IOCM Research in Support of Super Storm Sandy Disaster Relief

NOAA Co-operative Agreement NA14NOS4830001

Final Report: Executive Summary

December 29, 2015

Principal Investigator
Brian R. Calder
Center for Coastal and Ocean Mapping
University of New Hampshire
24 Colovos Road
Durham, NH 03824
brc@ccom.unh.edu
+1 (603) 862-0526

Co-Principal Investigator
Larry A. Mayer
Center for Coastal and Ocean Mapping
University of New Hampshire
24 Colovos Road
Durham, NH 03824
larry@ccom.unh.edu
+1 (603) 862-2615

Executive Summary

Overview

This report documents research conducted under co-operative agreement number NA14NOS4830001 between the National Oceanic and Atmospheric Administration (NOAA) and the Center for Coastal and Ocean Mapping (CCOM) at the University of New Hampshire (UNH). The co-operative agreement was competitively awarded to CCOM to support "relevant research and development activities associated with with FY13 Disaster Relief Appropriations Act-related LIDAR and acoustic coastal/ocean mapping and marine debris mapping data processing problems," as called for by the original Federal Funding Opportunity (FFO) document. This report covers a performance period from October 2013 to September 2015.

The primary objectives of the research were to develop methods for detection, aggregation, and characterization of marine debris; to examine the performance envelope of a variety of remote-sensing instruments; to investigate methodologies for data product construction and communication; and the public communication of the results of the research through outreach efforts, expressed within the framing structure of surveying in a storm-response scenario.

To support these objectives, research was conducted in five primary themes that were aligned with the programmatic priorities of the original FFO:

1. "LIDAR, habitat, and specialized data processing," which looked at extracting extra information from Light Detection and Ranging (LIDAR) return waveforms in order to support habitat research and change monitoring, with particular emphasis on submersed aquatic vegetation (SAV); determination of the minimum observable differences in repeated LIDAR mapping; methods for habitat classification and change detection; use of satellite-derived bathymetry (SDB) for change detection in shoreline and volumes; use of SDB to highlight areas of charts that might require update; use of satellite imagery for SAV mapping; and the limitations of these various instruments.

2. "Marine object management," which developed a robust method for detection of marine debris with multiple non-ideal detectors and use of semi-empirical prior knowledge on likely prevalence of marine debris as a means to control the complexity of this problem; and methods to package these results and com-

municate them correctly, and compactly, between parties involved in a storm response.

3. "Improved storm-response surveying with phase-measuring bathymetric sidescan echosounders," which developed methods for processing phase-measuring bathymetric sidescan (PMBS) data through conventional hydrographic tools; developed best practices for surveying with these instruments in a storm-response scenario; examined the concerns relevant to object detection with such systems; proposed methods for data analysis to assist in storm-response (and general) surveying; and demonstrated how PMBS systems could be integrated into a conventional multibeam echosounder (MBES) survey scheme.

4. "Visualization," which developed a new tool to assist with the automated selection of viewpoints for complex data, with particular application to marine debris identification; and developed this into a crowd-sourcing opportunity.

5. "Outreach," which communicated the purpose and results of the research via the public website; interaction with K-12 students and their educators through the SeaPerch and Ocean Discovery Day events; the development of infographics in print and interactive electronic form; and the co-development of a museum exhibit on the theme of hurricanes and marine debris.

This final report demonstrates that all of the proposed milestones for the project were achieved, and in many cases exceeded. Many of the techniques developed were also found to have impacts beyond the scope of the current project. A total of 25 publications were generated as part of the project, including one journal article, 11 conference papers or presentations, and 13 white-papers or best practice documents. The project website, `http://sandy.ccom.unh.edu` contains all materials related to the project, including the original proposal, all progress reports, all white-paper and best-practice documents, and all available conference papers or presentations. The website also hosts the crowd-sourcing marine debris experiment, and the interactive infographics.

Research Conducted

LIDAR, Habitat, and Specialized Data Processing

Research in this theme was focused primarily on applications, rather than instruments, since LIDAR and satellite imagery were both used for shoreline/bathymetric change detection and habitat monitoring/classification. A Super Storm Sandy-affected area in Barnegat Bay, NJ, was chosen as a common site for testing many of the techniques developed, primarily due to data availability.

The availability of multiple LIDAR datasets for the area, from different LIDAR systems, was used to identify the minimum observable difference for repeated surveys,

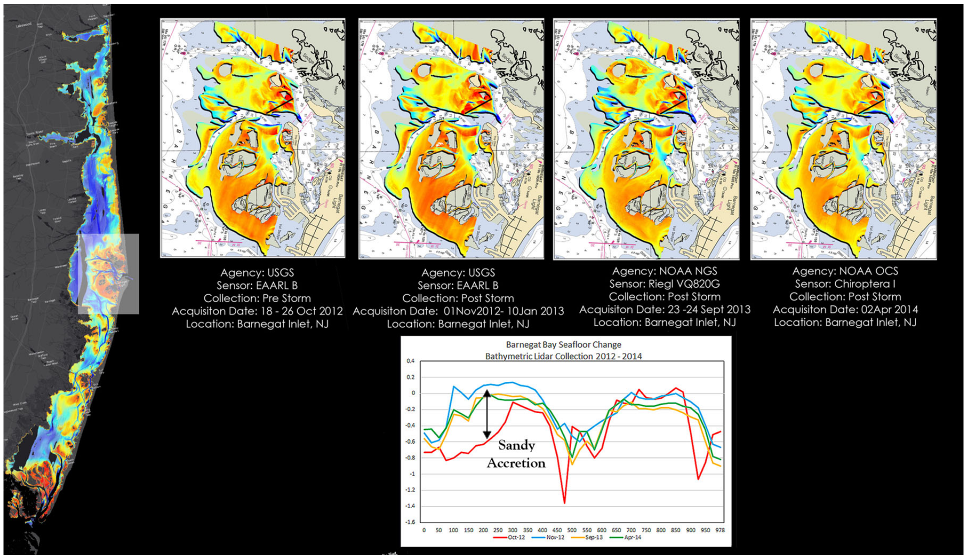

Figure ES.1: Depth as a function of distance for four bathymetric LIDAR collections over three years of data from three different LIDAR systems in the Barnegat Bay Inlet region. The change pre- and post-storm (red and blue lines) is clearly significant with respect to the self-noise of the systems.

i.e., the minimum amount that two surveys have to differ for the difference to be considered more than observational uncertainty. The results (Figure ES.1) indicate that the minimum difference considered to be "observational" is on the order of ± 0.1 m. SDB techniques cannot be used to provide absolute depths since it is assumed that there will be a lack of reference depths from a conventional survey in a storm-response scenario. Relative estimates of slope can be constructed, however, which are indicative of change (Figure ES.2) and can also be used to show levels of seasonal variability, which are used for calibration purposes.

Research into the use of LIDAR and satellite imagery for shoreline change was also conducted, which showed that a long-term trend for shoreline change rates could be derived from satellite imagery. The effects of Super Storm Sandy could be identified in some areas, implying that significant changes can be detected using these methods. Repeated LIDAR surveys were also used to derive direct estimates of deposition and erosion rates around Mantoloking, NJ. Procedure documents were generated for both processes.

Classification features, derived from LIDAR waveforms, were used as the basis of a classification scheme for SAV (Figure ES.3). Object-based image analysis (OBIA) was used in Trimble eCognition to construct a rule-set for four different habitat classes of sand, mixed macroalgae and sand, sparse eelgrass, and dense eelgrass, and comparison against ground-truth data showed an overall classification accuracy of 85%. The classifications used were shown not to be statistically different from manual classifications for the same area, and the rule-sets used were shown to be portable to different

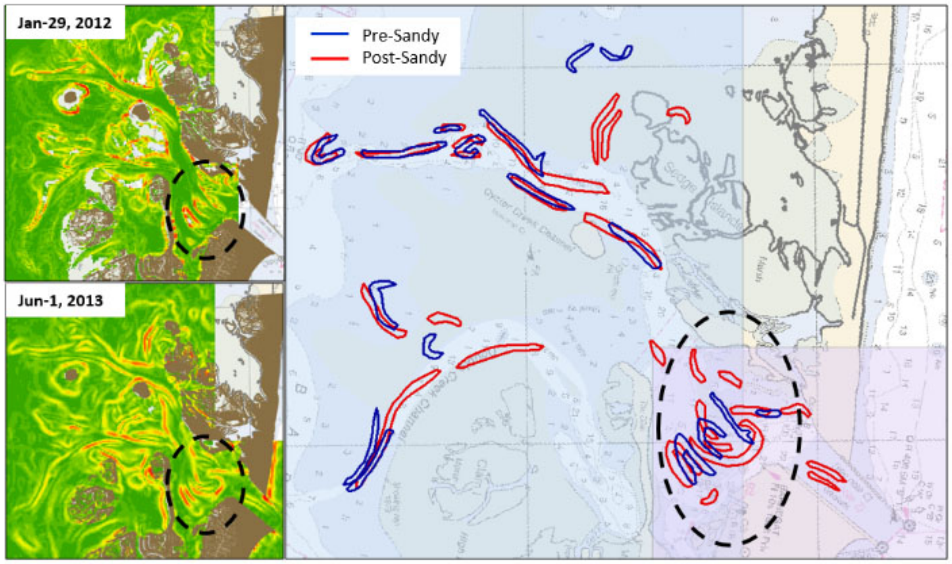

Figure ES.2: Preliminary results showing morphological changes at the entrance of Barnegat Bay Inlet pre- and post-Super Storm Sandy. The two images on the left are the slope maps from 2012-01-29 (pre-Sandy) and from 2013-06-01 (post-Sandy) acquired by WorldView-2 and Landsat 8, respectively.

areas and different LIDAR systems with compatible waveform features, although the specific parameterization of the rule-sets had to be adjusted.

Techniques were also developed to use satellite imagery for SAV mapping, particularly as a source for fine time-step estimates of change. Using Landsat 8, it was demonstrated that estimates of SAV density could be constructed from the tri-band imagery (Figure ES.4) and comparison against ground-truth data from a long-term study by Rutgers University showed agreement on the order of 75–88%, with some of the discrepancy potentially due to seasonal variability of the SAV.

Throughout the research, care was taken to ensure that the data products being generated would be compatible with the construction of Coastal Engineering Indices (CEI), although since there is currently no consensus on what a CEI would entail, no index was proposed. Procedures documents were developed for all of the techniques proposed, including use of SDB to assist in chart update and comparison, particularly so that they could be readily communicated to the Integrated Ocean and Coastal Mapping (IOCM) contract group at the NOAA-UNH Joint Hydrographic Center, a sister project, where they are currently in active use.

Marine Object Management

This theme focused on developing a model for the robust detection of marine debris using remote sensing techniques, accepting that this problem is inherently difficult because of the ill-defined nature of what constitutes "marine debris." The work uses

Figure ES.3: Benthic habitat map for the Barnegat Inlet flood tidal delta complex created using NOAA NGS Riegl VQ-820-G data (including auto-generated waveform features), Applanix DDS digital aerial imagery, and an object-based image analysis approach in eCognition.

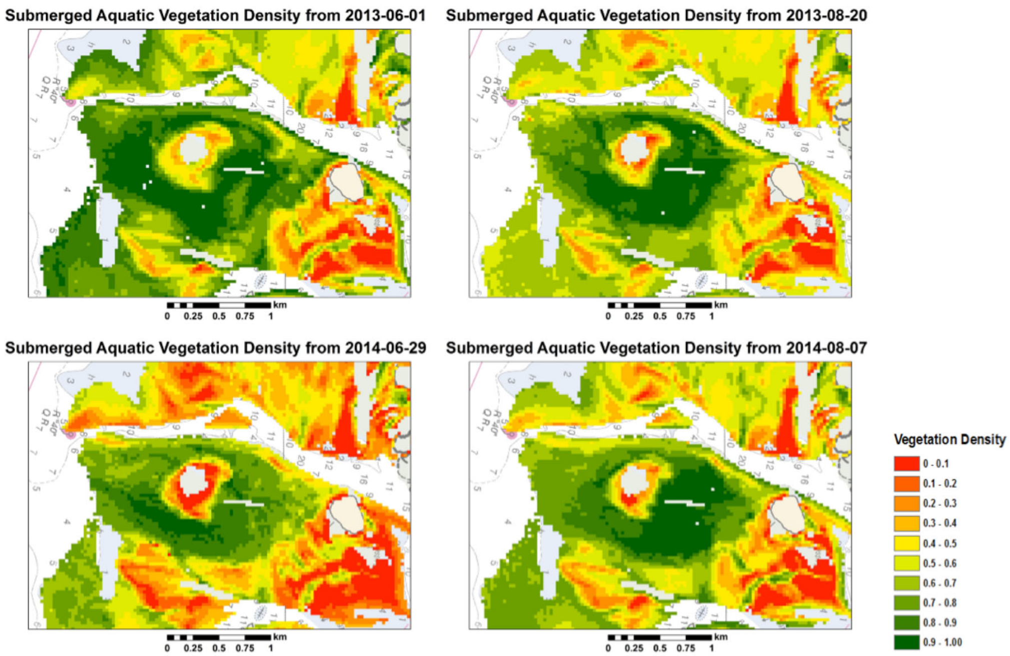

Figure ES.4: SAV density using Landsat 8 imagery from four different time periods in Barnegat Bay Inlet, NJ: (a) 2013-06-01; (b) 2013-08-20; (c) 2014-06-29; and (d) 2014-08-07. Density values range from 0% (red) to 100%, normalized to 1.0 (green).

a Bayesian hierarchical statistical model to generate a probability density map for marine debris presence, and builds an idea of the potential for debris abundance (Figure ES.5) from observations associated with previous storms. This is used to provide a prior estimate as to debris prevalence, which can help in constraining the overall estimation problem. Empirical data from the Gulf of Mexico Marine Debris Program, NOAA's Marine Debris Program and Office of Coast Survey responses to Super Storm Sandy were used for construction of the prior model, while NOAA Office of Coast Survey data in Jamaica Bay, New York, NY, was used for case-study testing of the methods developed.

The algorithm developed combines prior information with multiple non-ideal detectors of marine debris, which are based on automated analysis of data products typically generated in the normal course of survey operations. The logic is that in a storm-response scenario, it would be unlikely that there would be resources available for more specialized data collection. Each of the detectors is expected to be fallible, but since they are not all fallible in the same way, the research shows how they may be fused together to form a detector that is more robust.

A case study was conducted against ground-truth marine debris data collected by NOAA contractors as part of the Super Storm Sandy response, and was shown to develop probability maps that correspond to the density of objects identified by hand (Figure ES.6). Receiver Operating Characteristic (ROC) curves for the same area show an Area Under the Curve (AUC) value of 0.880 for the model when spatial context

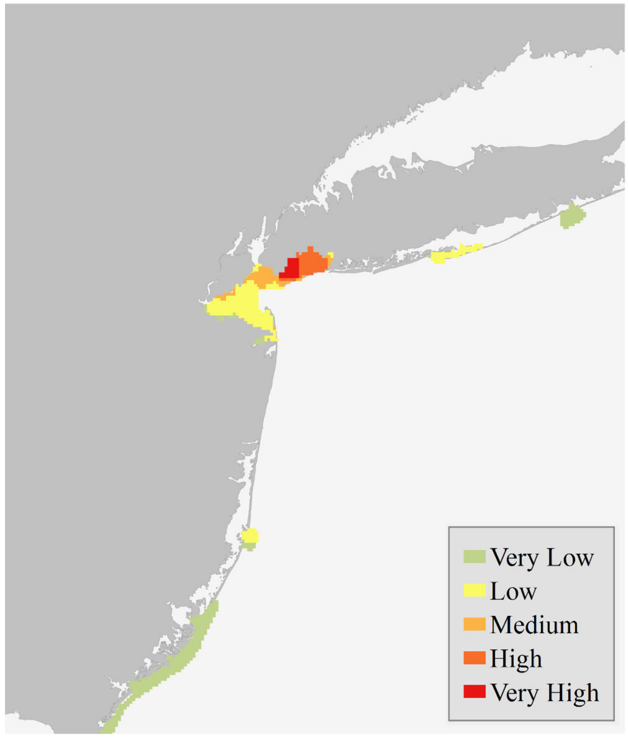

Figure ES.5: Predicted distribution density of marine debris in the SSS study area.

was taken into account, which indicates strong detection capabilities with few false positives. The ROC curves also demonstrate that the addition of spatial context to the estimation problem has positive benefit.

Finally, the research addressed the question of how to readily transfer information on marine debris objects between the various entities involved in a marine debris response, driven by the observation that no common vocabulary for such purpose existed. A "markup" language was developed from the core objects in the Geographic Markup Language (GML), a commonly-implemented standard, which allow marine debris objects described in the Marine Debris Markup Language (MDML) to be readily processed with standard applications.

Improved Storm-Response Surveying with Phase-Measuring Bathymetric Sidescan Echosounders

Research on the use of phase-measuring bathymetric sidescan (PMBS) sonars balanced concerns of exploring the limitations of these systems and developing best-practice information for their use in a storm-response scenario. The research highlighted historical problems with PMBS systems, and showed that hardware and software advances by some manufacturers have largely resolved these issues for their systems. These improvements have increased the ability of PMBS systems to detect and maintain in-

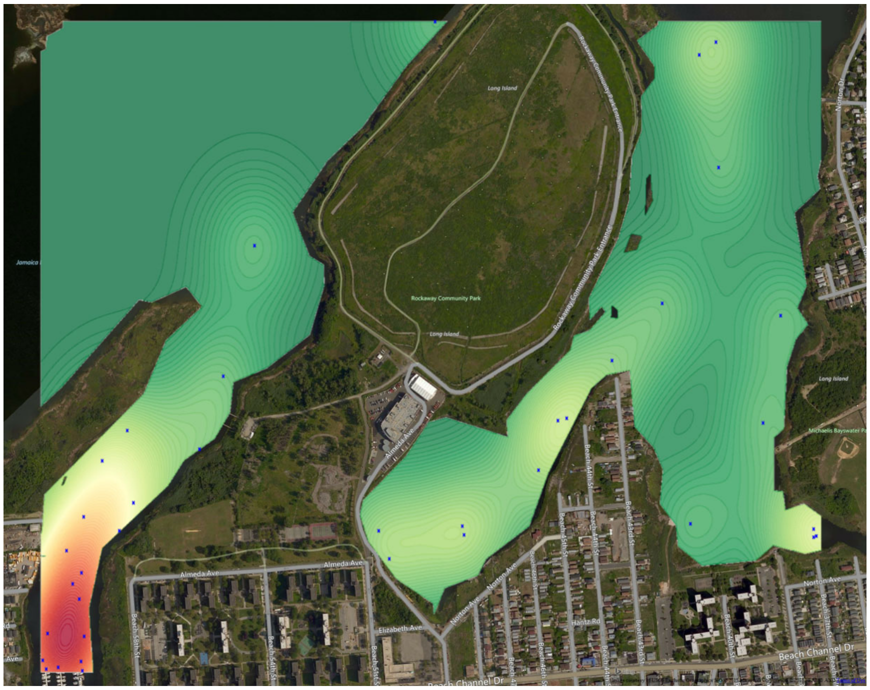

Figure ES.6: Results of the hot spot analysis in Jamaica Bay, New York, NY, with the ground-truth positions of the marine debris designated by human analysts showed as blue dots.

formation on objects of hydrographic significance (such as marine debris), such that they can now be routinely and reliably detected in data (Figure ES.7). Identification of objects remains a challenge, but it is argued that co-located sidescan generated by a PMBS in addition to the bathymetry improves on this situation, and its use is strongly recommended. It is argued that the most effective strategy for survey in a storm-response scenario may very well be to have more widely spaced survey lines in order to improve efficiency, relying on the sidescan data to identify potential targets, which can then be re-surveyed with optimal survey geometries.

A series of best-practice suggestions are presented, among them to require water column data, or sidescan in order to assist in object detection; to require uncertainty estimates from manufacturers of PMBS systems; use of the outer swath to increase detectability; to filter data to omit only outliers and not the tails of noisy data thereby maintaining the original statistics; and to build CUBE statistical surfaces to assist in data processing rates.

Previous arguments emphasized the importance of simultaneous sidescan and bathymetry information from PMBS systems; to capitalize on this, a prototype graphical user interface (GUI) was developed to demonstrate the benefits of co-analysis of such data (Figure ES.8), a tool which is conspicuously absent in conventional hydrographic data processing software. A mock-up of a suitable GUI demonstrates that simple techniques such as showing the same cursor position in all data views, or

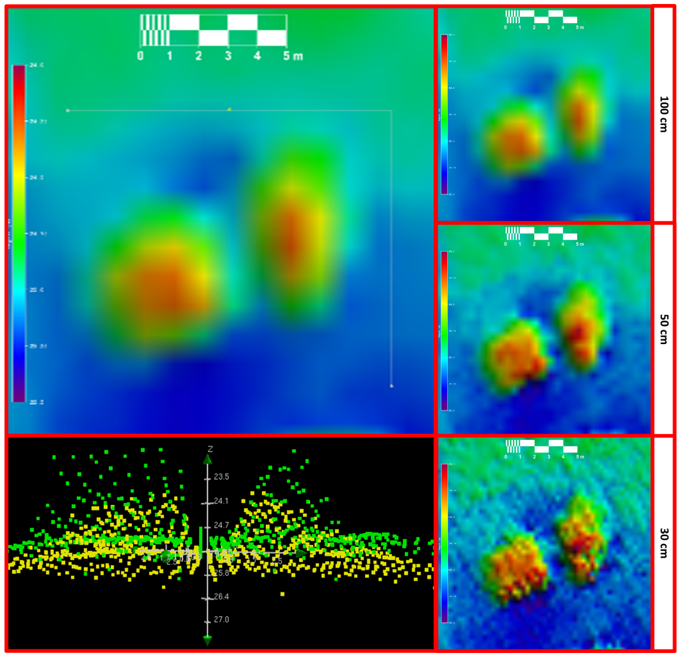

Figure ES.7: Visibility of distinct objects in PMBS data, here 5 m apart (note 5 m total length scale bar in all images). Evidence in multiple paths shows that these are distinct objects, but does not necessarily support identification.

showing a range-ring about the PMBS corresponding to a target position can radically improve user understanding of data.

Finally, the research demonstrates that PMBS estimates of depth constructed through completely automatic means using the CUBE algorithm applied to a shallow water survey in Plymouth Harbour, England, are comparable with MBES estimates in the same area, with the only significant disagreement being on steeply sloped areas.

Visualization

Visualization research focused on how to optimize operator output when attempting to identify marine debris. The Marine Debris Rapid Decision Tool (MDRDT) was developed (Figure ES.9) which automatically selects multiple, optimal views of the target object that are expected to best highlight the shape of the target and thereby assist the operator in identification. The views are embedded in a fully-functional 3D visualization system so that the viewpoint can be adjusted as required, but it is argued that the more often the views allow for early identification of the object without the need for adjustment, the more efficient the operator will be. Simplified tools to mark objects as debris, and to associate a confidence of identification, are provided.

The techniques developed for MDRDT were also applied in a web-based tool (Figure ES.10) as a model for a crowd-sourced approach to marine debris identification.

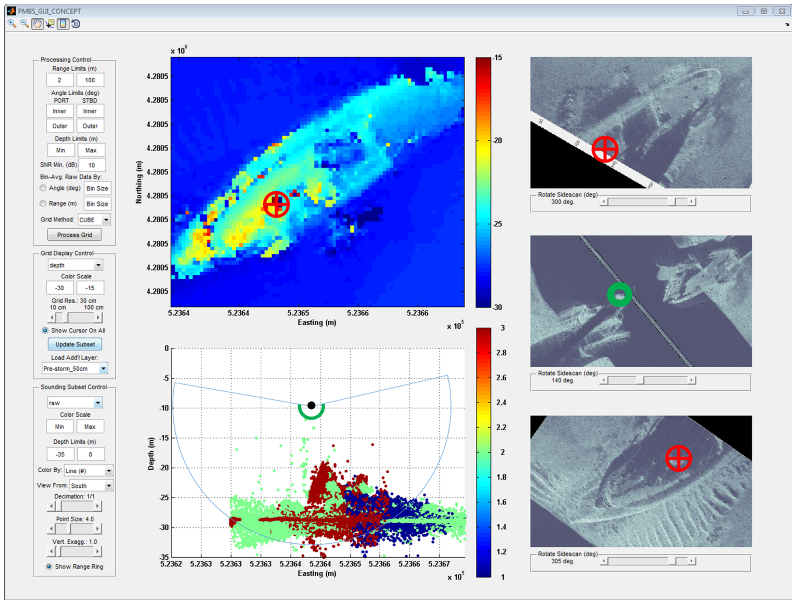

Figure ES.8: Prototype GUI for simultaneous review of bathymetry and sidescan imagery from a PMBS system. The “Show Cursor On All” option has been selected to assist in cross-identification of a target in all views (red crosshairs), and the “Show Range Ring” option has been used to correlate a target in sidescan with a particular range from the PMBS in the bathymetry.

It is argued that the lack of trained operators can be a significant limitation during a marine debris project, and therefore that it might be advantageous to use a group of volunteers to assist. An experiment hosted on the project website demonstrated that the identification performance of untrained volunteers, neglecting the (automatically identified) lowest quality volunteers, showed 84% agreement with a trained operator.

Outreach

Outreach efforts were conducted across a variety of media. The simplest outreach opportunities were afforded by the project's website, which was used to host all of the documents generated by the project, but was also used to host informal "infographics" explaining general topics such as marine debris and survey protocols as well as interactive infographics showing simplified versions of marine debris data, and experimental data analysis techniques.

The project was afforded a more permanent outreach opportunity through a collaboration with the Seacoast Science Center (Rye, NH), a local interactive science museum. This collaboration supported the development of an interactive exhibit that explores hurricanes, the marine debris problem, methods for debris identification, and the decisions associated with whether and how to remediate debris. An

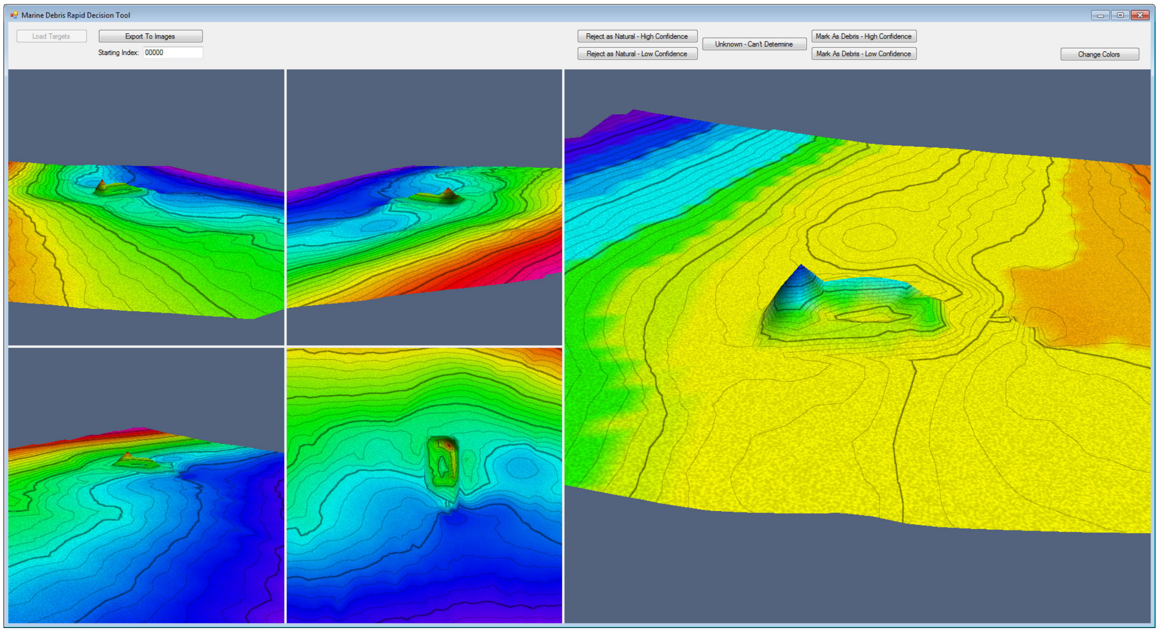

Figure ES.9: Screenshot of the Marine Debris Rapid Decision Tool. The multiple views of the target under investigation are automatically selected to assist the operator in identifying the target, ideally without having to adjust the viewpoints or manipulate the data.

interactive, touch-screen exhibit was developed with the aid of undergraduate computer scientists (Figure ES.11) which demonstrates principles of survey and marine debris identification. The exhibit will open at the Seacoast Science Center during winter 2015.

Further outreach opportunities were fostered through collaboration with UNH-led STEM events. The project provided several interactive demonstrations of mapping technologies and related research during the UNH Marine School's Ocean Discovery Day in 2014 and 2015, and partnered with the regional SeaPerch competition (Figure ES.12) in 2014 to introduce K-12 students and their educators to the problems of marine debris, the aims of the project, and the issues surrounding debris remediation.

Conclusion

The co-operative agreement has resulted in research on a number of themes, all of which have been documented through academic papers, conference presentations, and white paper documents, hosted on the project's website. This research has shown that there are significant benefits to be had through their adoption for the collection, processing, and dissemination of multi-use IOCM data products. Active efforts to transfer the research into operational use have taken place.

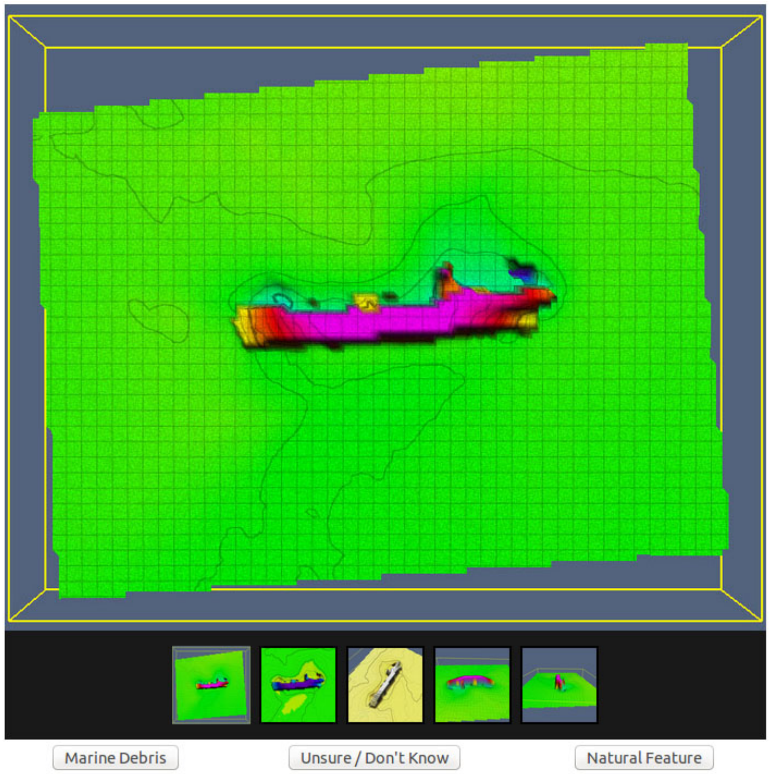

Figure ES.10: A screenshot of the web-based crowdsourcing interface. Users see a single zoomed-in image, and can scroll through or click on the thumbnail images at the bottom to view each of them as many times as needed.

(a) Conceptual design. (b) Exhibit screenshot.

Figure ES.11: The "A Hurricane Hits Home" exhibit at the Seacoast Science Center, Rye, NH, and an example screen-shot from the interactive exhibit.

Figure ES.12: SeaPerch afternoon "team challenge" event, 7 June 2014. Clockwise from top left: divers deploying simulated "marine debris" in the engineering test tank; a team adapting their SeaPerch; a dual-Perch marine debris removal system; SeaPerch ROVs removing simulated debris.

In addition to the specific benefits associated with the immediate fields of application of the various techniques developed, there is potential for wider impact of many of the techniques. LIDAR-derived waveform features could be used more generally for rapid habitat assessment as an add-on product for conventional LIDAR surveys, and the use of multiple passes of satellite imaging could be used to provide a baseline for seasonal or long-term habitat change. The marine debris detection model could also be used for general hydrographic feature detection and management, and the techniques developed for PMBS data collection and processing could be used to support the use of such systems for general hydrography. The techniques developed to select viewpoints for marine debris inspection could also be applied to the general problem of selection of data orientation for hydrographic data processing. And the proposed crowd-sourced debris identification application could be used for future storm events, or even for general hydrographic practice.

Many of the techniques developed for this project have already had an influence on practice within the IOCM sister-contract at the Joint Hydrographic Center. It is argued, however, that there is significant potential for loss of capabilities as the immediate projects (eventually) come to an end. It is recommended that efforts to preserve the gains achieved through this project are pursued.

IOCM Research in Support of Super Storm Sandy Disaster Relief

NOAA Co-operative Agreement NA14NOS4830001

Final Report
December 29, 2015

Principal Investigator
Brian R. Calder
Center for Coastal and Ocean Mapping
University of New Hampshire
24 Colovos Road
Durham, NH 03824
brc@ccom.unh.edu
+1 (603) 862-0526

Co-Principal Investigator
Larry A. Mayer
Center for Coastal and Ocean Mapping
University of New Hampshire
24 Colovos Road
Durham, NH 03824
larry@ccom.unh.edu
+1 (603) 862-2615

Contents

List of Figures

List of Tables

Chapter 1

Introduction

1.1 Background to the Project

At 1930 EDT on the 29th of October 2012, Super Storm Sandy[1] made landfall on the U.S. east coast near Brigantine, NJ (Figure 1.1–1.2). The convergence of the storm with an intense low-pressure system, its unusual approach direction (from the east rather than from the south) and its coincidence with astronomically high tides made Super Storm Sandy one of the deadliest and costliest hurricanes in U.S. history, causing 147 deaths in the U.S. and more than 70 billion dollars in damages [1]. Most of the damage caused by Super Storm Sandy was focused on the coastal zone, with flooding (the hurricane caused record high storm surges in New York, New Jersey and Connecticut), high winds and powerful waves resulting in the destruction of buildings, homes, roads, vehicles, and many other objects over hundreds of miles of coast.

In the wake of Super Storm Sandy, it became clear that many of the techniques and tools used for surveying were not optimal for use in the response to a storm event. Storm response surveying requires a different approach from that in which hydrographic tools and techniques are generally used, as the emphasis is often on more rapid processing of data, or less stringent standards of accuracy traded off against more area covered in less time. Consequently, there was a clearly felt need for investigation of how standard survey techniques and tools could be modified, or extended, to be more effective in response to the result of a storm on the coastal environment, and in particular to the concept of Integrated Ocean and Coastal Mapping (IOCM), where data might be gathered for one purpose, but usefully applied to a variety of problems.

In addition, it was clear that a significant amount of data was going to be collected in the wake of the storm, and that there was likely to be a processing bottleneck in dealing with all of that data in a timely manner. Although a separate funding in-

[1] The storm is variously known as "Super Storm Sandy," "Hurricane Sandy," and "Post Tropical Cyclone Sandy, " depending on the author. The term "Super Storm Sandy" is used consistently within this report for convenience, and consistency with the initial proposal document, but without any intent of limitation, or of precise meteorological definition.

Figure 1.1: Satellite image of Super Storm Sandy on 2012-10-30, approximately at its maximum extent, a day after making landfall. Photo: NASA.

(a) Aftermath, Seaside Heights, NJ

(b) Aftermath, Mantoloking, NJ

Figure 1.2: After-effects of Super Storm Sandy land-fall, which included the generation of some obvious (and much more not so obvious) marine debris. Photos: AP Photo/Julio Cortez.

strument was used to support the IOCM Center at the NOAA-UNH Joint Hydrographic Center, it was clear that new techniques and tools would likely be required to assist in the processing task, for which some research effort was going to be required.

While the damage caused by the storm can easily be documented by airborne or satellite imagery for those areas that are above sea level, the impact of the storm on those areas at or below sea level (i.e., the presence of debris and changes in the shape of the seafloor that can create navigational hazards, or the impact on benthic marine habitat) is much more difficult to assess. Recognizing this, the FY-13 Disaster Relief Appropriations Act contained funds to support state and Federal efforts to acquire and process coastal and ocean mapping data in order to support marine debris removal and beach nourishment efforts, as well as to update nautical charts, create more accurate inundation models and better understand the impact of the storm on marine habitat.

In response to this, the National Oceanic and Atmospheric Administration (NOAA) released a federal funding opportunity (FFO) document, number NOAA-NOS-OCS-2013-2003801, calling for "relevant research and development activities associated with the FY13 Disaster Relief Appropriations Act-related LIDAR and acoustic coastal/ocean mapping and marine debris mapping data processing problems," with the expectation that proposals "shall provide beneficial outcomes for the affected coastal areas through improvements in Integrated Ocean and Coastal Mapping processing." A proposal was subsequently submitted by the Center for Coastal and Ocean Mapping (CCOM) to carry out research in line with the FFO, which was selected for funding as a co-operative agreement between the University of New Hampshire and NOAA.

This document is the final report on that research, and seeks to summarize the research conducted during the period 2013-10-01 to 2015-09-30 under the agreement.

1.2 Goals and Objectives

The proposed research was predicated on three primary goals:

1. Improving the efficiency and scope of survey operations conducted in support of post-storm disaster recovery;

2. Raising awareness of best practices and procedures for data collection, processing, and management; and

3. Supporting flexible and efficient planning and preparedness for, and response to, significant storm events through provision and wide dissemination of appropriate data products;

which were designed to support the programatic goals of the FFO, particularly with respect to the NOAA priorities of coastal resiliency, safe marine transportation system, ecosystem-based management, and the ability to plan and respond to climate variability.

The emphases of the research conducted were directly informed by these goals. In particular, each segment of the research has attempted, whenever possible, to document the procedures and tools that have been developed, many of which are referenced through this report, and which are also available through the project's website. In addition, the research has considered a number of new improvements on data processing techniques for commonly available data, for example the use of satellite-based imagery to support submersed aquatic vegetation (SAV) detection, or the extraction of waveform features from LIDAR data; and has considered better methods for surveying with current tools, such as phase-measuring bathymetric sidescan (PMBS) sonars, which will also cross-over into standard hydrographic practice. Finally, all phases of the research have ensured that the products being generated are constructed in a fashion that is compatible with down-stream decision-making tools, such as conventional geographical information systems (GIS) and more specialist tools such as the Emergency Response Management Application (ERMA), but particularly those tools being utilized by the Integrated Ocean and Coastal Mapping (IOCM) team at the Joint Hydrographic Center (JHC) in their sister-project on Super Storm Sandy response.

Specifically, however, the research was structured with respect to four overall objectives:

1. Development of methods for detection, aggregation, and characterization of marine debris;

2. Examination of the performance envelope of a variety of remote-sensing instruments;

3. Investigation of methodologies for data product construction and communication; and

4. Communication of the results of the research through outreach efforts;

which have guided the overall direction of the effort. As detailed in the remainder of this report, these objectives have been largely achieved.

With respect to development of methods for marine debris processing, the project has developed a new technique, based on a robust statistical model, which combines *a priori* knowledge derived from marine debris cleanup of previous storms with a set of object detection techniques so that the overall complexity of the marine debris problem is constrained, and the non-ideal detections from the different detectors can be fused in a robust manner. The resulting output is a statistically robust estimate of the probability of marine debris presence that can be used as a guide for clean-up operations. The technique also includes a language for cross-vendor description of marine debris that can bring some commonality and consensus in transferring information between participants in a clean-up effort, easing communication of data products through the processing and decision-making chain. In addition to this direct approach to the objective, the research conducted has also looked at the human-factors involved in marine debris data analysis, considering new visualization techniques to improve human operator efficiency when tackling the difficult (and often tedious) task of identifying marine debris, and at how to make this task into something that might potentially be crowd-sourced in the event of another storm event, addressing the resource limitations that are often observed in such situations.

The research addressed the question of limitations of performance of current systems primarily through examination of the PMBS systems often used for surveying in very shallow water, and the capabilities of LIDAR systems. For PMBS systems, the primary concerns for their use in production hydrographic surveying are processing the data using conventional tools, and their ability to detect and maintain the presence of small objects through the processing chain. The research reported here demonstrates that advances in data pre-processing developed by the manufacturers of PMBS systems, and particularly the availability of nadir data and uncertainty estimates, make it possible to process such data through conventional toolchains without difficulty; and that, constructed correctly, grids made from PMBS data can preserve the presence of objects (although the use of the co-located sidescan data from PMBS systems is also strongly recommended). The best practices and procedures are summarized in a series of white-papers. For LIDAR systems, the research demonstrates that shoreline and volumetric changes due to storm events can be reliably captured in LIDAR data (i.e., are beyond the measurement uncertainty).

Almost all of the themes of the research program address the objective of product creation and communication in some sense. For example, in the marine debris work, the research has developed, in conjunction with NOAA's Marine Debris Program, a computer mark-up language that allows marine debris objects to be concisely and unambiguously described, avoiding the problem of, for example, the remains of a ship being classified variously as "ship," "boat," "wreck," "ships," and "SHIP," as has been observed in some databases of marine debris in the Sandy-affected area. Within the LIDAR and satellite imagery work, products are generated as standard GIS-style objects which are readily exchangeable, while within the PMBS theme, standard hydrographic tools are used. In all themes, the procedures have been documented, and are available on the project's website.

Finally, the objective of outreach and communication of results has been addressed in three separate efforts: construction and maintenance of a public-facing website (including the crowd-sourcing experiment for marine debris identification), participation in K-12 STEM[2] activities, and development, in conjunction with a local interactive science museum, of a child-friendly exhibit exploring marine debris issues in the context of storm response.

Through all of the research, however, one primary objective has guided the effort, which is a focus on developing practical tools to support storm-response surveying. That is, surveying in the wake of a storm is not necessarily the same as surveying for primary hydrographic purposes. For example, if the purpose of the survey is

[2]Science, Technology, Engineering, and Math.

to identify marine debris objects that are going to be removed, it does not matter so much if a precise least-depth is determined, and approximate techniques can be used. Or it might be permissible to use wider line-spacing to improve efficiency (using sidescan imagery to fill gaps), or alternative (approximate) data sources such as satellite-derived bathymetry, if they are more readily available and give a better time series of changes in order to assess the significance of a storm's effects. This focus on *practical* tools is driven primarily by the connection to the IOCM sister project, but has the happy coincidence in making the tools developed more readily useful in the event of the response to a future storm event.

1.3 Structure of the Report

1.3.1 Topic Areas

The structure of this report follows directly from the research themes proposed, which themselves reflect the programatic priorities of the FFO, and cut across the objectives outlined in the previous section. The proposed research covered five major themes:

1. LIDAR and satellite remote-sensing data processing, with connections to habitat monitoring. The research has looked at new techniques for extracting better information metrics from LIDAR waveforms, and use of these metrics for habitat classification and change analysis; use of LIDAR for shoreline and volumetric change in the wake of a storm; use of satellite-derived bathymetry for shoreline and volumetric change analysis with emphasis on time-history of the changes to identify when significant change has occurred; and application of these to chart update and change determination.

2. Use of Phase Measuring Bathymetric Sidescan (PMBS) sonars for response surveying, and the associated data processing requirements. The research has looked at some of the processing chain problems associated with PMBS data, and shown that PMBS can now be processed with conventional techniques; methods to improve on deployment of PMBS systems for surveying in storm response situations; the ability of PMBS systems to detect and preserve objects, and the conditions under which these can be optimized; and best practices for selecting and deploying such systems.

3. Marine debris detection, databasing, and communication, including the use of different data sources to augment the detection process. The research has looked at models of debris prediction from extant data, and how to translate them into structuring information to assist models of marine debris detection; how to analyze survey data that would be conventionally acquired during storm response surveying for marine debris; and how to combine the results of a number of non-ideal (i.e., realistic) debris detectors in a principled manner to generate an overall estimate of the probability of marine debris.

4. Visualization of the results of marine debris detection, and better tools for informed decision-making. The research has looked at automatic viewpoint selection in 3D visualization systems so as to minimize the time required to identify marine debris; how to translate these tools into something that can be deployed on a website; and the use of the same as a means to crowd-source marine debris classification problems.

5. Public outreach, conducted through direct events (including a permanent museum exhibit in a local science center) and through data products and guides, available from the project's website.

Each of these themes is covered in more detail in one section of this report. The original proposal document, as well as all of the interim progress reports, submitted quarterly, can be found on the project's website, `http://sandy.ccom.unh.edu`.

1.3.2 Project Products

Throughout the project, a central theme of the research was to provide, whenever possible, advice, guidance, and procedure documents to capture the methods and tools developed during the research. In part this was motivated by sound scientific principles, but was also informed by the need to propagate new methods to the IOCM team at the Joint Hydrographic Center, who are tasked with using these techniques to process all of the data being collected in support of Super Storm Sandy remediation efforts.

A list of the products generated during the project can be found starting on page 133; electronic versions of all of the documents can be found on the project's website, `http://sandy.ccom.nh.edu/publications/library.html`.

1.3.3 Data and Techniques

Much of the data used in this project has been sourced from public archives, or has been provided by collaborators within the Federal government, or State organisations. CCOM is not the data custodian or responsible party for any of the raw data sources, and readers should note that some of the data are preliminary, and subject to modification by their respective owners.

Data examples are presented here and in related documents for demonstration purposes only and do not represent any guarantee of performance by any sonar system or software package. No part of this report or related documents shall be taken as a recommendation or endorsement of any particular product.

Chapter 2

Lidar, Habitat, and Specialized Data Processing

2.1 Introduction

In the wake of a storm event on the scale of Super Storm Sandy, there is often a strong need to provide rapid assessment of the state of harbors, channels, and other hydrographically significant features, primarily as an aid to re-opening ports and providing support to the recovering communities affected by the storm. There is often, however, also a requirement to understand the effects of the storm on marine habitats within the area affected, where the problem can be made more difficult because of the lack of a time history of the natural variation of the area. In both cases, physical access to the locations of concern can be limited by the infrastructural damage caused by the storm.

Airborne remote sensing techniques are tempting tools for these types of problems. Not only can they cover ground rapidly, they can also do so from bases more remote from the storm-affected area, which eases logistical difficulties. In addition, satellite-based optical and multi-spectral imaging (MSI) provide the opportunity to recover a more dense time series of older datasets from a given area simply by searching the appropriate archives, which is more difficult with terrestrial remote sensing techniques such as multibeam echosounders, or bathymetric LIDARs. Since the location where a response is going to be required is not readily predictable, this can be a significant advantage.

This chapter considers the opportunities for, and potential of, airborne remote sensing techniques to assist in the estimation of the effects of a significant storm, such as Super Storm Sandy. In particular, it considers the use of LIDAR data for classical roles such as shoreline change detection and morphological change, but also as a source of waveform features that can be translated into maps of submersed aquatic vegetation (SAV), or other habitat features. It also considers the use of visible-light satellite imagery as a source of bathymetric information using Satellite-derived Bathymetry (SDB) techniques, to detect morphological changes, and as an alternative

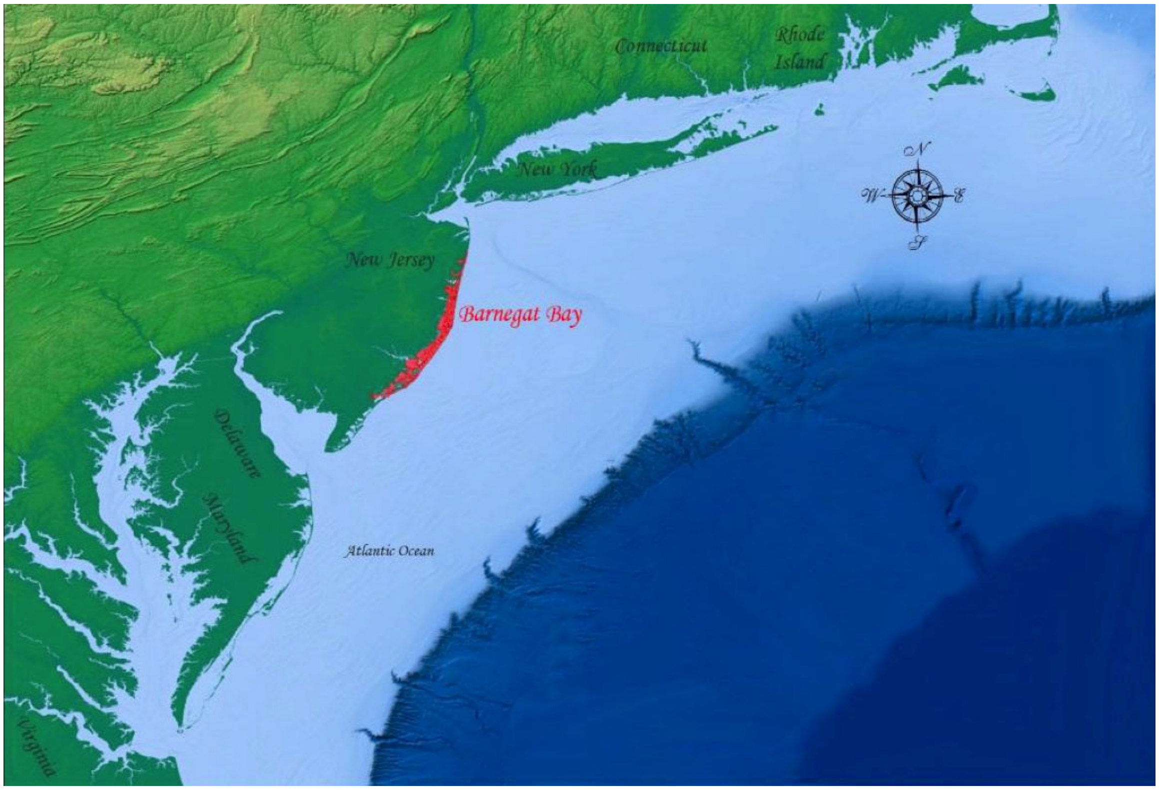

Figure 2.1: Location of Barnegat Bay, NJ, the site of much of the work conducted for the LIDAR and SDB themes.

source of habitat information on SAV. Finally, it addresses the possibility of constructing Coastal Engineering Indices (CEI) from the various products constructed, with the goal of providing source material for CEIs, rather than the CEIs themselves.

2.1.1 Analysis Location

In order to allow for comparison of results between the various techniques being developed, a common location for analysis was sought. The basic requirements were availability of suitable datasets, relevance to the types of techniques being developed, and a demonstrated impact by Super Storm Sandy. (This last was added in order to demonstrate that the techniques could be used in areas likely to be affected by storms of this type.) A number of potential locations were considered, but the best match was in the Barnegat Bay–Little Egg Harbor region of coastal New Jersey (Figure 2.1).

Barnegat Bay-Little Egg Harbor (BB-LEH) forms a long, narrow, tidal basin on the coastline of central New Jersey. The water mass extends approximately 70 km north-south, separated from the ocean by a series of barrier islands. Exchange of bay and ocean water occurs through three inlets: Pleasant Canal in the northern segment, Barnegat Bay Inlet in the central segment, and Little Egg Inlet in the southern segment. The bay water has an extended residence time due to the limited number of exchange points (74 days in the summer, [2]). It ranges from one to six meters in depth with a volume of approximately $2.4 \times 10^8\,\mathrm{m}^3$ and a surface area of approximately $280\,\mathrm{km}^2$ [3]. Tides are semidiurnal with a range of 0.5–1.5 m. Water temperature ranges from −1.5°C to 30°C and salinity ranges from about 10 to 32 [4] (as cited in [5]). Freshwater supply is dominated by groundwater (> 80%) with a smaller component of surface water discharges [3].

Within the greater context of BB-LEH, the area around Barnegat Bay Inlet is of particular interest. Barnegat Bay Inlet provides a passage for small-craft and fishing-boat traffic from the Atlantic Ocean through Oyster Creek Channel to the New Jersey Intracoastal Waterway (Figure 2.2). The sediments around Barnegat Bay Inlet are sandy, which is typical for the coastal areas of New Jersey. These coastal areas experience heavy wave action with a high average grain size (0.4–0.5 mm). The tidal ranges along the New Jersey coastline are between 1.5 m during neap tides to 2.3 m during spring tides according to NOAA's Center for Operational Oceanographic Products and Services (CO-OPS). The Oyster Creek Channel at the entrance to Barnegat Bay Inlet is characterized by strong tidal currents. Jetties at the entrance of the inlet provide stabilization to the shoreline along the inlet, but necessitate frequent dredging. Recent U.S. Army Corps of Engineers works using Post-Sandy Supplemental Funds (PL 113-2) include: dredging of shoaling that occurred in Oyster Creek (work completed December 2013) and repairing post-Sandy damage to the north jetty that began in February 2014. In April 2014, the New Jersey Department of Transportation (NJDOT) announced that navigational buoys in the Double Creek Channel were removed due to severe post-Super Storm Sandy shoaling that created a severe navigation hazard and unsafe channel conditions, redirecting all navigation through Oyster Creek Channel [6]. Consequently, Barnegat Bay Inlet is a very good example of an area strongly affected by Super Storm Sandy, and therefore where the sorts of techniques being developed for this work are likely to be applied in the event of future storms.

2.1.2 Dataset Selection

A primary reason for the selection of BB-LEH, and Barnegat Bay Inlet in particular, as an exemplar area for technique development is the availability of datasets in the area. As part of the preliminary work for this project, available datasets were identified and catalogued.

Imagery datasets were used as part of the overarching goal of identifying spatial-temporal morphological or biological changes caused by a natural event and therefore data sources which provided a time series of products were preferred. National and State archives were searched for appropriate imagery (e.g., USGS EarthExplorer[1]). The data downloaded from the archives included: three-band Red-Green-Blue (RGB), four-band visible and near-infrared (VNIR), and multispectral imagery (MSI) that contains more than four bands. The use of these imagery datasets spans a wide range

[1] http://earthexplorer.usgs.gov

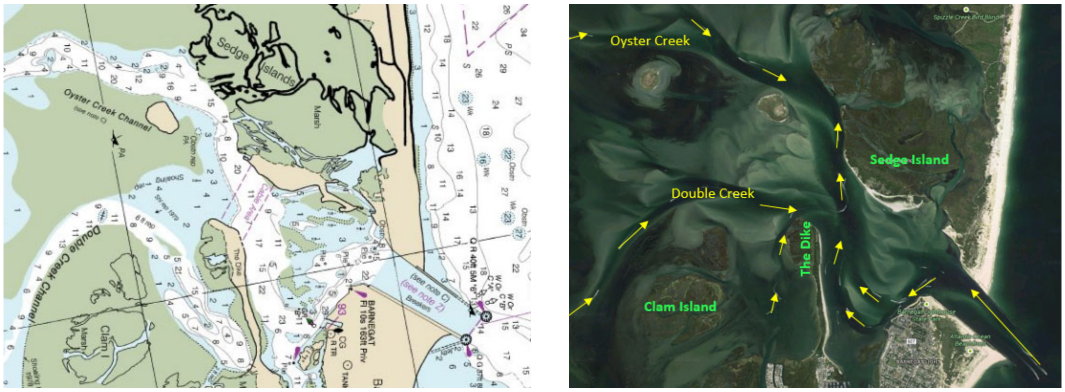

(a) NOAA Chart 12324 (b) Satellite RGB imagery

Figure 2.2: Overview of the Barnegat Bay Inlet. The yellow areas in 2.2(b) mark the traffic routes into Barnegat Bay through the two main channels: Oyster Creek and Double Creek.

of applications. In order to define the scale of the mapping products, the frequency of the imagery was evaluated as a function of the image resolution (Figure 2.3). It was concluded that the resolution of the IOCM products to be evaluated should be at 30 m, where 2 m products could be used as a control measurement.

LIDAR data were collected for Super Storm Sandy response both before and after the storm passed through the New Jersey area; see Figure 2.4 and Table 2.1 for collection details. The presence of multiple pre- and post-storm datasets in Barnegat Bay, and especially Barnegat Bay Inlet, were a primary driver for selection of this area for analysis.

2.2 Morphological and Shoreline Change

2.2.1 LIDAR Bathymetry

Storms on the scale of Super Storm Sandy can make significant changes to the morphological configuration of back bays and estuaries, in addition to the more recognized effects on large-scale structures. An initial, basic, method to address this is simply to consider multiple datasets within a common area, and examine the differences observed from appropriately configured bathymetric models constructed from remotely sensed data. A more complex, and less well addressed problem, however, is to determine when the changes observed from such methods are actually significant, rather than a product of the uncertainty of the measurement and processing methods.

For the study site selected, many overlapping datasets were available, and therefore the site is an ideal spot for data inter-comparison. Data were collected before and after Super Storm Sandy by the USGS using the EAARL-B system, by the U.S. Army Corp of Engineers (USACE) using the CZMIL system, by the National Geodetic Survey

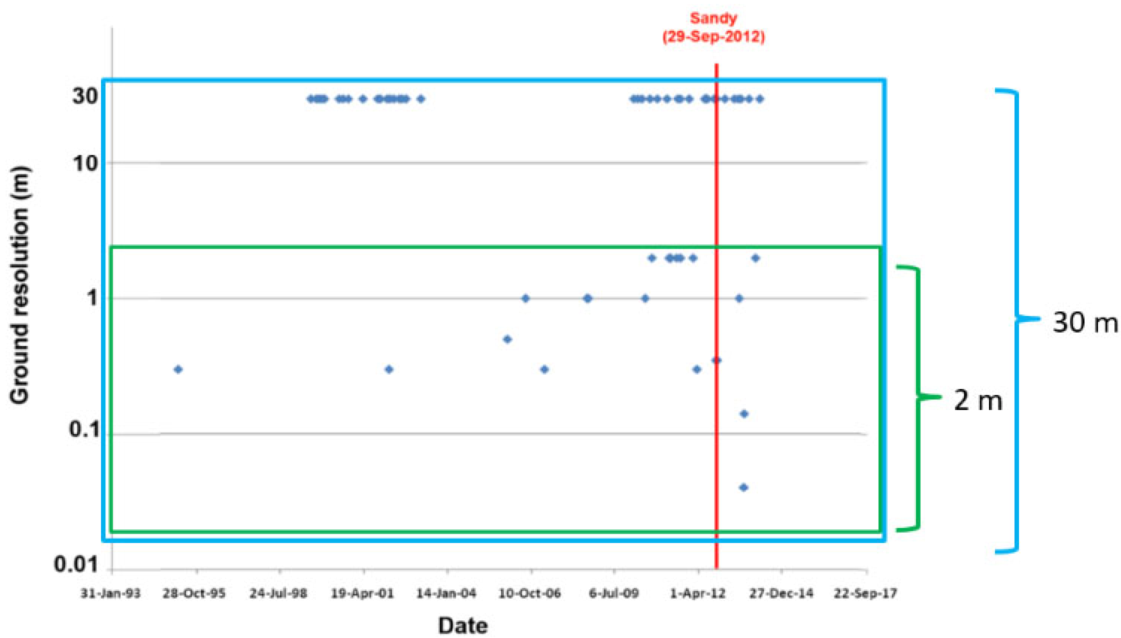

Figure 2.3: Scatter plot showing availability of imagery for the Barnegat Bay, NJ study site. The scatter plot is based on the ground resolution as a function of date with respect to the Super Storm Sandy event over New Jersey (October 29, 2012). The green and blue boxes shows all the datasets that will be used for 2 m and 30 m products, respectively.

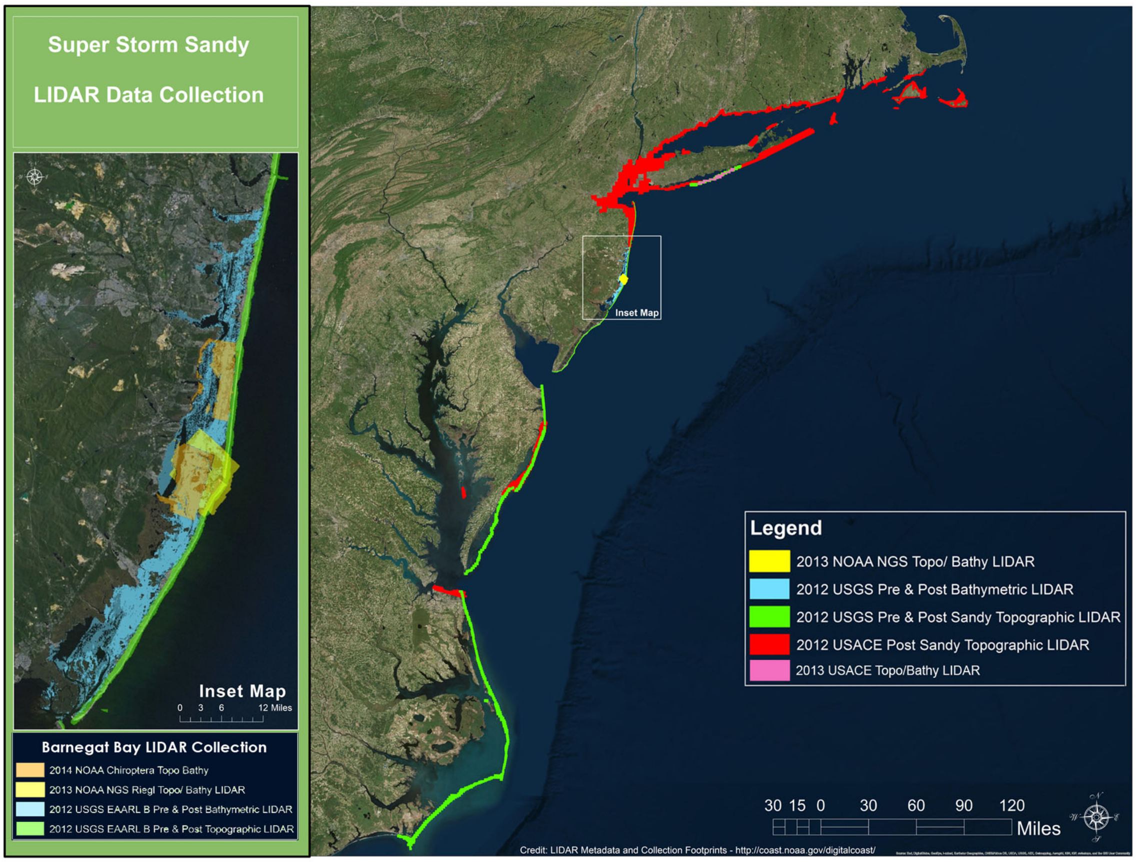

Figure 2.4: Super Storm Sandy LIDAR data collection overview. The collection includes data from Riegl VQ-820-G (NOAA National Geodetic Survey), EAARL-B (USGS), Chiroptera I (NOAA Office of Coast Survey), and CZMIL (U.S. Army Corps of Engineers) systems.

Dataset	**Type**	**Sensor**	**Date**	**Dist. Delay**	**Purpose**
USACE Post-Sandy LIDAR: CT	Topographic	Leica ALS60	Nov-2012	1 week – 1 month	Obtain LIDAR for digital elevation models and contours for use in damage assessment to USACE projects.
USACE Post-Sandy LIDAR: Eastern Long Island, NY	Topographic	Optech Gemini	Nov-2012	1 week – 1 month	
USACE Post-Sandy LIDAR: MA & RI	Topographic	Optech ALTM 3100	Nov-2012	1 week – 1 month	
USACE Post-Sandy LIDAR: MD & VA	Topographic	Optech Gemini	Nov-2012	1 week – 1 month	
USACE Post-Sandy LIDAR: NJ & NY	Topographic Bathymetric	CZMIL	Nov-2012	1 week – 1 month	Depict elevations above and below the water in the NY coastal zone.
USGS LIDAR: Post-Sandy (DE, MD, NC, NY, VA)	Topographic	Optech Gemini	Nov-2012	2 weeks – 1 month	Obtain MHW shoreline, dune crest (DHIGH) and dune toe (DLOW) elevation.
USGS LIDAR: Pre-Sandy (NJ)	Bathymetric	EAARL- B	Oct-2012	2 years	Pre- and Post-Hurricane Sandy highly detailed and accurate digital elevation maps of NJ coastline.
USGS LIDAR: Post-Sandy (NJ)	Bathymetric	EAARL- B	Nov-2012	2 years	
USGS LIDAR: Pre-Sandy (NJ)	Topographic	EAARL- B	Oct-2012	1 year	
USGS LIDAR: Post-Sandy (NJ)	Topographic	EAARL- B	Nov-2012	1 year	
USACE LIDAR: Post-Sandy Fire Island (NY)	Topographic Bathymetric	CZMIL	Sept-2013	1 year	Data collected to depict the elevations above and below water.
NOAA NGS LIDAR: Post Sandy Barnegat Bay NJ	Topographic Bathymetric	Riegl VQ820G	Sept-2013	6 months	Research efforts for testing and developing standards for LIDAR.
NOAA OCS LIDAR: Post-Sandy Barnegat Bay, Atlantic City, NJ	Topographic Bathymetric	Chiroptera I	03Apr14	4 months	Provide current surveys to update (NOS) nautical charting products following Sandy.

Table 2.1: Available LIDAR datasets in the Barnegat Bay area. Dates obtained from LIDAR source metadata and from http://www.lidarnews.com/PDF/LiDARMagazine-_WozencraftHurricaneSandy_Vol3No2.pdf and http://coastal.er.usgs.gov/hurricanes/sandy.

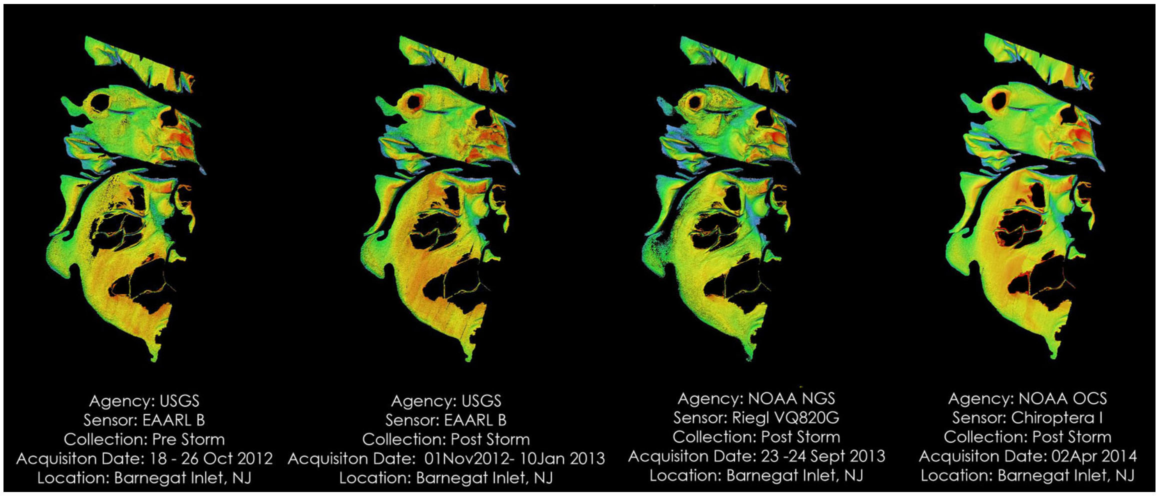

Figure 2.5: LIDAR bathymetry coverage from four LIDAR surveys over three years from three different LIDAR systems in Barnegat Bay Inlet, NJ.

(NGS) using the Riegl VQ-820-G system, and by NOAA's Office of Coast Survey (OCS) using a Leica AHAB Chiroptera I system. Bathymetric LIDAR datasets were canonicalized in the GIS sense, meaning organized to have a consistent footprint, resolution, and horizontal and vertical datum, etc., and clipped to areas of overlapping coverage in order to allow for comparison of erosion and deposition patterns (Figure 2.5). NOAA's VDatum tool was used to convert ellipsoidal heights to orthometric heights and finally to the Mean Lower Low Water (MLLW) tidal datum, which was used consistently as the vertical datum for this portion of the project. Data was gridded using Fledermaus (QPS, b.v., Zeist, The Netherlands) to the coarsest resolution of the four datasets, 2.5 m.

Comparison of results from multiple surveys in the region of Barnegat Bay Inlet over the course of three years (Figure 2.6) shows that the repeatability of surveys, including seasonal variability, is on the order of ± 0.1 m, and in some cases (Figure 2.8) better than this. A result like this provides a reference point to judge the scale of change due to Super Storm Sandy, and therefore makes it possible to conclude that in the section of Figure 2.6 from 50–450 m along the profile, there has been a significant change in bathymetry due to the effects of the storm. Similarly, Figure 2.7 shows an area near the barrier island breach at Mantoloking, NJ, where there has been significant change in bathymetry due to overwash effects. The converse is also true, meaning that the lack of change between 2013 and 2014 shown in Figure 2.6 shows that the system is now stable (in this region at least) after the effects of the storm, and is not recovering to its original configuration.

Availability of estimates of the distinguishable scale of change in any remotely-sensed dataset, as well as being scientifically important, allow for alternative processing techniques to be developed. For example, Figure 2.9 shows an estimate of volumetric change based on EAARL-B LIDAR data from the Mantoloking area. Previous

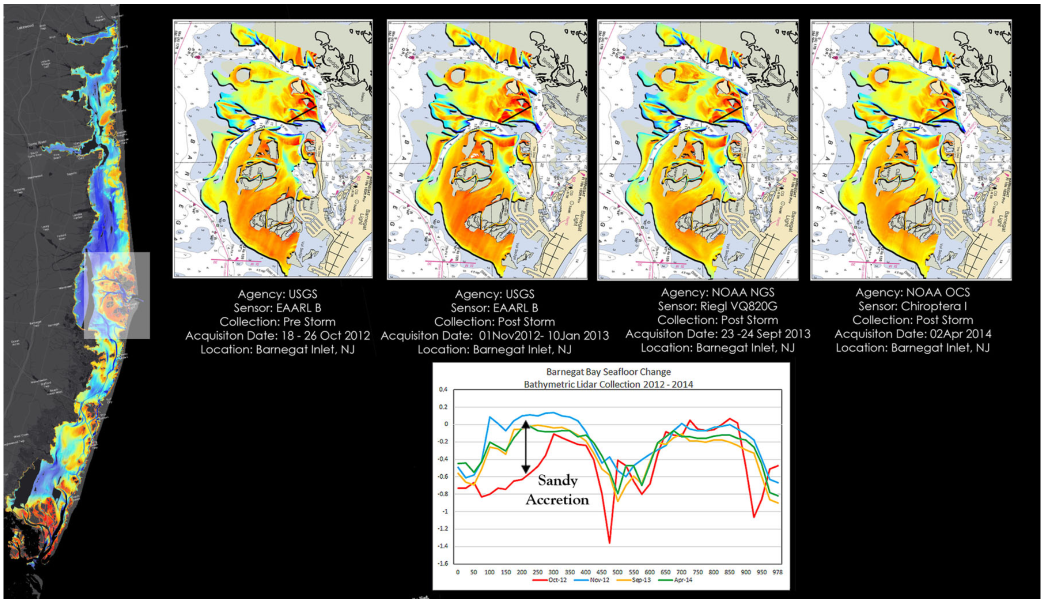

Figure 2.6: Depth as a function of distance for four bathymetric LIDAR collections over three years of data from three different LIDAR systems in the Barnegat Bay Inlet region. The change pre- and post-storm (red and blue lines) is clearly significant with respect to the self-noise of the systems.

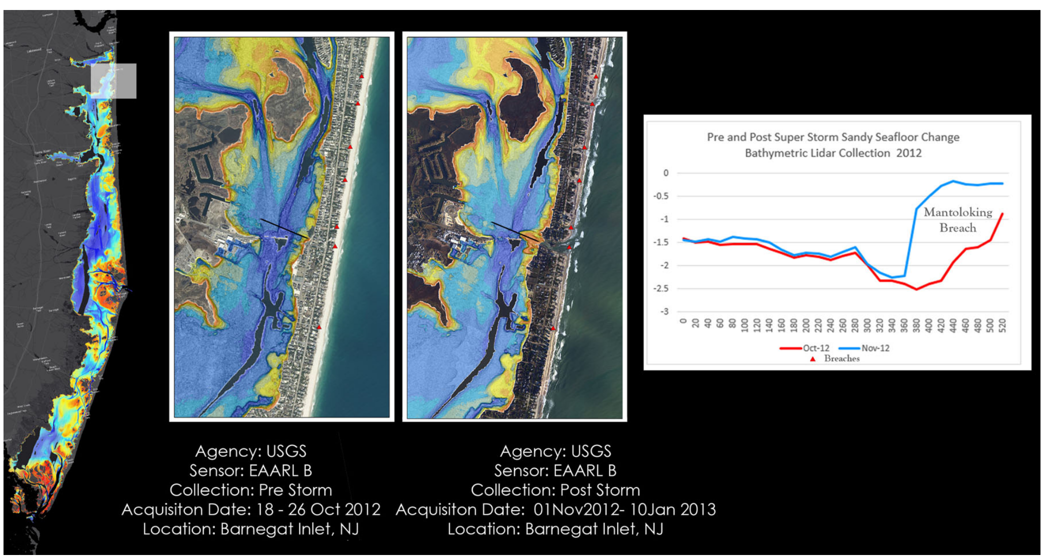

Figure 2.7: Depth as a function of distance for two bathymetric LIDAR collections over two years of data from the USGS EAARL-B LIDAR system in the Barnegat Bay Inlet region, focusing on the Mantoloking Breach.

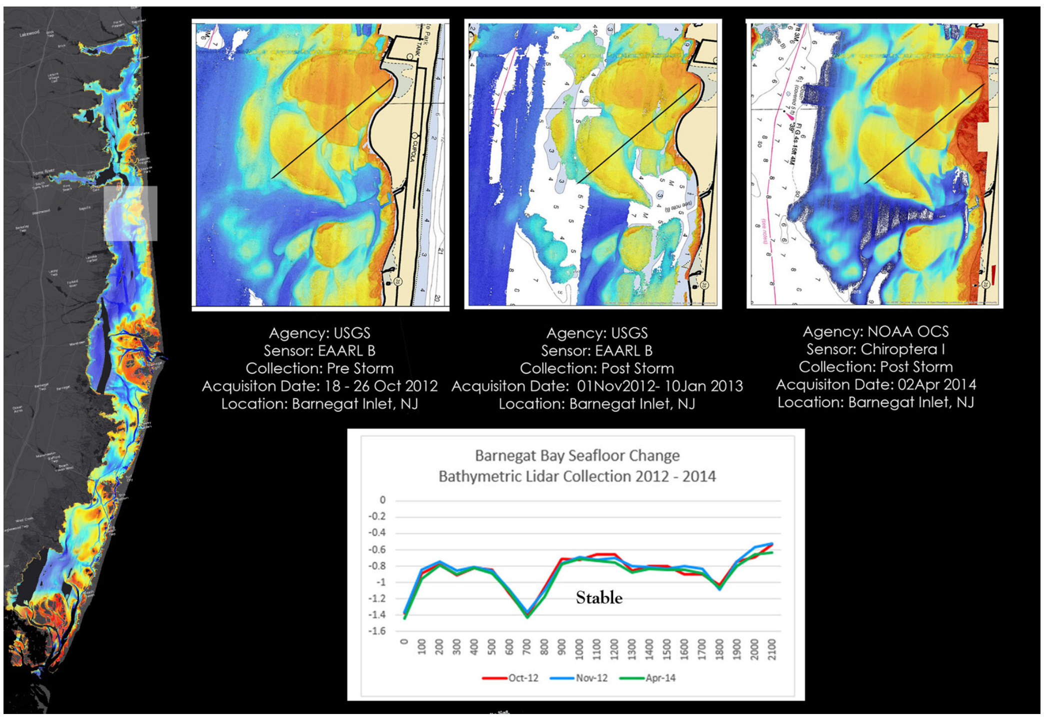

Figure 2.8: Depth as a function of distance for three bathymetric LIDAR collections over three years of data from two different LIDAR systems in the Barnegat Bay Inlet region. No Change is observed in the area before and after the storm.

techniques for change detection were usually limited to photogrammetric estimates of dune height and, thereby, of change. With reliable LIDAR data, estimates of volumetric effects pre- and post-storm can be readily constructed, showing that in an area of $120,600\,\mathrm{m}^2$, the total volume change was $34,900\,\mathrm{m}^3$, with $33,300\,\mathrm{m}^3$ deposited and $1,600\,\mathrm{m}^3$ eroded.

2.2.2 Satellite Imagery

Morphology

Although morphological changes are readily detected where there are multiple surveys before and after an event, it is often not the case that a pre-event dataset is available against which changes can be assessed: there is often no way to predict where an event will happen, and prioritization of survey effort means that many areas will not have up-to-date information prior to an event occurring. Satellite-derived bathymetric data is therefore an intriguing possibility: since satellites can regularly cover the same area of ground, it is possible to build up a time series of data from the area, and therefore monitor continuously (or at least regularly) for changes. This allows for an estimate of the magnitude of seasonal variability as well as any event-driven change. The key issue, however, is to establish a reliable estimate of the bathymetry in any given area from a single satellite image, so that change detection techniques can be applied.

The methods for establishing satellite-derived bathymetry, and the limitations and uses of such products, are still developing, and were developed further during the course of this work [7, 8]. Using data from Landsat 8 and WorldView-2, the key element of SDB is to compute a ratio of the signals in the blue and green bands of the imagery, matching the estimated depth to charted depth in order to provide the absolute vertical reference required for useful products. Auxiliary steps are required to ensure that the data is of sufficiently high quality for use, and to pre-process the data, so that the procedure becomes:

- **Pre-processing:** Satellite imagery is downloaded based on the geographic location and environmental conditions (e.g., cloud coverage and sun glint).
- **Water separation:** Dry land and most of the clouds are removed.
- **Spatial filtering:** "Speckle noise" in the imagery (particularly Landsat) is removed using spatial filtering.
- **Applying the bathymetry algorithm:** The bathymetry is calculated using the blue and green bands.
- **Identifying the extinction depth:** The optical depth limit for inferring bathymetry (also known as the extinction depth) is calculated.

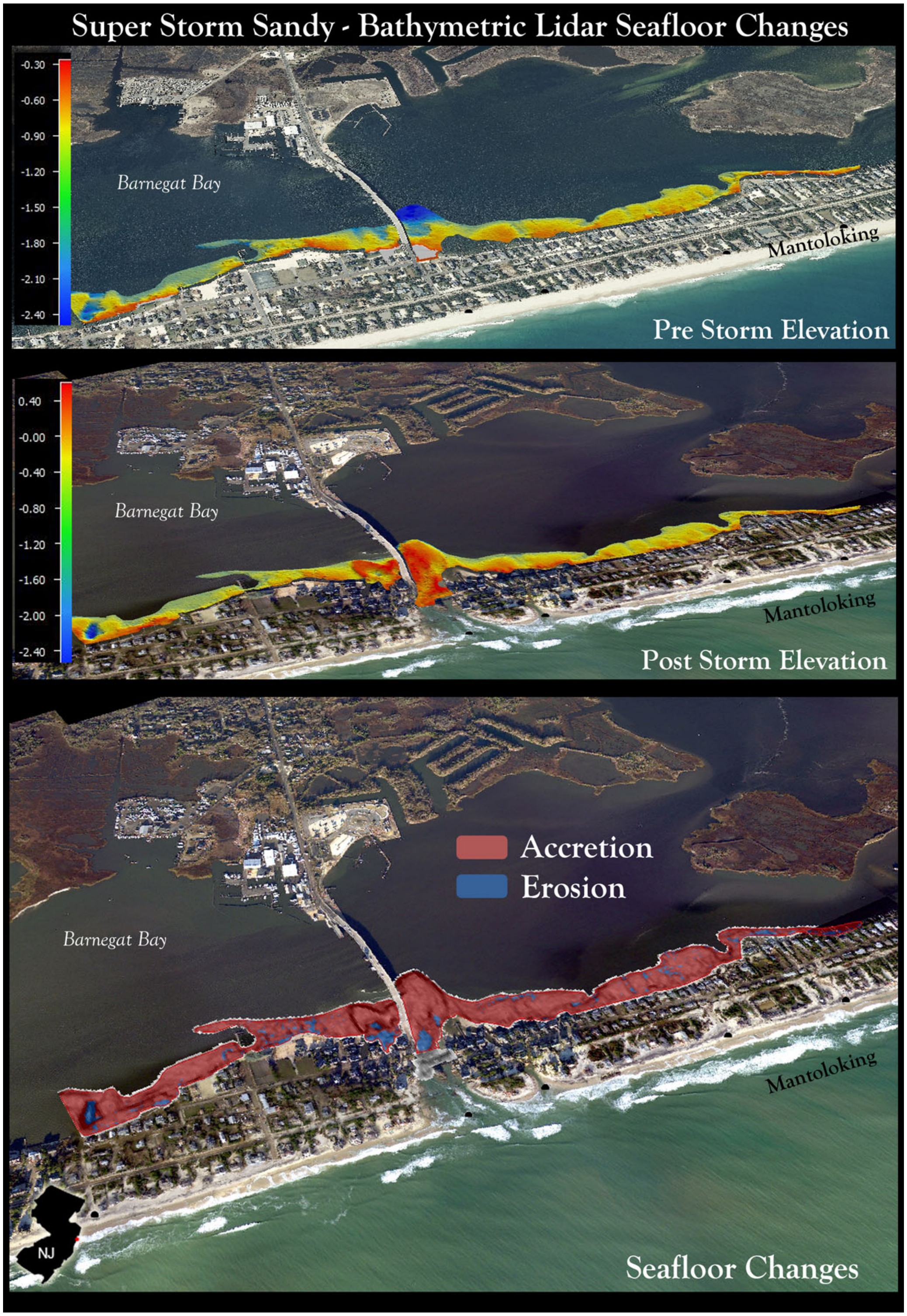

Figure 2.9: Super Storm Sandy seafloor changes from breaches and overwash in Mantoloking, NJ derived from topobathymetric LIDAR. The storm deposited $33,300\,\mathrm{m}^3$ of material.

- **Vertical referencing:** A statistical analysis between the algorithm values to the chart soundings references the Digital Elevation Model (DEM) to the chart datum.

The vertical referencing phase is a critical aspect of this technique, with modern survey data (either acoustic or LIDAR) being preferred. However, it is not always the case that such data exist where a SDB estimate is required, and therefore a procedure was developed [9] to provide a robust estimate of morphological change without requiring a high-resolution vertical referencing step. In this procedure, the first derivative of the bathymetry (i.e., the slope) was used to reduce the dependence on the vertical accuracy of the produt, with the bathymetry resulting from the algorithm being converted to a slope map, where only significant slopes (large slope values) that represent the edges of shoal features and banks of channels were retained, represented as contours. This was tested in the Barnegat Bay Inlet region, since during the early stages of the project, airborne LIDAR bathymetry (ALB) data was not available to provide vertical control—as would often be the case in the first response scenario for any storm—and the only vertical control was provided by hydrographic smooth-sheet soundings from the 1930s (or earlier). The results here (Figure 2.10) show that areas of significant effect were observed in the inlet area, but consistent with other findings, the remainder of the bay appeared to be more stable. A SDB map of slopes could therefore have a role to play in the early stages of a storm-response scenario as an approximate—but readily computable—estimate of change.

In any environment with natural variability in a particular parameter, having some estimate of the variability of that parameter is a necessary first step in understanding whether any significant change has taken place as the result of a storm event. As for the LIDAR techniques described previously, SDB can be used to identify seasonal variabilities in a region, with the significant benefit that a more consistent, and generally longer, time series of data is usually available. To demonstrate, and refine, these techniques for use in a storm response scenario, Landsat 8 satellite imagery acquired after Super Storm Sandy was processed to identify areas of morphological changes that were not related to this major storm event [10]. (No new WorldView-2 data, at high resolution, was available for the appropriate time period of 2015-01–2014-07.) Using the methods of [9, 10], all vegetated areas, dry land, and optically-deep areas were removed from the imagery and bathymetry for the remaining sandy/muddy areas were calculated at 30 m resolution. A slope map was derived from the bathymetry and the spatial differences between the slopes were used to identify the dynamic and stable areas.

From the analysis, seasonal and annual morphological changes (dynamic shoals) can clearly be identified within the bay (Figure 2.11). For example, the shoals on the eastern side changed with season, while the channels within the bay were stable, although their location was different from where they were charted. This demonstrates that the techniques developed could potentially be used prospectively to provide baseline information on seasonal variability, as well as being used for storm response.

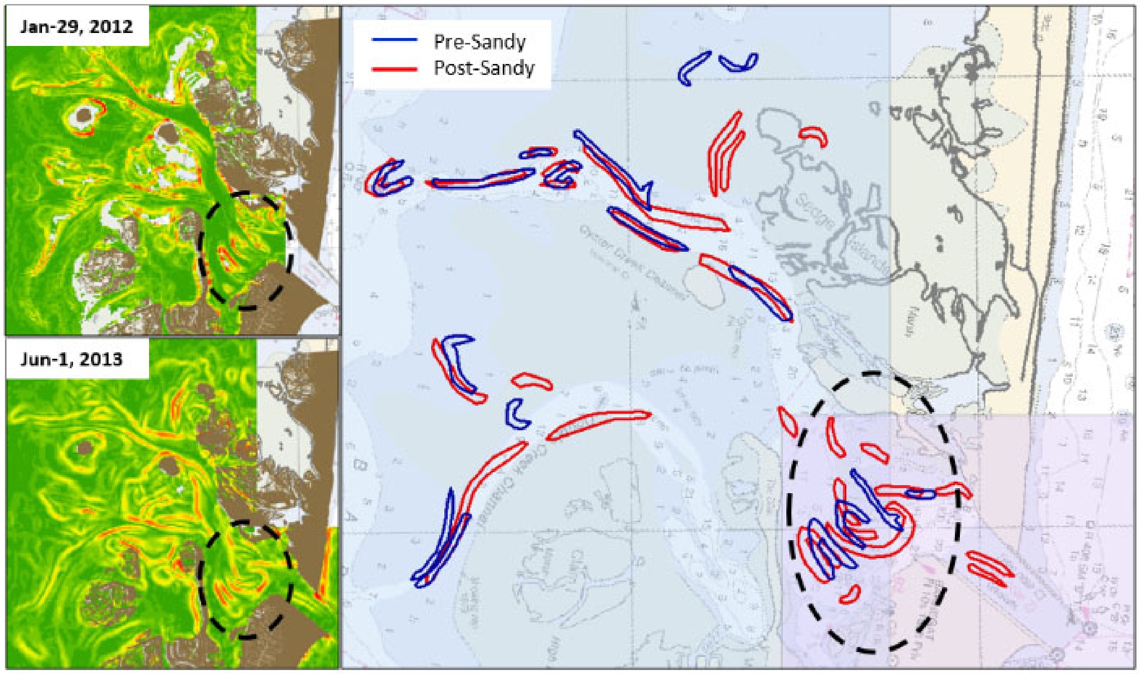

Figure 2.10: Preliminary results showing morphological changes at the entrance of Barnegat Bay Inlet pre- and post-Super Storm Sandy. The two images on the left are the slope maps from 2012-01-29 (pre-Sandy) and from 2013-06-01 (post-Sandy) acquired by WorldView-2 and Landsat 8, respectively.

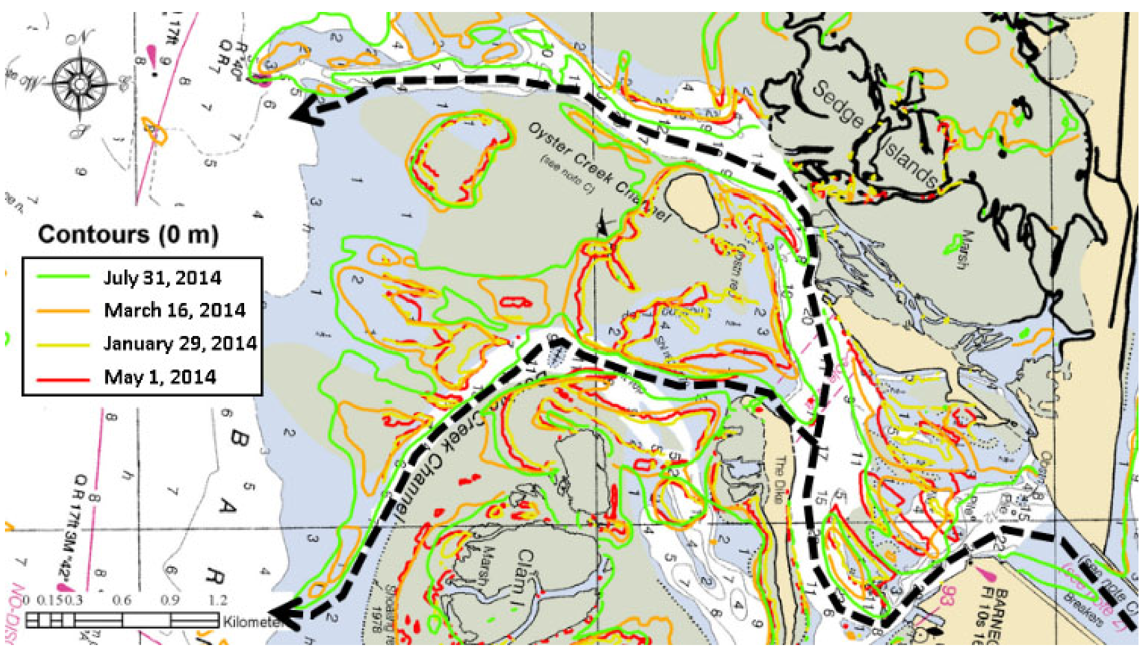

Figure 2.11: Seasonal changes in bottom morphology near Barnegat Bay Inlet during 2014, based on Landsat 8 imagery.

Shoreline Change

In the wake of a significant storm event, knowledge of changes to the shoreline are often high on the list of requirements for response and restoration events. Having a reliable method of estimating the change in shoreline and, again, determining whether it is significantly higher than the normal seasonal variability in any given area, is therefore important.

Using the USGS Digital Shoreline Analysis System (DSAS), a standard utility implemented within the ArcMap application framework [11, 12], as a starting point, a procedure [13] has been developed to assess the level of change in a shoreline, using linear regressions against the results of the same analysis applied to prior shorelines to determine the natural variability, or expected rate of change. The core concept is to estimate the distance from a known, fixed, baseline to the shoreline by projecting rays orthogonal to the baseline until they intersect with the shoreline. The variability between shorelines along each transect is then estimated and a regression model is used to estimate the mean rate of change, so that in the wake of a storm it is possible to determine whether any observed change is significantly different from the historical mean rate. The procedural steps are therefore:

- **Baseline selection:** Arbitrary baselines are selected for all candidate shorelines. The baseline are linear features located away from the land and shoreline.
- **Transect construction:** Perpendicular transect lines were constructed from the baseline to intersect with the candidate shorelines. In this study, transects were generated at an interval of 25 m or 50 m, depending on the shoreline.
- **Analysis:** Changes of distance between the baseline and shoreline are computed using DSAS.
- **Trend calculations:** The shoreline distances are processed in MATLAB to determine a regression line over the historical record.
- **Prediction:** The resulting regression lines are used for prediction of shoreline change. A root-mean-square error is used to assess the spread of mean predicted locations, allowing comparison of the observed location in post-storm imagery.

To illustrate this procedure, datasets from the Barnegat Bay Inlet region from as early as 1951 were recovered from NOAA's Shoreline Data Explorer (NSDE[2]), which includes an estimate of horizontal uncertainty, and the USGS' EarthExplorer archive (`http://earthexplorer.usgs.gov`) (Table 2.2). Shoreline change estimates were generated using the procedure outlined previously, resulting in estimates of change at five sites around the inlet (Figure 2.12). Pre-Sandy shorelines from 1995, 2002, 2007, and 2012 were used to estimate the historical trend at each location. Then, using linear

[2] `http://www.ngs.noaa.gov/NSDE`

Date	Collection	Horizontal Accuracy	Source	Notes
2013	2013-09-24	1 m or 5 m	NSDE	Post-Sandy
2012	2012-11-01	5.5 m	NOAA NGS	Post-Sandy
2012	2012-03-14 to 2012-04-16	5.5 m	EarthExplorer	Pre-Sandy
2007	2007-03-18 to 2007-05	5.5 m	EarthExplorer	Pre-Sandy
2001/2002	2001-07-21	4.3 m	NSDE	Pre-Sandy
1995	1995-03-29	5.5 m	EarthExplorer	Pre-Sandy
1951	1951-01-01	11.7 m	NSDE	Excluded

Table 2.2: Shorelines used for analysis example in Barnegat Bay Inlet, NJ.

Area of Interest	Average trend rate (m/yr)	Post-storm Rate (m/yr)
1 (inlet)	-6.94	-5.42
2 (inlet)	0.54	5.65
3 (inlet)	-2.70	-5.24
4 (beach face)	0.58	-42.0
5 (beach face)	2.54	-32.31

Table 2.3: Average trend rates of change prior to Super Storm Sandy (1995-2002) and the post-storm rate (Mar., 2012–Nov., 2012). Negative values indicate erosion, while positive values indicate deposition.

regression, the post-Sandy shorelines were compared to the predicted trend (with the associated uncertainty). The 1951 shoreline dataset was excluded from the regression because of the large gap in time period.

The analysis demonstrates that the bay-side sites (i.e., sites 1, 2, and 3) showed a slight accretion, whereas the ocean-side sites (i.e., sites 4 and 5) exhibited trends of erosion. The results (Figure 2.13; Table 2.3) indicate that the ocean-side sites were impacted by the storm, but the bay-side were within the erosion rates predicted using linear regression. Similar results were observed in the 2013 imagery over site 1. These results suggest that the Barnegat Bay Inlet region has not experienced further increased erosion (within the inlet).

While effective, these procedures would benefit from improved statistics and visualizations. An important caveat is that there is a potential difficulty in comparison of results derived from LIDAR data with those from imagery. In particular, it is possible that LIDAR-derived shorelines might not be at mean high water (MHW), unlike orthoimagery-derived shorelines. As a result, trends calculated with mixed datasets might generate an error in estimation of the extent of horizontal change, especially in areas with very shallow slope beaches [14].

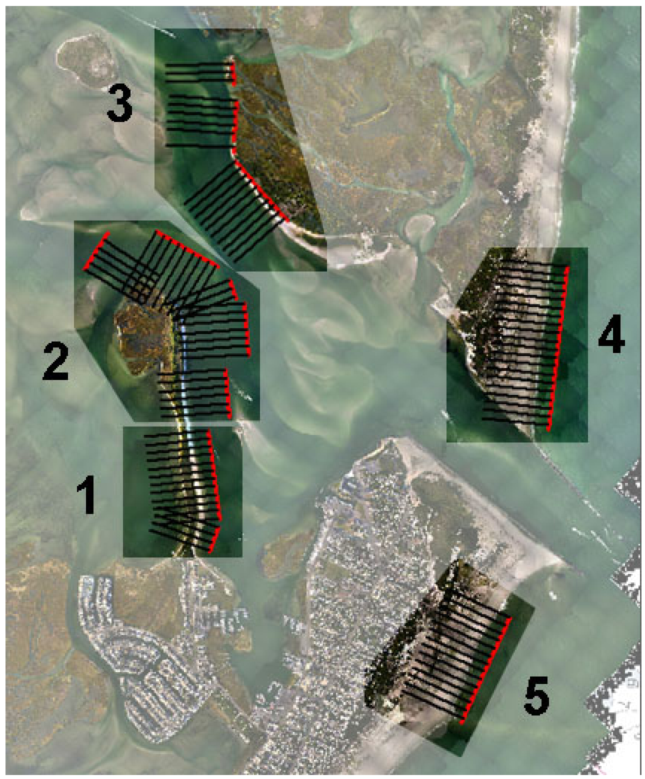

Figure 2.12: Study sites for shoreline change within Barnegat Bay Inlet, NJ.

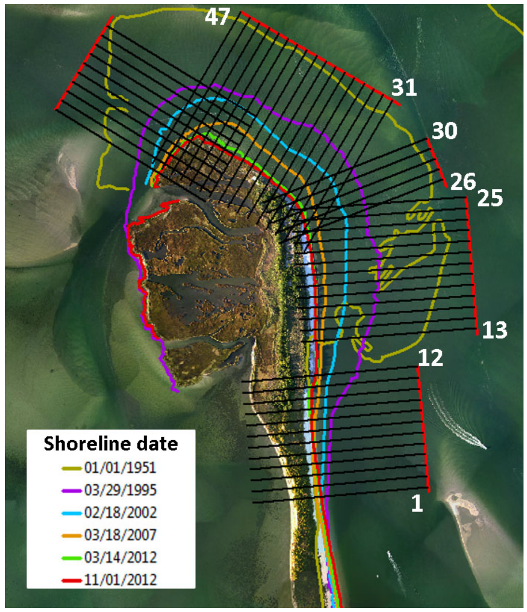

(a) Transect Line Numbers, Site 1

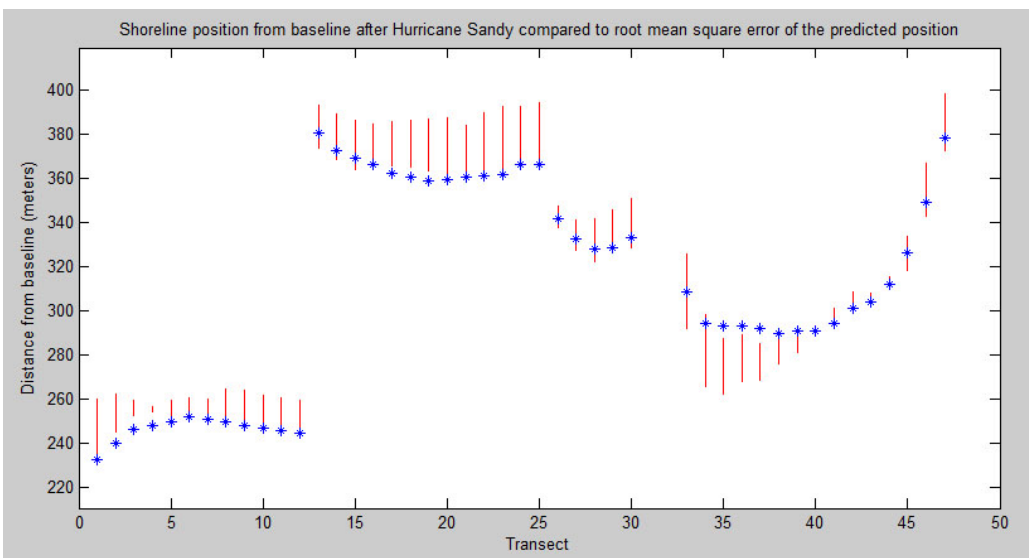

(b) Predicted Shoreline Locations (red) and observed (blue)

Figure 2.13: Estimate and prediction of shoreline at study site 1, Barnegat Bay, NJ. Red lines in 2.13(b) indicate the range of shoreline location predicted, while blue stars indicate the observed location in post-Sandy imagery. Stars that fall outside the range predicted show significant change.

2.3 Habitat Mapping

In the wake of a significant storm event, the focus is often, naturally, on the damage to the built environment, and restoring some vestige of normalcy to the people affected. However, damage to the environment, and particularly habitats in the near-shore, back-bays, and estuaries can be subtle, and long-lasting. Shallow-water habitats, such as eelgrass beds, can be critical to the health and well-being of the environment, since they can act as breeding grounds, provide shelter for some species, filter the water, and help to stabilize the sediment. Consequently, much effort has been expended during this project to address questions of how best to determine, evaluate, summarize, and communicate the effects of storms on shallow-water habitats.

The focus has been, in particular, on automatic, or semi-automatic methods to assess habitats, and how to estimate the natural variability that occurs over time, so that there is a baseline for assessing whether the change due to a storm has been significant. Automatic techniques are a significant departure from more traditional methods and processes, which are largely manual, and therefore subjective. However, automatic techniques, such as the Object-based Image Analysis (OBIA) methodology [15, 16] described below, can produce a finer-scale map which may lead to a greater overall accuracy in classification, allowing for a more detailed assessment of the impacts of storm events such as Super Storm Sandy. They are also less sensitive to the skill of the operator. Further, the OBIA methodology can produce an accurate habitat map in a fraction of the operational time and the methods can be applied to multiple datasets collected by multiple systems, possibly with modifications to the same basic rule-set to suit the different systems.

Habitat classification using remote sensing techniques is in general a complex problem. However, given the focus of this work on the area around Barnegat Bay, NJ, the emphasis here has been primarily on the detection, characterization, and description of submersed aquatic vegetation (SAV) using both LIDAR and satellite imagery data.

2.3.1 LIDAR Waveform Analysis

In addition to collecting information about the depth of water, some LIDAR systems are capable of recording the received waveform of the reflected light pulses. In addition to their use to estimate uncertainty of depths [17], shape parameters derived from these waveforms have the potential for habitat mapping applications, specifically for the assessment of submersed aquatic vegetation (SAV). Derivation of maps of SAV location from rapid-assessment remote sensing techniques such as LIDAR has significant benefit in the wake of a storm event, since it allows for efficient delineation of habitat status and, assuming that previous datasets are available, change detection.

Techniques for deriving such maps have been developed as part of the current grant. Preliminary work used Riegl VQ-820-G data collected in Barnegat Bay by NOAA's National Geodetic Survey (NGS) in September, 2013 (Figure 2.14). Because

Figure 2.14: Riegl LMS-Q680i and VQ-820-G LIDAR systems (left) operated by NOAA's National Geodetic Survey (NGS) in the Sandy impact area; USGS EAARL-B used to acquire data immediately before and after Sandy made landfall. Images courtesy of NOAA and USGS.

the Riegl VQ-820-G was not configured to store full-waveforms (i.e., time series representing backscattered signal strength) during the Barnegat Bay acquisition, it was not possible to perform custom waveform processing with the NGS topo-bathy lidar data set. However, this system does automatically compute and store two waveform features during data collection: Riegl reflectance and pulse shape deviation [15, 18]. The former refers to return waveform peak amplitude, normalized using Riegl laboratory calibration data and expressed in decibels, while the latter is a measure of the difference between the received signal and a stored reference pulse.

Through collaboration with the University of Vermont's (UVM) Spatial Analysis Laboratory (`http://www.uvm.edu/rsenr/sal`), the project team developed and tested an OBIA approach to habitat classification using the VQ-820-G Riegl reflectance and pulse shape deviation data, along with the LIDAR-derived bathymetry and Applanix DDS digital aerial imagery, which was simultaneously acquired by NOAA NGS. A final habitat map for a $\approx 18\,\mathrm{km}^2$ project site was produced in eCognition (Figure 2.15). Using ground truth data acquired by the project team in October, 2013 (Figure 2.16), a classification accuracy assessment was then performed on this habitat map. The overall classification accuracy was determined to be 85%, while users accuracies varied from 69% to 100%, and producers accuracies ranged from 73% to 100% [15]. The results of this phase of the project supported the conclusion that Riegl VQ-820-G

Parameter	Manual - OBIA	Chiroptera - Riegl
Number of Patches	0.06	0.19
Mean Patch Size	0.26	0.41
Patch Size Std. Dev.	0.41	0.41
Mean Patch Edge	0.41	0.41
Mean Shape Index	0.41	0.13
Perimeter to Area Ratio	0.25	0.02

Table 2.4: Mann-Whitney U test statistic p-values for landscape metrics derived from classification maps created from manual classification and OBIA methodologies (first column) and for OBIA with the same rule set applied to Riegl and Chiroptera datasets (second column).

data, including the auto-generated waveform features, are advantageous for benthic habitat mapping in the region impacted by Super Storm Sandy.

A common question with techniques of this kind, however, is how they compare with previous methods, and how well they adapt to different areas, and extend to different measurement systems. To investigate the limits of applicability of these systems, the rule set that was developed in eCognition using the Riegl VQ-820-G was compared to a manually classified dataset (Figure 2.17) using imagery only—the conventional methodology—and then applied to bathymetry, LIDAR reflectance, and aerial imagery collected by the Leica AHAB Chiroptera system in an effort to assess the efficacy of the rule set across LIDAR systems (Figure 2.18). The same rule set was finally used to classify habitat from an additional Chiroptera data set that was collected in a different area of Barnegat Bay (Figure 2.19). No significant differences, with the exception of patch-perimeter to area ratio, in the spatial extent of the classified habitat were found between LIDAR systems (Table 2.4). Patch-perimeter to area ratios were greater in the classification from the Chiroptera data, indicating that while the total habitat surface area is the same between the LIDAR datasets, the habitat patches themselves are smaller in the Chiroptera dataset. It is likely this difference is due to natural seasonal expansions and contractions of eelgrass beds as the Riegl data was collected in June 2013 while the Chiroptera data was collected in October 2014. Minor changes to the rule set needed to be made when classifying habitat using different LIDAR systems. This was also found to be true even when classifying habitat from two different data sets collected by the same Chiroptera system. While each individual rule remained in the same order, the parameters within each rule needed adjustment based on the individual values collected by each system [16].

As with the other techniques developed during this project, knowledge of the natural variability of the habitats being considered is essential if the changes observed in the wake of a storm event are to be assessed: if the changes are within the scope of the natural variability, then the observed change might be simply the normal change in density over time. In order to demonstrate the scope for the techniques

Figure 2.15: Benthic habitat map for the Barnegat Bay Inlet flood tidal delta complex created using NOAA NGS Riegl VQ-820-G data (including auto-generated waveform features), Applanix DDS digital aerial imagery, and an object-based image analysis approach in eCognition [15].

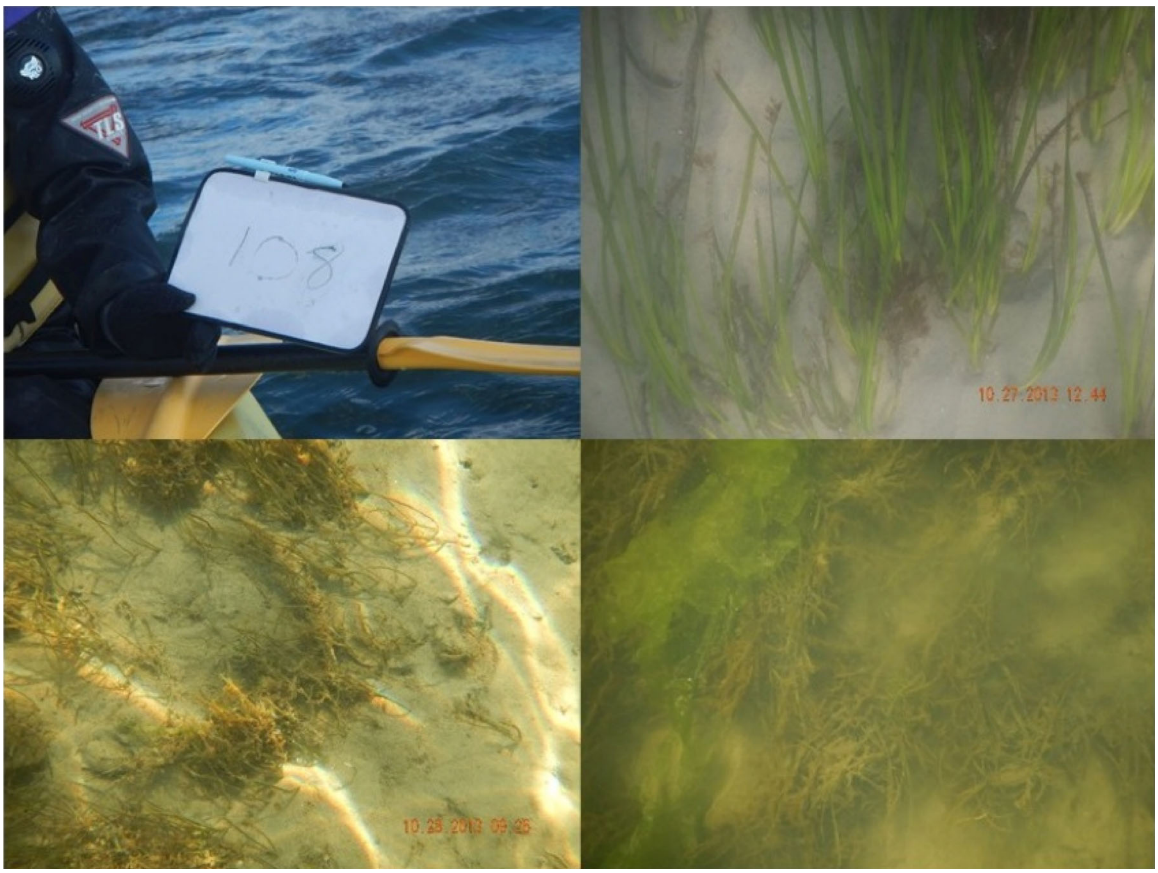

Figure 2.16: Reference data acquired in Barnegat Bay in October, 2013, for assessing the classification accuracy of habitat maps generated from LIDAR and imagery. The majority of the fieldwork was performed in shallow water from kayaks.

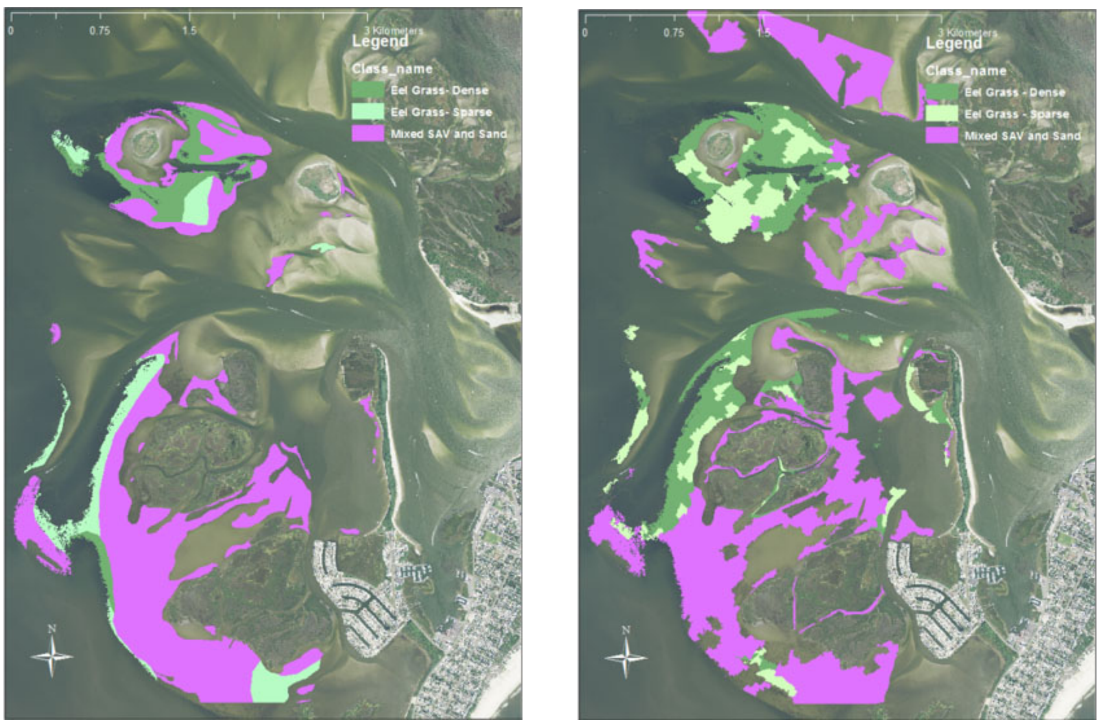

(a) Manual classification (b) OBIA classification

Figure 2.17: Habitat classification of Barnegat Bay Inlet generated from imagery (left) and Rielg lidar and imagery (right).

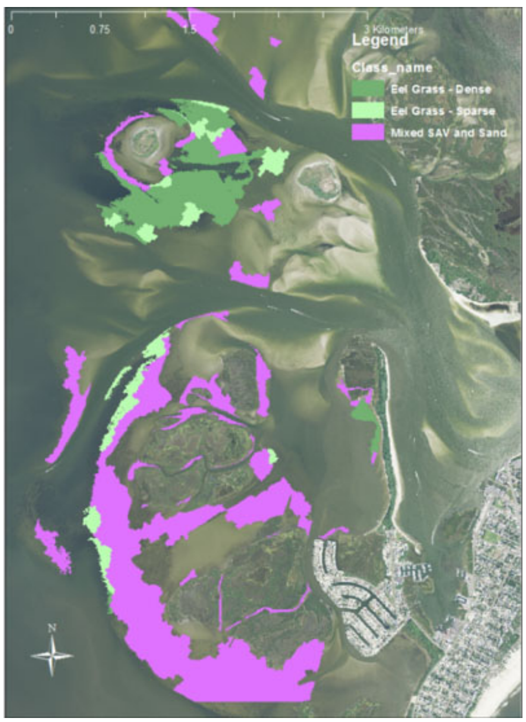

(a) Chiroptera imagery and LIDAR

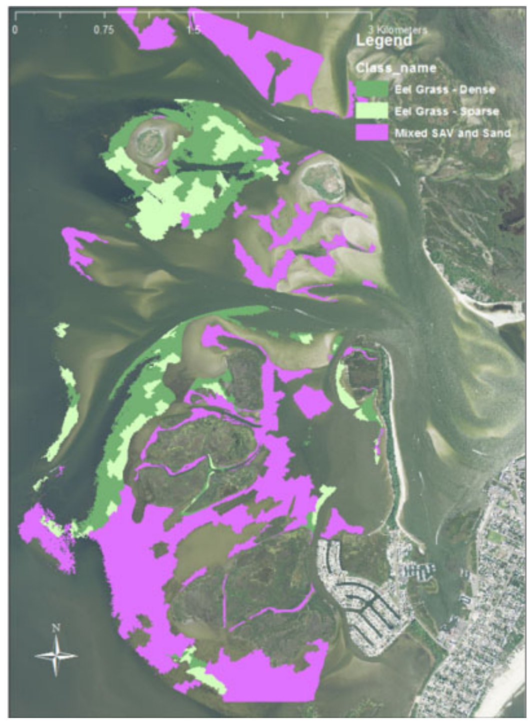

(b) Riegl imagery and LIDAR

Figure 2.18: Habitat classification of Barnegat Bay Inlet generated from Chiroptera LIDAR and imagery (left) and Riegl LIDAR and imagery (right).

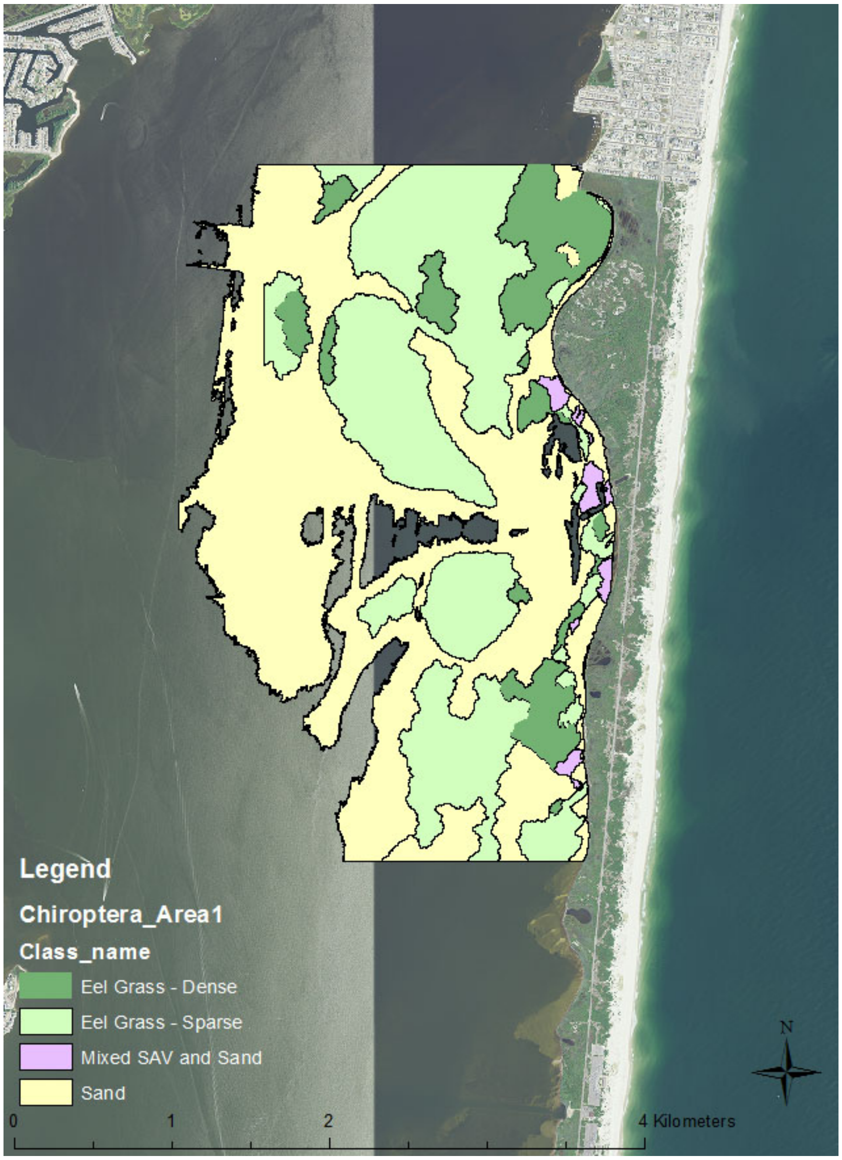

Figure 2.19: Classification of habitat of an area north of Barnegat Bay Inlet from topo-bathy LIDAR data collected by NOAA's AHAB Chiroptera system.

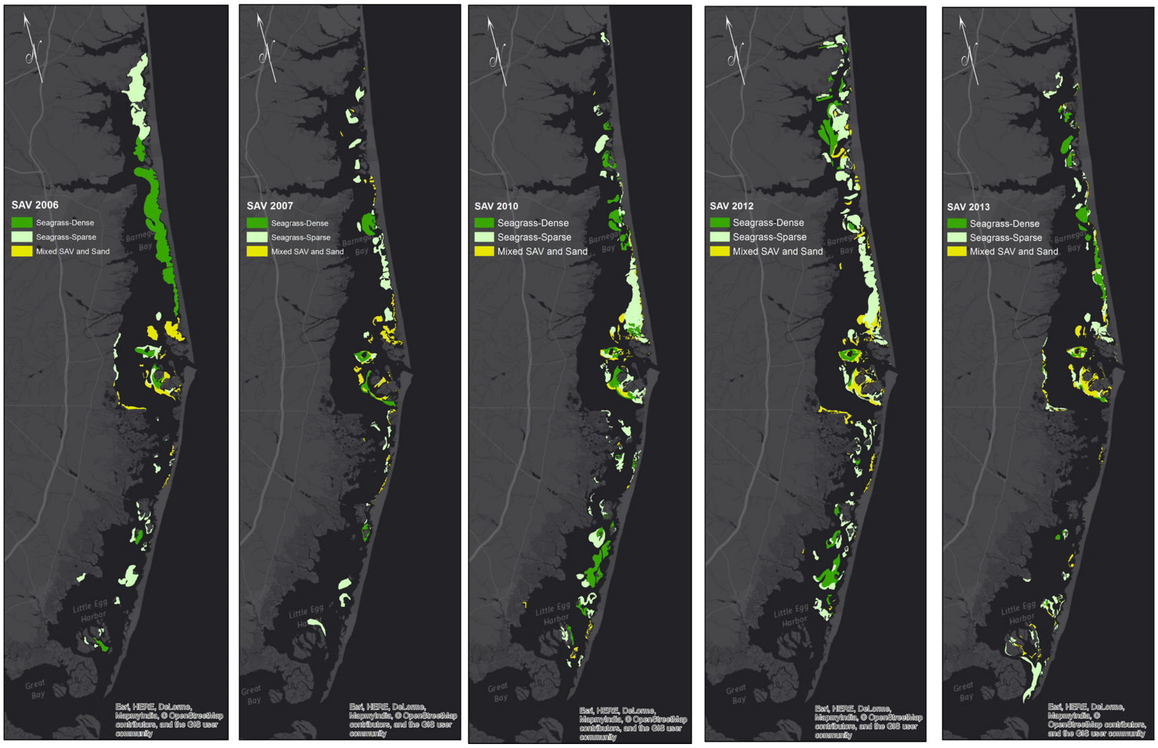

Figure 2.20: Time-series of manual classification of seagrass and mixed SAV and sand cover between 2006 and 2013.

developed in this regard, manual classification of dense and sparse seagrass as well as mixtures of SAV and sand were implemented for data collected between 2006 and 2013 using orthophotos collected by the state of New Jersey and the National Agricultural Imagery Program (NAIP; Figure 2.20). The remotely-sensed and manually classified 2006–2013 trend map suggests a decline in seagrass cover, particularly at the southern portions of Barnegat Bay. The June 2012 and 2013 field campaigns conducted for this project corroborated the remotely-sensed results indicating the presence of seagrass along the northern portion of Barnegat Bay and Barnegat Bay Inlet. Further, the remotely-sensed monitoring trend indicated a decline in the area of dense seagrass in 2013 compared to 2006. Differences in image quality and the seasonal period of image acquisition may account for the differences in the mapped area and in the apparent thinning of seagrass density as imagery for 2006, 2010, and 2013 were acquired in the growing season (July and August), while the 2007 and 2012 surveys were acquired earlier in the season (March and April).

These maps were then compared to earlier base GIS layers of SAV identified by the Center for Remote Sensing and Spatial Analysis (CRSSA), Rutgers University. Preliminary results indicate that SAV cover is temporally variable with a noticeable decadal decline in SAV from 1968 to 2013, specifically with seagrass (Figure 2.21). It appears that the decline in seagrass is not confined to one particular region, but

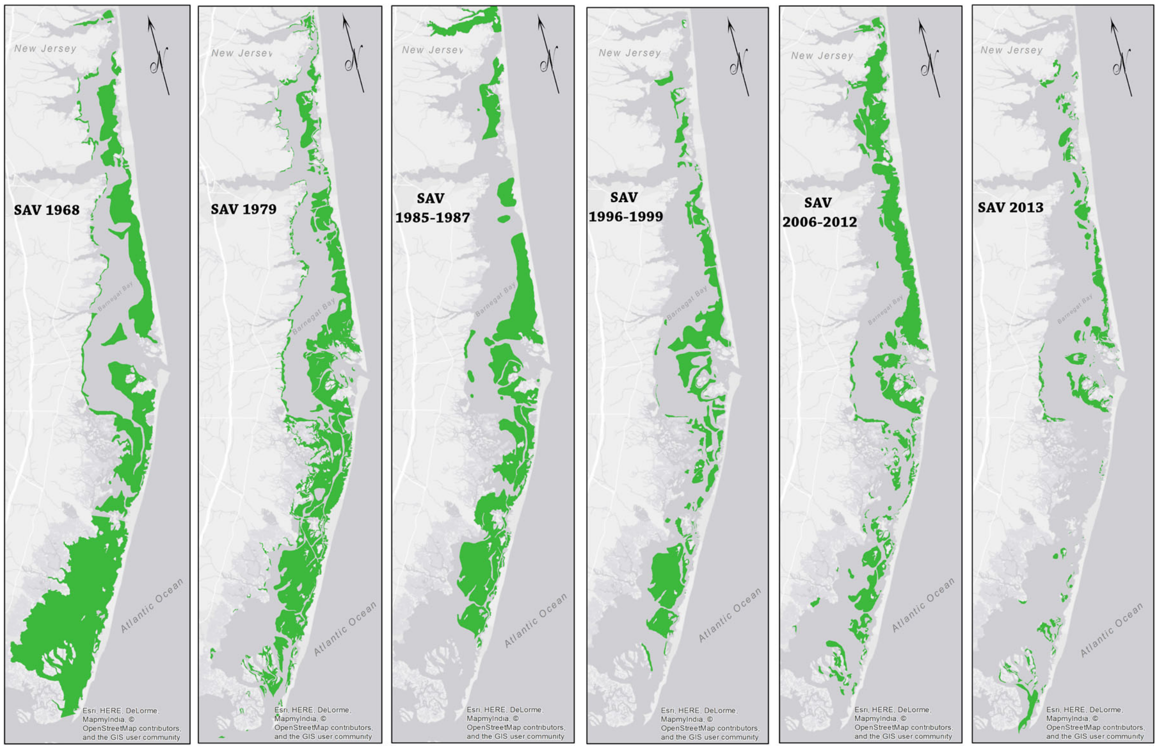

Figure 2.21: Temporal maps displaying SAV coverage from 1968 to 2013. Maps for 2006–2012 and 2013 were manually classified from orthophotos that were collected by the state of New Jersey. SAV from 1968 to 1999 were identified and analyzed by the Center for Remote Sensing and Spatial Analysis, Rutgers University.

has occurred throughout the entire bay. These results are consistent with previous studies demonstrating decadal loss of seagrass habitat (e.g., [5, 19–22]).

It therefore appears that the techniques developed for this project are sufficiently sensitive to pick up natural variabilities in the SAV distribution in Barnegat Bay, such that an analysis like this could be used to provide a baseline for a given area against which changes due to a storm event could be judged.

In order to extend these results, access to a system that stores full waveforms was required. The USGS EAARL-B topo-bathy lidar system (Figure 2.14) [23] has this feature [24], and was used by the USGS to collect both pre- and post-Sandy data in Barnegat Bay just days before Sandy and again within a week after the storm made landfall [25, 26], affording unprecedented opportunities for change assessment. Through work with David Nagle (USGS) and Wayne Wright (NOAA NGS), waveform feature extraction algorithms developed previously [17] were implemented in ALPS (Airborne LIDAR Processing System), the EAARL-B processing software. These algorithms were then used to output waveform feature files for all of Barnegat Bay in both the pre- and post-Sandy data.

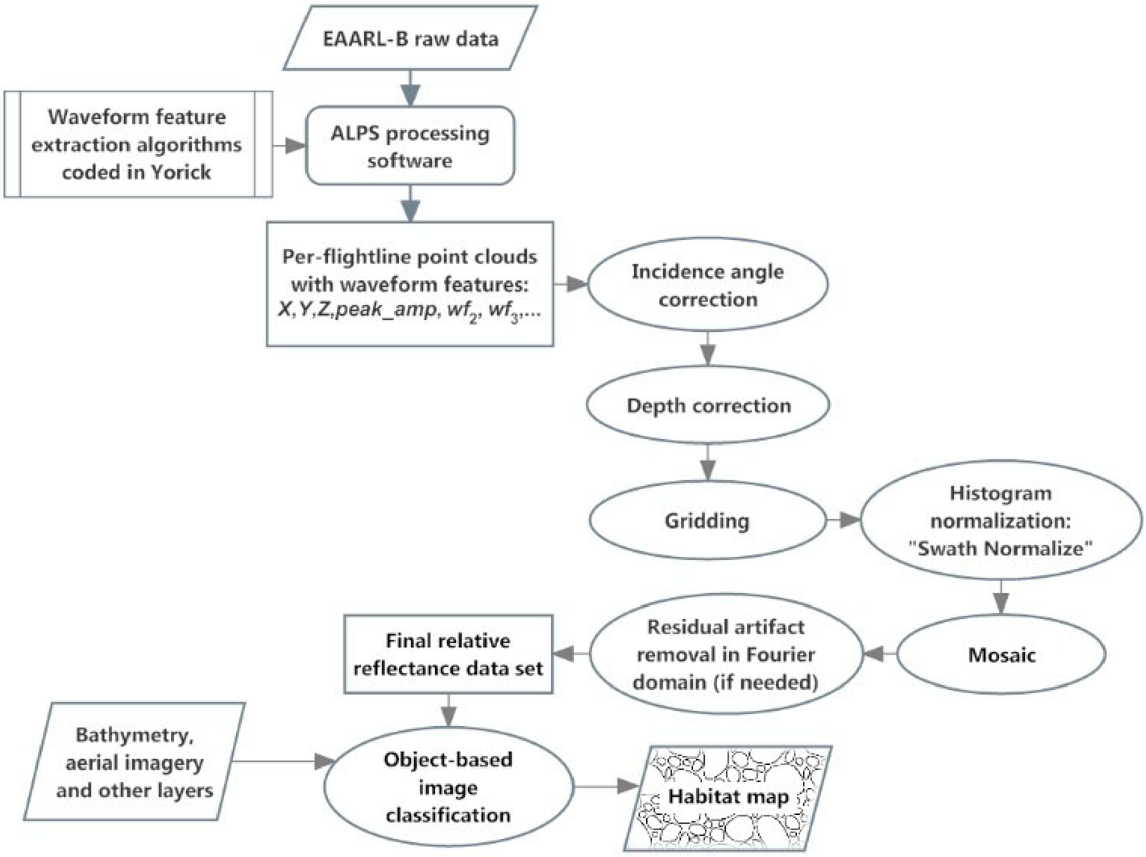

Figure 2.22: Workflow for seafloor relative reflectance mapping with the EAARL-B LIDAR [26].

The EAARL-B system is unlike other LIDAR systems in that it does not use a circular scan pattern or fixed forward tilt angle to maintain a nominally-constant incidence angle on the water surface. Instead, the system scans back and forth, passing nearly through nadir. This scan pattern necessitates a robust incidence angle correction algorithm to compensate for the great variation in waveform features as a function of incidence angle. New algorithms and workflows for applying corrections for depth and incidence angle to bottom return peak amplitude in order to generate seafloor relative reflectance images [26] were then developed. The final workflow is illustrated in Figure 2.22, while Figure 2.23 shows the results of applying these procedures to generate seafloor relative reflectance imagery in the Barnegat Bay Inlet study site. Development of these features can allow EAARL-B data to be used with similar methods as developed for the Riegl VQ-820-G.

Practical application of the algorithms developed through this project is an important part of the work, since a parallel program of work is currently under way in the IOCM Center at the NOAA-UNH Joint Hydrographic Center. The algorithms and procedures developed here have been transferred to the IOCM Center, where work

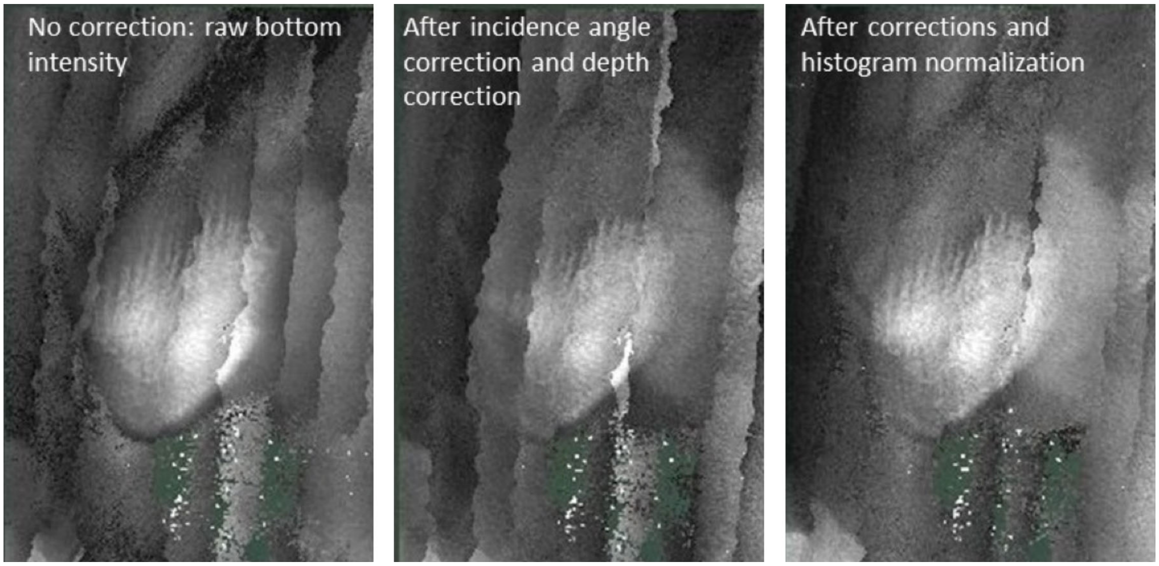

Figure 2.23: Example of applying the procedure illustrated in Figure 2.22 to generate seafloor relative reflectance imagery in Barnegat Bay.

is now under way to extract waveform features for Barnegat Bay Inlet. These new software and procedures could be applied to future storm events to map and assess change. Specific outputs include: new procedures for benthic habitat mapping with NOAA NGS's Reigl topo-bathy LIDAR system; new software and procedures for waveform feature extraction from the EAARL-B; and eCognition rule sets that can be used in future projects and possibly adapted for use with data collected with other sensors.

2.3.2 Satellite Imagery

As with morphological change detection (Section 2.2), satellite-derived measures of habitat potentially have the significant advantage of a more consistent time series, which makes it possible to provide finer time resolution for assessment of historical rates of change. In turn, this makes it possible to provide better calibration for expected rates of change against which to compare any potential storm-induced changes. Consequently, a procedure for determining SAV distribution (including both macroalgae and seagrass) using satellite multispectral imagery (MSI) was developed with the overall goal of being able to demonstrate the detection of a change in SAV coverage before and after Super Storm Sandy.

The procedure was built around satellite imagery from Landsat 8 and WorldView-2. Preliminary SAV maps were created over the Barnegat Bay Inlet area using the following steps [27]:

- Band-ratio index algorithms were applied to the imagery: blue/green for satellite derived bathymetry (SDB) and a green/red band ratio to determine the location of optically deep waters, including deep channels of the inlet.

- Dry land and optically-deep waters were removed from the imagery.
- The green band in the satellite imagery was used as a condition to separate areas of vegetation from those of sandy/non-vegetated regions depending on the return strength.
- The resulting vegetated areas were classified based on vegetation density.

The preliminary version of this algorithm was focused on detecting presence of SAV (Figure 2.24) and demonstrated changes between September, 2010 and September, 2014. However, using only the green band it is difficult to determine vegetation density or other properties of the SAV, mainly due to the spatial and spectral resolution limitations of the available sensors. The algorithm was therefore extended to estimate vegetation density.

In this extension, the red, green, and blue image bands are treated as a vector in three dimensional space, and the angle between any test vector and a vector from an area of known density is used as a discriminator in a supervised classification. The training sets are developed from areas identified through an unsupervised classification using an ISODATA algorithm [28, 29], field work, and optical properties of the satellite imagery, and the spectral signature of the non-vegetated bottom (i.e., the background signature) was used to normalize the results (Figure 2.25), converting the angle values that the algorithm natively produces to a density proxy.

To provide some assessment of the accuracy of the method, coverage and density of the SAV mapping results from satellite imagery were compared to the results of a Rutgers University survey from 2009 (Figure 2.26 [5]). The overall accuracy of the classification was assessed using a confusion matrix approach, and ranged between 75% and 88% (Table 2.5). In the first column, the accuracy assessment results considered sparse vegetation regions (based on Lathrop and Haag [5]) were counted as part of the SAV. In the second column, the accuracy assessment results did not consider the sparse vegetation regions as vegetation (i.e., counting them as "bare"). Although the satellite imagery was collected four to five years after the Rutgers University habitat mapping (which was based on aerial imagery analysis acquired on June 28, July 7 and August 4, 2009), the accuracy assessment is good. Given that the imagery used for comparison was not collected at the same time as the reference data, it is possible that some of the variability in accuracy is attributable to seasonal changes.

2.4 Coastal Engineering Index Support

A priority for work in this project was to ensure that the products derived were suitable for inclusion in downstream processing. Few of the products are end results in themselves: most will be input components for more integrative analyses. A particular example of this is the concept of Coastal Engineering Indices (CEI) [30], which are intended to provide comparable combined indices for engineering, environmental, and human use, which provide a snap-shot of coastal conditions. CEIs are also intended

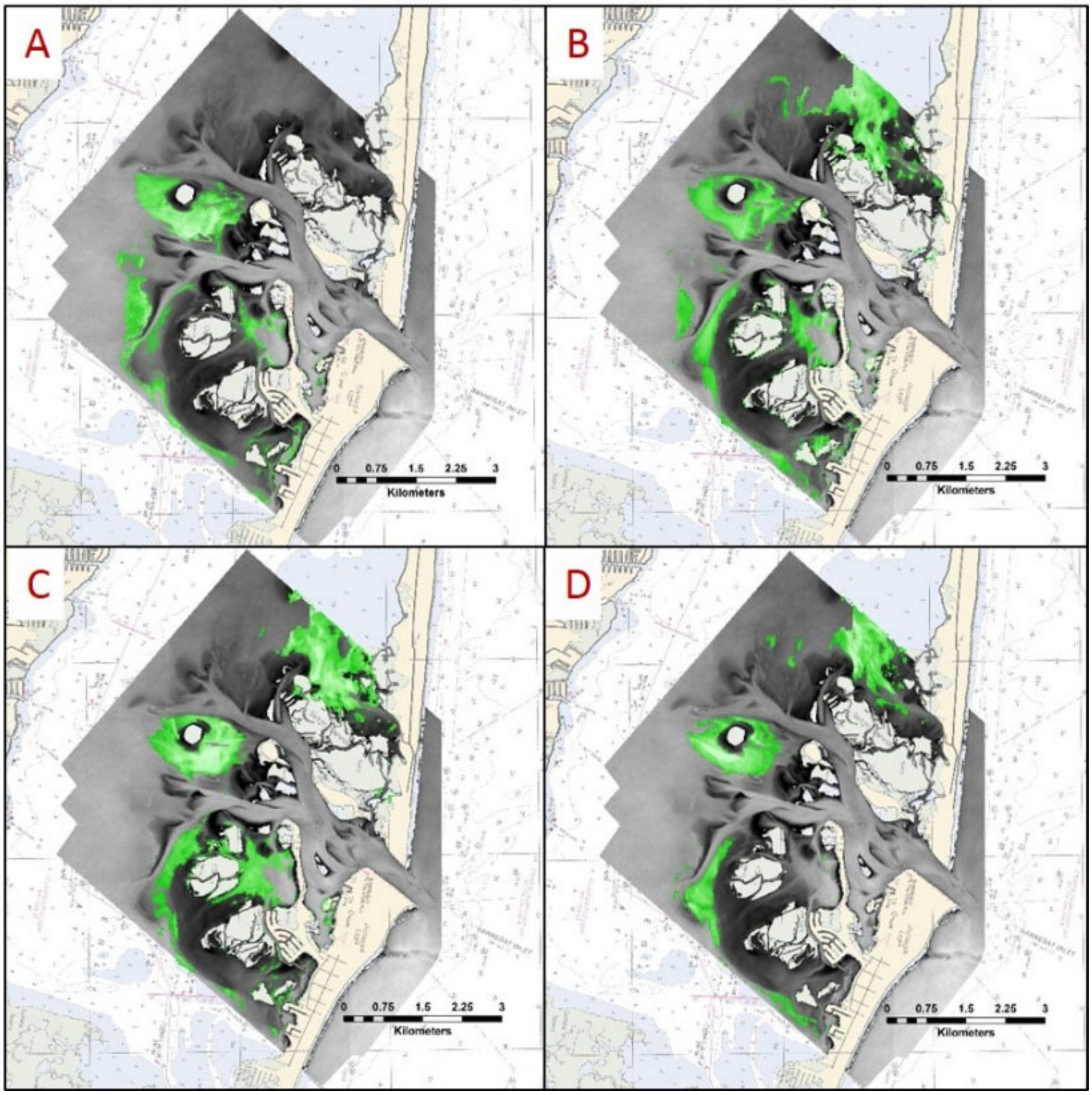

Figure 2.24: Preliminary results of vegetation mapping around Barnegat Bay inlet, NJ: (a) 2011-05-01 (WV-2); (b) 2013-06-01 (Landsat 8), (c) 2013-08-20 (Landsat 8); and (d) 2014-06-29 (Landsat 8). SAV regions are shown in green and are overlaid onto satellite-derived bathymetric image and a NOAA chart. This series of images shows SAV extent and changes from (a).

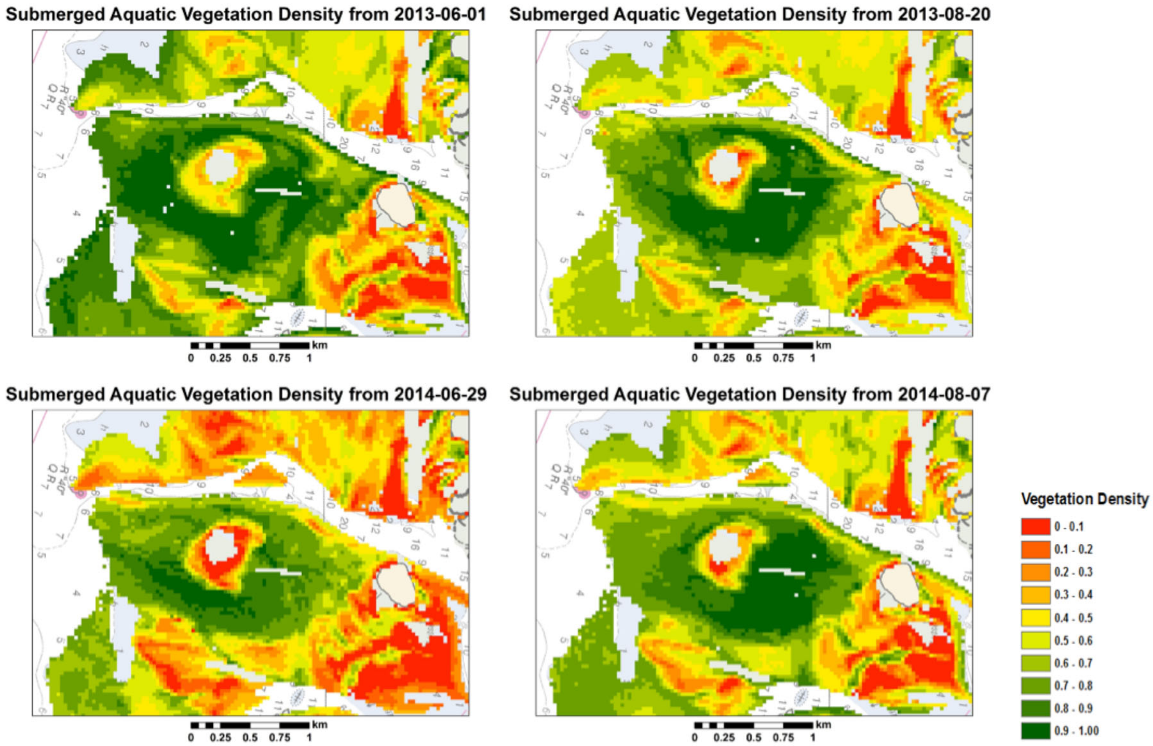

Figure 2.25: SAV density using Landsat 8 imagery from four different time periods in Barnegat Bay Inlet, NJ: (a) 2013-06-01; (b) 2013-08-20; (c) 2014-06-29; and (d) 2014-08-07. Density values range from 0% (red) to 100%, normalized to 1.0 (green).

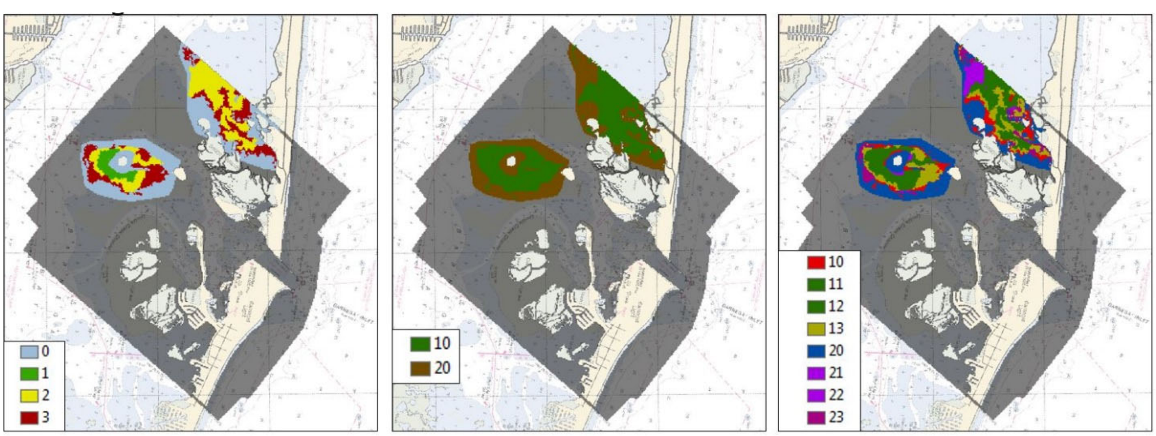

Figure 2.26: Confusion matrix between the Rutgers survey results to one of the study results (satellite imagery from 2014-04-10). Rutgers University classes were classified as: Very sparse (0), Sparse (1), Dense (2), Very Dense (3). The study results were classified as Sparse (10) and Dense (20). The intersection between the two classifications is shown in the image on the right.

Date	**Accuracy (“Sparse” ≡ SAV)**	**Accuracy (“Sparse” ≡ Bare)**
June 1, 2013	0.79	0.79
August 20, 2013	0.83	0.80
April 10, 2014	0.85	0.75
June 29, 2014	0.80	0.84
July 22, 2014	0.73	0.82
July 31, 2014	0.84	0.85
August 7, 2014	0.76	0.80
September 17, 2014	0.76	0.89

Table 2.5: Accuracy assessment (probability of class agreement) of sparse vegetation coverage between Landsat 8 results and Rutgers University measurements. Two conditions are considered to map the current measurements to the categories used by the Rutgers study: in the first “sparse” eelgrass is mapped to SAV; in the second, “sparse” is mapped to bare ground.

to synthesize data needed to assess coastal conditions, compare regions, and monitor change using parameters extracted from spatial data, and examine how it can be integrated and/or transformed into a regional index.

In order to support the objective of providing products that can be used for CEI construction, products derived from topo-bathymetric LIDAR and high resolution imagery for the Super Storm Sandy habitat mapping effort, including bathymetry, slope, rugosity, bottom return, and peak amplitude, have all been generated in standard, documented [31], formats. Having the products generated as standard imagery makes them more generally useful to the scientific and management communities.

These products have already been used to create habitat maps [31, 32] (Figure 2.27), and can be used to generate features for environmental applications and CEI that focus on habitat analysis. These data can also be easily cross-walked to other standard classification systems such as NOAA’s Coastal Marine Ecological Classification Standard (CMECS). Many of the parameters that can be derived map well into the benthic habitat CMECS that has been approved by the Federal Geographic Data Committee and adopted as a standard for benthic habitat classification by many NOAA labs.

The exact forms of specific CEIs are not, at the time of writing, well defined. However, the products being derived from this work are at least well-placed to be inputs into this process.

2.5 Chart Update

Much of the work in this project has focused on non-hydrographic products and processes that might support storm response and restoration efforts. However, many of

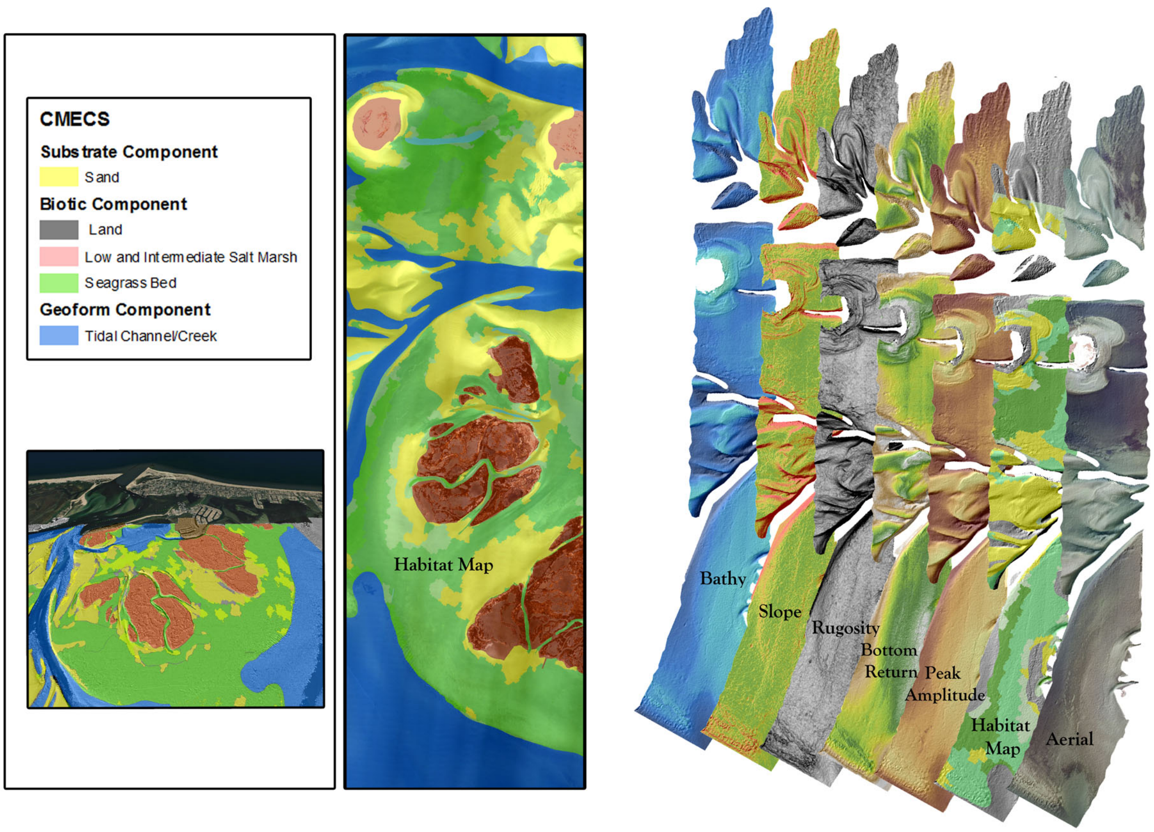

Figure 2.27: Products derived from the USGS EAARL-B Topo-bathymetric LIDAR system that can be incorporated into a Coastal Engineering Index.

the techniques are also suitable for support of more traditional hydrographic practice. Even when not collected to hydrographic surveying standards, for example, LIDAR data can serve as a critical source of bathymetry in areas too shallow to survey with conventional acoustic technologies. Similarly, although SDB might provide the lowest quality of bathymetry data from the publicly-available datasets, it provides a reconnaissance tool with large coverage (185 km swath width) and can fill gaps that may exist between the other available datasets. LIDAR and SDB data are particularly valuable in emergency response scenarios, including post-hurricane mapping, due to their ability to efficiently survey large areas from an airborne platform. As estuarine and shallow, near-shore areas may be severely impacted during a storm event, the ability to quickly survey these areas and identify potential navigational hazards (both manmade and natural) is crucial.

Thus, for example, USGS EAARL-B LIDAR data can be used to identify features that are not on the chart, and might need to be updated (Figure 2.28) while Landsat 8 imagery can be used to generate SDB where other data is not available (Figure 2.29), using EAARL-B LIDAR data as vertical referencing information.

An important facet of the work conducted under this project is transfer of techniques, in particular to the IOCM group working at the Joint Hydrographic Center. In addition to white-papers[3] published, CCOM researchers have been actively assisting the IOCM group, and NOAA's Marine Chart Division, to use SDB for evaluating chart adequacy and chart preparation [33]. Based on this experience, the IOCM group now plan to derive bathymetry from the New York coastal areas using procedures pioneered through this grant.

[3] `http://sandy.ccom.unh.edu/publications/library.html`

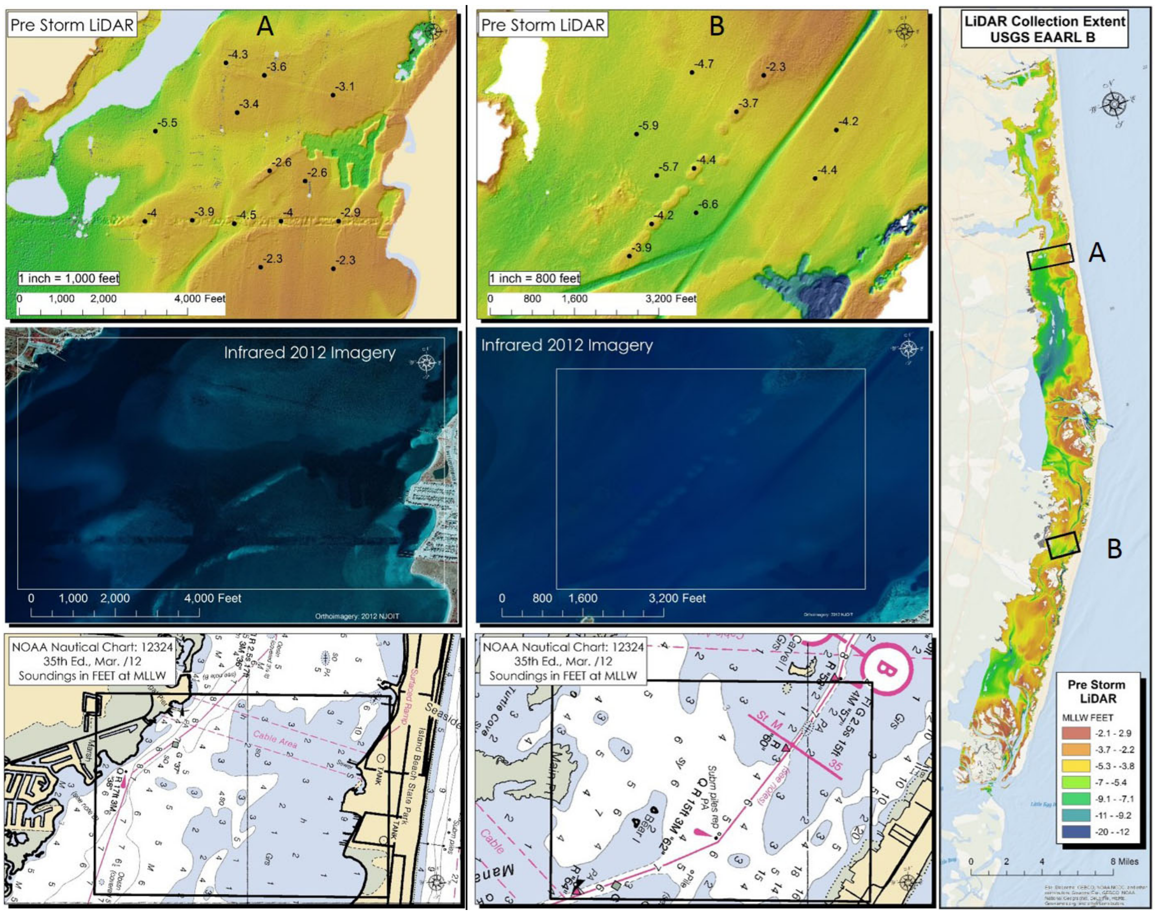

Figure 2.28: Examples of pre-storm EAARL-B data showing potential uncharted submerged objects. Left: a cable within the designated cable area, and uncharted shoal immediately south. Right: a small chain of shoals parallel to the deeper channel.

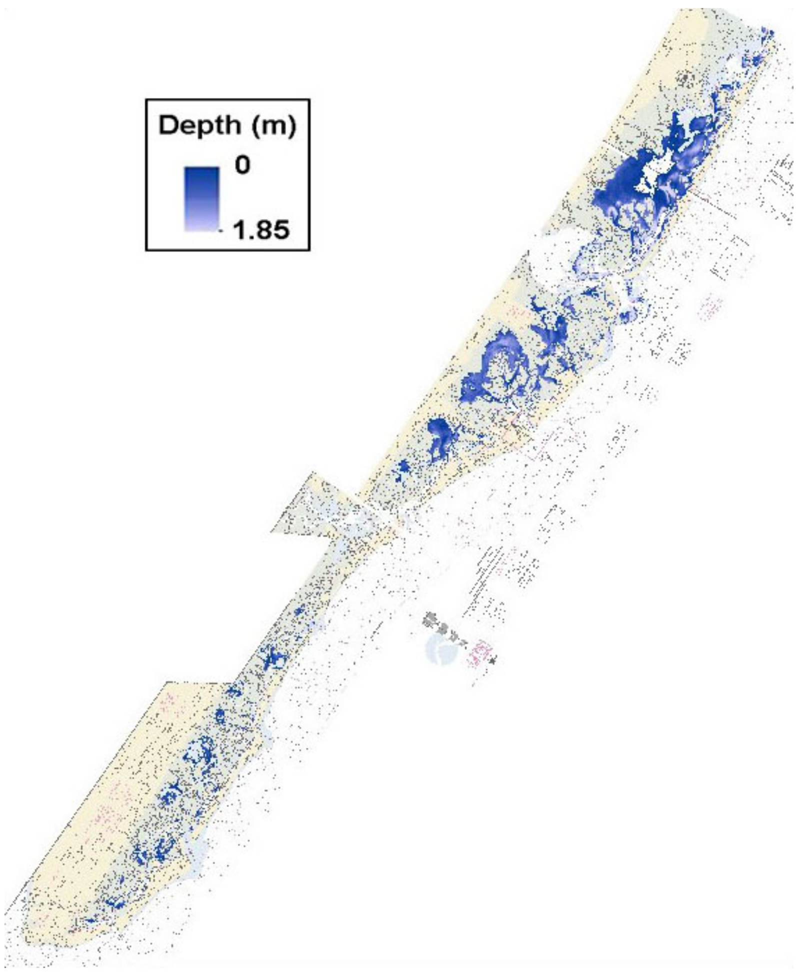

Figure 2.29: Coverage of satellite derived bathymetry derived from a Landsat 8 satellite image collected on 2014-04-10.

Chapter 3

Marine Object Management

3.1 Introduction

3.1.1 The Marine Debris Problem

Marine debris is a general problem in the oceans, and a particular problem in coastal areas due to the proximity to human activities. Although marine debris enters the environment continuously, storm events can significantly accelerate this process, breaking down the built environment and anthropogenic materials and washing them into local waterways. In the wake of a significant storm event, therefore, there is an immediate need to identify marine debris in the affected area, and then to decide whether it should be left *in situ* or removed. In some cases, this process might be due to concerns for navigational safety (e.g., sunken barges blocking the entrance to a port), in others due to concerns about potential pollution (e.g., oils and gasoline in cars washed into a river), and in still others due to concerns of safety (e.g., building detritus in populated areas). Whatever the reasons for concern, however, the primary goal is identification of marine debris, and management of this information from survey to restoration.

In practice, however, this process is generally not straightforward. Marine debris is often not well defined, and therefore the extreme variability of shape, size, material, etc., can make robust identification difficult. In other fields, particularly mine counter measures and pipeline inspection, there has been a lot of work done on marine object detection. However, although several of these techniques have been modified and adopted here [34–36], these techniques are often successful because they can rely on knowledge of specifics of the targets [37], which makes the problem somewhat simpler. In other words, if one is looking for mine-like objects, for example, the target can be modeled quite well since one generally knows at least roughly what they look like. With marine debris, the loose definition of "target" means that this is generally not the case [38].

The objective of this work is therefore to develop a model that allows for the detection of marine debris in a suitably robust manner, taking into account as many sources of information as possible, providing the results in a manner that can be readily transferred to others in a standardized format, so that it can be used for further downstream studies and remediation/restoration efforts. In this context "information" includes not only what can be found from direct and remotely sensed data, but also *a priori* information on the possible locations of debris, and predictive models based on previous storm events, that can be used to constrain the overall complexity of the detection problem. The result is an algorithm that can flexibly assimilate data from a variety of sources, and declare its results in an appropriately intuitive manner, and then summarize them in a standard interchange data format.

3.1.2 Sources and Types of Marine Debris

Marine debris are commonly defined, in approximate terms, as being any man-made object discarded, disposed of, or abandoned, that enters the coastal or marine environment [39]. They can be made of a variety of materials, directly related to those commonly used by modern society: plastics, from industrial products (strapping bands, resin pellets, plastic sheeting) to common domestic material (bags, bottles), as well as other materials (metal, styrofoam, rubber, glass) that, like plastic, have a wide range of uses [40]. They tend both to break down into smaller fragments and to be worn away, but they do not biodegrade entirely. Marine debris span in size from the millimetric size of resin pellets to entire sunken vessels [39]. Thousands of abandoned and derelict craft are presently close to the shoreline, in a multiplicity of states (e.g., semi-submerged in the intertidal zone, or stranded on reefs or in marshes) [41]. When present in protected areas (e.g., lagoons), these shipwrecks may persist for years, while exposed environments can force their disintegration, and litter thereby generated may be distributed widely through multiple habitats [39, 42]. Marine debris are commonly classified by source type into ocean-based and land-based [39]. The primary ocean-based sources are vessels (e.g., derelict fishing gears such as nets, traps, buoys, lines lost by commercial fishing vessels and recreational boats, entire containers from cargo ships in rough seas), but stationary platforms also play an important role since all items lost from these structures become litter (e.g., hard hats and gloves, storage drums). However, the largest part of debris along the shoreline comes from land-based sources [39].

Debris may be blown, swept, and washed out to sea after their accidental or intentional disposal as domestic or industrial wastes on land or in streams. In normal conditions, rain and snow melt-waters are the usual means by which these materials are carried to a nearby river or canal, or even directly to the ocean. However, natural disasters such as hurricanes, tsunamis, mudslides and floods are usually coupled with devastating effects such as heavy rains, flooding, strong winds, high waves, and storm surges [43, 44], leading to a peak of new deposition (in both intertidal and subtidal areas) of marine debris, and an additional problem for regions already impacted by a natural disaster. In fact, this abnormal amount of marine debris may create threats to navigation, fishing activities, recreation, sensitive ecosystems, and generally to the environment and human safety [39, 44]. Effectively and quickly processing large amounts of hydrographic data collected using commercial systems for detection of marine debris would be highly advantageous to remediation operations [45].

3.1.3 Workflow Overview

The complex nature of marine debris demands that a coherent framework for the detection task must take into account as much available information as possible. From the spatial relationship between the marine debris distribution and explanatory variables to an effective way to merge the results of different detection algorithms, the vague definition in size, shape and material of the investigated targets demands a technique that can synthesize all available data into a coherent decision. At the same time, some degree of modeling and approximation is required to make the analysis computationally attractive and sufficiently effective to be practical [46, 47].

The developed workflow is therefore structured in three stages: a prediction model that provides *a priori* information to constrain the problem; a detection step to fuse information into a probability map; and a data format and transfer step that allows for simple transfer of results into further processing stages.

The prediction step analyzes the marine debris distributions in recent available data sets, from which a forward predictive model for marine debris presence is developed. This predictive step provides the initial state for a Bayesian spatial hierarchical model, but can also be used as a post-hurricane survey planning tool.

For detection, a target model was built postulating a simplified description of debris properties, and a set of detection algorithms were developed to target different possible characteristics of marine debris, detecting discrete objects which differ (e.g., protrude) from the surrounding seafloor, being close or connected to the bottom [45]. The scope of these algorithms was constrained to analyze products commonly available in existing post-processing software (e.g., bathymetric digital terrain models and backscatter mosaics with associated data sets such as statistics derived from the core data) so that the technique may be quickly inserted into existing workflows, easing resource management in a response situation.

For data exchange, a data model was developed that provides a common vocabulary for describing marine debris objects, which was found to be a particular problem with data collection in the wake of Super Storm Sandy. Based on standard techniques for geospatial data exchange, this model and its implementation, are readily implemented in standard data processing packages, making it simple to transfer data from the core algorithm into further processing steps.

The workflow was developed for storm response in general, but is illustrated here on data collected in the wake of Super Storm Sandy, specifically around Jamaica Bay, New York, NY, where there are appropriate bathymetric and backscatter data, along with hand-picked marine debris locations to use as ground-truth for the results of the detection algorithm. The area is also of interest to restoration efforts, since it has a high density of objects in a heavily populated area.

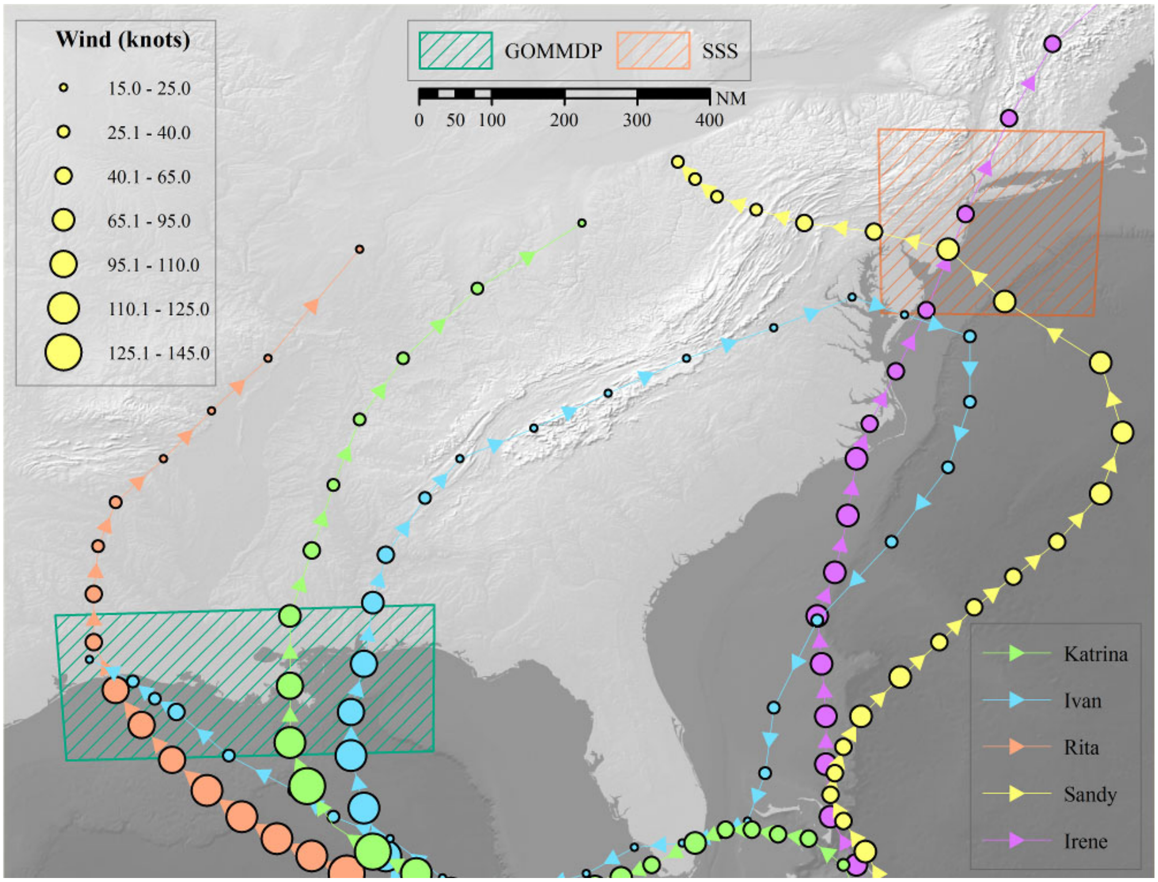

Figure 3.1: Study areas, and the best estimate track (associated with peak winds) of the five hurricanes of interest for marine debris prediction models.

3.2 Case Studies and Data Sources

Super Storm Sandy was a natural disaster with unusual characteristics [1]. Starting as a classical late-season hurricane in the Caribbean Sea, a complex evolution made Sandy grow considerably in size, moving parallel to the coast of the United States (Figure 3.1). After turning northwestward over much cooler waters, Sandy weakened and started to lose its tropical characteristics about 45 nautical miles off Atlantic City, becoming an extra-tropical cyclone (that is, relying mainly on baroclinic processes), to make landfall near Brigantine, NJ, around 7:30 p.m. on October 29, 2012. Because of Sandy's unusually large size, the New Jersey and New York coastlines were hit by a catastrophic storm surge, accompanied by powerful damaging waves and enhanced by the fall full moon period. The impacts of Sandy were widespread, with at least 650,000 houses damaged or destroyed, cars tossed about, boats pushed well inland from the coast. Sandy represented a massive source of marine debris deposition for impacted coastal areas. However, being relatively close in time, Hurricane Irene most likely also influenced the debris distribution [48].

Survey data collected after Sandy, concentrated in the Redbird Reef area (off the coast of Delaware), and Jamaica Bay, New York, NY, were used to test the algorithms under development. However, in order to generate the predictive models, information from previous storm events was required. Three datasets were considered, two in the Sandy-affected area, and a third in the Gulf of Mexico; specifically, the projects used were:

- The NOAA Marine Debris Program (MDP) dataset, mainly focused on intertidal coastal areas (hereafter, SSS-ID), which was based on NOAA NGS imagery acquired during post-storm overflights, and follow-up shoreline survey [49] of the Sandy-affected area. The data set is made up of almost 70,000 debris records: 52% identified via automated Object Based Image Analysis (OBIA) [50], and the remaining targets marked via manual heads-up digitization by imagery analysts.

- NOAA's Office of Coastal Survey (OCS) dataset, which is a growing collection of subtidal marine debris (SSS-SD), mainly based on surveys using a variety of acoustic sensors (e.g., Multibeam Echosounders, Side Scan Sonars) performed by contractors. This preliminary data set (some processing is still ongoing) was retrieved directly from NOAA OCS. This data covers many areas of the Sandy-affected region, but the focus here was on Jamaica Bay, New York, NY.

- The Gulf of Mexico Marine Debris Project (GOMMDP) data set, a large collection of marine debris items related to Hurricanes Katrina, Rita and Ivan, and identified via side scan sonar during several surveys conducted in 2006 [51].

There are several differences between the GOMMDP and the Sandy area that influence the expected debris distribution. The former project area is quite flat, while in comparison the latter is characterized by moderate bathymetric and topographic relief. The complex geography of New York Harbor and Long Island Sound generated quite distinct patterns for the maximum elevation of storm surge and peaks of strong winds, while for Katrina these were almost coincident. Sandy also affected one of the most densely populated areas along the East Coast, giving it a much higher potential for debris creation due to the abundance of debris sources, while much of Katrina effects were on rural or low-density suburbs [1, 52].

3.3 Predictive Model

The predictive model was developed to spatially constrain the marine debris detection problem. Although such problems are notorious for having multiple possible solutions, the objective here is to specify a likely solution that can be used as a prior for Bayesian inference. In essence, the predictive model helps to identify the right haystack, and the Bayesian inference finds the needles.

Based on the data availability of previous hurricane events, the correlation between several possible explanatory layers collected in the wake of recent Gulf of Mexico and

East Coast storms (like Katrina and Sandy) and the likelihood of generation and deposition of marine debris was studied. Data related to the track and the intensity of the storm, to the human environment in the area (which are sources of much marine debris), and to the size of the effects (significant wave, storm surge, and so on) were used as information layers [53]. The combination of these layers provided a means to obtain a rough prediction, for a given storm, on where there is a larger likelihood of being significant marine debris creation.

The outcomes of the predictive model become very useful when there are detection algorithms that throw up a number of false positives. In such a case, the model results are used to effectively tune back these algorithms, and thus provide better constraint to the overall solution to the problem.

3.3.1 Spatial Analysis Tools

Spatial data are often characterized by a phenomenon, known as spatial auto-correlation (SAC), that occurs when the values of variables sampled at nearby locations are not independent from each other [54]. In marine debris data, SAC may arise from a multitude of possible causes, both from intrinsic processes, such as debris size and target-seafloor interactions, and in response to unknown (or partially known) environmental drivers, e.g., non-linear relationships between predictors and dependent variables that are modeled (erroneously) as linear, or failure in accounting for an important environmental determinant that is itself spatially structured [55]. SAC often poses serious shortcomings for hypothesis testing and prediction by violating the assumption of independently and identically distributed errors required by most commonly-used statistical procedures [56]. In the absence of a perfectly correctly specified model, SAC cannot be accounted for by non-spatial models [57], and some kind of correction, such as the one introduced by auto-covariate regression, is required [58]. However, SAC may also be seen as an opportunity since it provides useful information for inference of a process [59].

The distribution of marine debris density over a seafloor area is a spatially-distributed stochastic phenomenon. The density values represent a set of variates, and the task is to decide whether there is any evidence that these variates are spatially correlated. However, real scenarios such as the case studies usually present a quite complex hierarchical structure that cannot be simply modeled as regular or clustered point processes, and they may exhibit different spatial pattern characteristics at different scales [60]. The verification of the hypothesis that the debris locations tend to cluster rather than following a complete spatial randomness (CSR) process, under which their patterns are realizations of a Poisson point process, is thus an important preliminary step. Dedicated methods can be classified as global (throughout the whole study region) or local. For global methods, there are several established procedures (Moran's I plots, Geary's C correlograms and semi-variograms), in which a measure of similarity or variance of data points is plotted as a function of the distance between them, to check whether spatial correlation is likely to impact the data analysis [61]. Morans I varies between -1 and $+1$, and a value close to 0 indicates a random pattern or absence of spatial autocorrelation [62]. Calculation of the z-score provides a means to evaluate the intensity of spatial clustering, looking for clustering lags with statistically significant peak z-scores (based on a randomization null hypothesis). Given the kind of pattern of this study, the focus of most algorithms is on a small, local level of clustering, and this method allows the correct size of the analysis to be determined from the data. Local methods such as Local Indicator of Spatial Association (LISA) and hot-spot analysis, when used in conjunction with Moran's I applied globally, deepen the knowledge of the processes that give rise to spatial association, enabling the detection of local pockets of dependence that may not show up when using global methods [63]. LISA is a local Moran index proposed by Anselin [64]. This method highlights clusters as well as possible outliers, a low value surrounded by high values (low–high) or a high value surrounded by low values (high–low). The hot-spot analysis identifies local spatial clusters of statistically significant high (hot spot) and low (cold spot) number of debris targets for a grid cell by calculation of the Getis-Ord Gi* statistic [65].

The popular K-means algorithm was also adopted as an exploratory tool, applying a cluster analysis to identify possible structure between the available data in the absence of category information [66]. The selection of the number of groups was based on the pseudo F-statistic, a ratio reflecting within-group similarity and between-group differences [67].

3.3.2 Model Implementation

SAC occurs at all spatial scales (from meters to dozens of kilometers) for many reasons. Since these reasons are mostly unknown, one cannot readily derive a spatial correlation structure for an entirely new and unobserved area, although it is possible to derive predictions by interpolation for missing data within the study area (e.g., by using a Gibbs Sampler) [68, 69]. When models are projected into different areas the handling of spatial auto-correlation is quite problematic, sometimes even impossible. Extrapolation in space can only be based on the coefficient estimates, not on the spatial component of the model [46, 62]. Extrapolation is further complicated by model complexity: the use of non-linear predictors and interactions between environmental variables usually increases model fit, but with the price of compromising model transferability in time and space. Given such intrinsic limitations, a predictive model was created with the main aim of providing a reliable initial state to the Bayesian inference; however, the evaluation of areas where the presence of marine debris is more probable, coupled with considerations related to the economic relevance of specific waterways, may also help to effectively prioritize the areas to survey and the data to process, speeding up identification of detected possible targets and their eventual removal. A limited number of predictive debris models have been recently developed: the web-based HurDET model [70]; USACE HAZUS-MH models [71, 72]; and, the Marine Debris Distribution model of the Gulf of Mexico, from the NOAA Marine Debris

Data Product	Predictor	Source
H* Wind Surface Wind Analysis	Wind	NOAA
Experimental Extratropical Surge and Tide Operational Forecast System	Storm surge	NOAA
NGDC 3-Arc Second Coastal Relief Model	DEM	NOAA
International Best Track Archive for Climate Stewardship	Hurricane best-track	NOAA
Global Self-consistent, Hierarchical, High-resolution Geography Database	Shoreline	NOAA
Natural Waterway Network	Waterway	USACE
Topologically Integrated Geographic Encoding and Referencing	Population	Census Bureau

Table 3.1: Proxy sources for marine debris prevalence model predictors.

Program (MDP) [44]. While the first two are focused on terrestrial debris, some of the findings and the results from the MDP model have been adapted and incorporated in the present model, attempting both to generalize the approach (to increase flexibility) and to cast the modeling results to feed a probabilistic algorithm for marine debris detection.

A list of intuitive marine debris predictors (Table 3.1) was created, informed by comparison with existing similar work, and data availability. This latter criterion is for model flexibility, avoiding a model based on peculiar predictors that, although highly explanatory of debris presence, will likely not be available in case of natural disasters in different areas, as well as in the immediate proximity of the event. The selected predictors can be clustered in two groups: those related to the storm energy (wind, storm surge, bathymetric profile, etc.) and those capturing the spatial distribution of debris sources (concentrations of highly populated human areas, waterways, etc.). The intuition behind such a choice is that coastal urban areas impacted by high storm energy should have larger amounts of anthropogenic debris, due to higher potential for debris creation and mobilization.

The wind-based predictor was created by summarizing into a single layer, representing the peak intensity, the surface wind analysis of tropical cyclones produced by the NOAA Hurricane Research Division as part of the H* Wind Project [73], a project that merges a variety of coastal and inland data from land, space, and marine platforms. Data from the Extratropical Surge and Tide Operational Forecast System [74], a new generation hydrodynamic modeling system using the Advanced Circulation (ADCIRC) model, was used as storm surge predictor. The National Geophysical

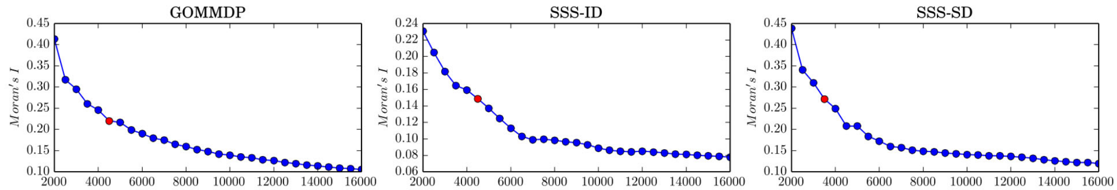

Figure 3.2: Moran's I statistic, globally applied, calculated for the case study data sets. Red dot indicates the first peak of the associated z-scores.

Data Center[1] 3-Arc Second Coastal Relief Model [75], integrating bathymetric and topographic information from a variety of data sources, was used to explore the relationship between debris and depth. The best tracks for the hurricanes in the study were retrieved from NOAA's International Best Track Archive for Climate Stewardship project [76], collecting the historical tropical cyclone best-track data from all available Regional Specialized Meteorological Centers and other agencies [77]. The distance of each cell in the lattice grid has been calculated having as reference the World Vector Shorelines, present in the Global Self-consistent, Hierarchical, High-resolution Geography Database [78], while for the waterways the USACE Natural Waterway Network was adopted [79]. Finally, a population index was derived from the 2010 census Topologically Integrated Geographic Encoding and Referencing product [80].

A classic ordinary least squares [62] was adopted to create an equation relating marine debris density (dependent variable) to the selected set of explanatory variables. Exploratory regressions were used to find a well specified model by evaluation of all the different possible combination of explanatory variables, balancing statistical significance, redundancy and multi-collinearity [46, 47, 62]. The balance was mainly evaluated by comparison of Adjusted R-squared, Akaike Information Criterion (AIC) and Variance Inflation Factor (VIF) values [46, 47].

3.3.3 Exploratory Analysis of Available Data

Moran's I statistic, which is used to test the null hypothesis that the spatial autocorrelation of a variable is zero, was applied globally to the study case data sets. The results are presented in Figure 3.2, with the first peak of z-score plotted as a red dot.

The results from LISA and hot-spot analysis are presented as Pane A and B in Figure 3.3 for the GOMMDP data, in Figure 3.4 for the SSS-ID data, and in Figure 3.5 for the SSS-SD data; while Pane C was used to spatially identify the areas resulting by the grouping analysis, performed using K-mean algorithms and based on the pseudo F-statistic to identify the parameter for the number of groups: two for GOMMDP and SSS-ID data sets, three for SSS-SD data set. For this last, a plot with the resulting inter-group relationships is presented in Figure 3.6.

[1] Now National Centers for Environmental Information

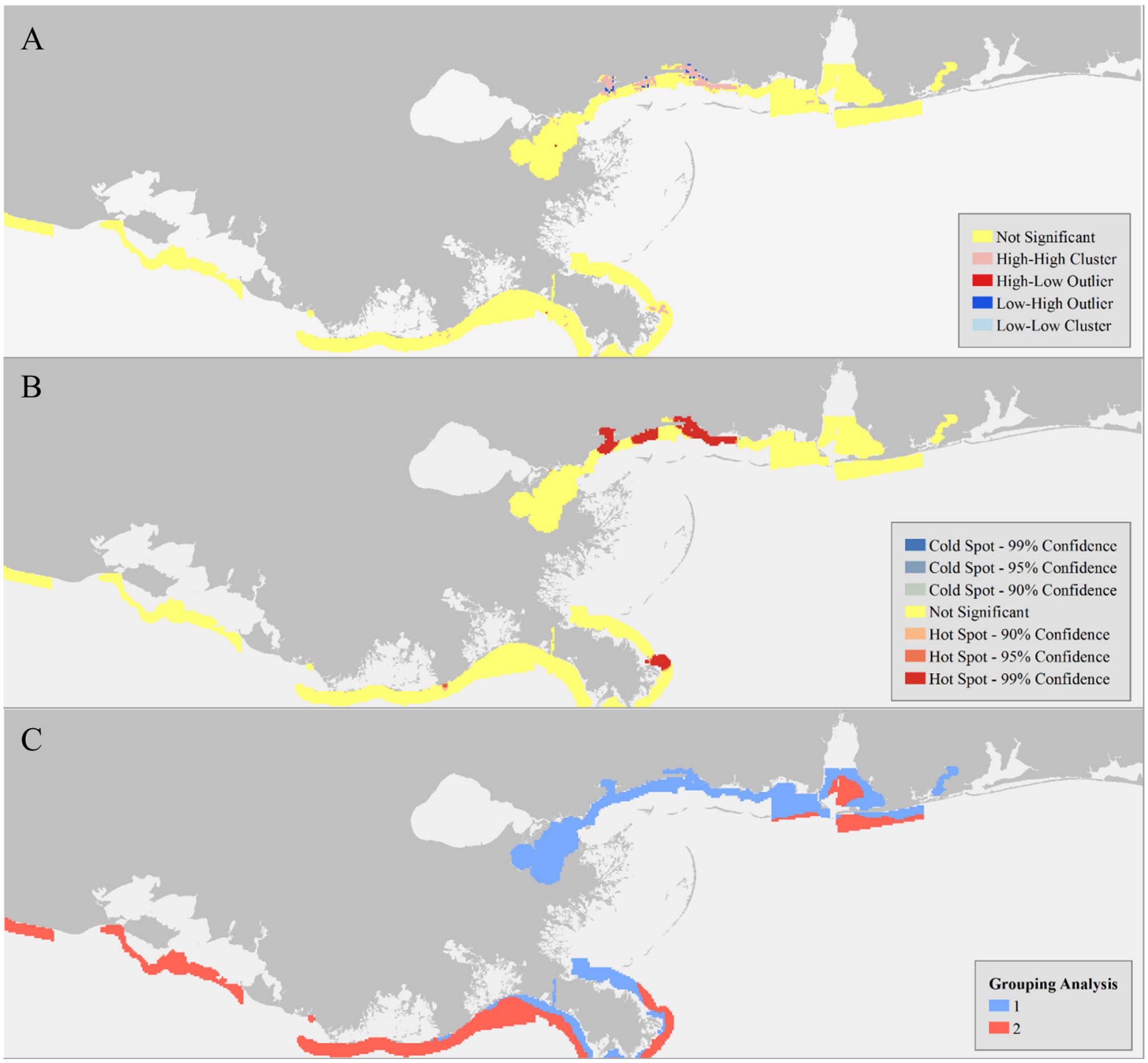

Figure 3.3: Moran's I statistic, locally applied (pane A), hot-spot analysis (pane B) and grouping analysis (pane C) for the GOMMDP data set.

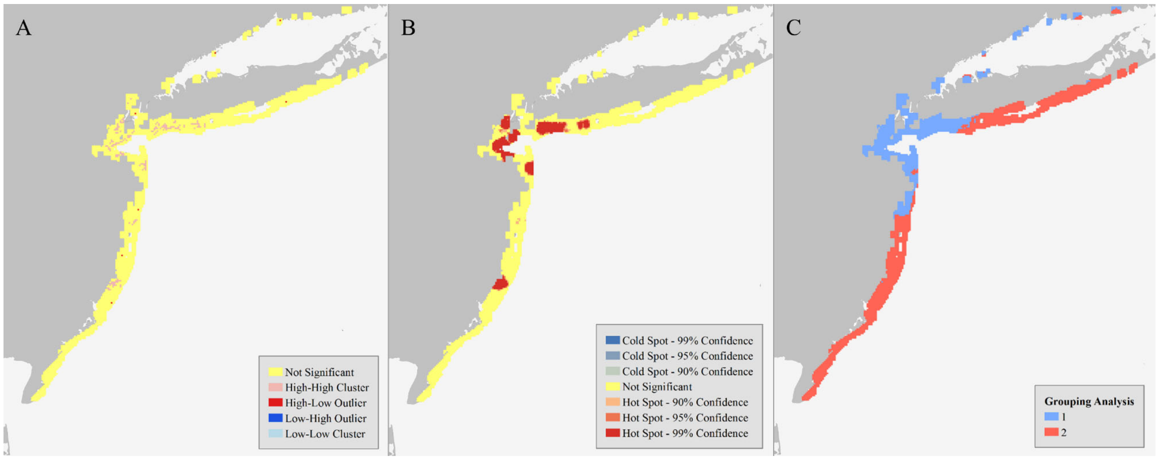

Figure 3.4: Moran's I statistic, locally applied (pane A), hot-spot analysis (pane B), and grouping analysis (pane C) for the SSS-ID data set.

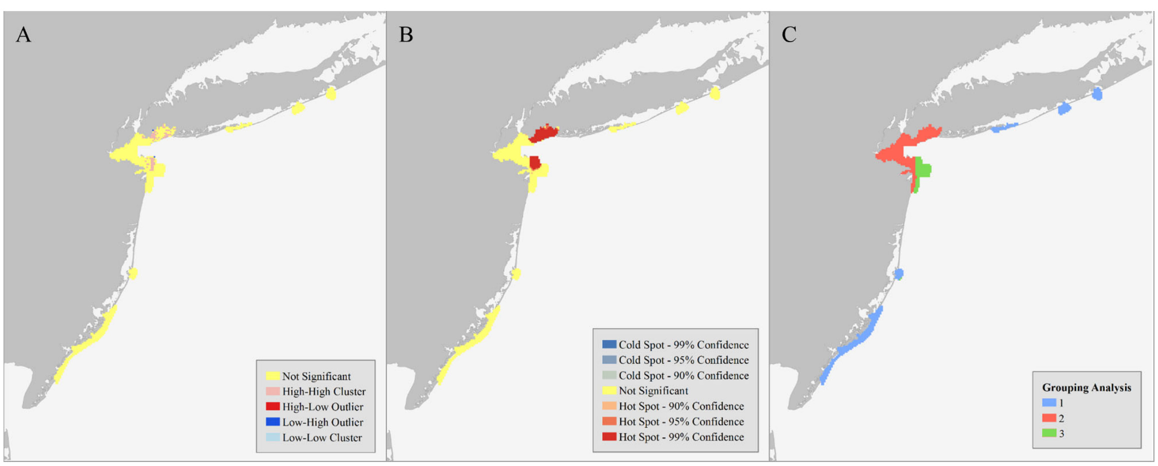

Figure 3.5: Moran's I statistic, locally applied (pane A), hot-spot analysis (pane B), and grouping analysis (pane C) for the SSS-SD data set.

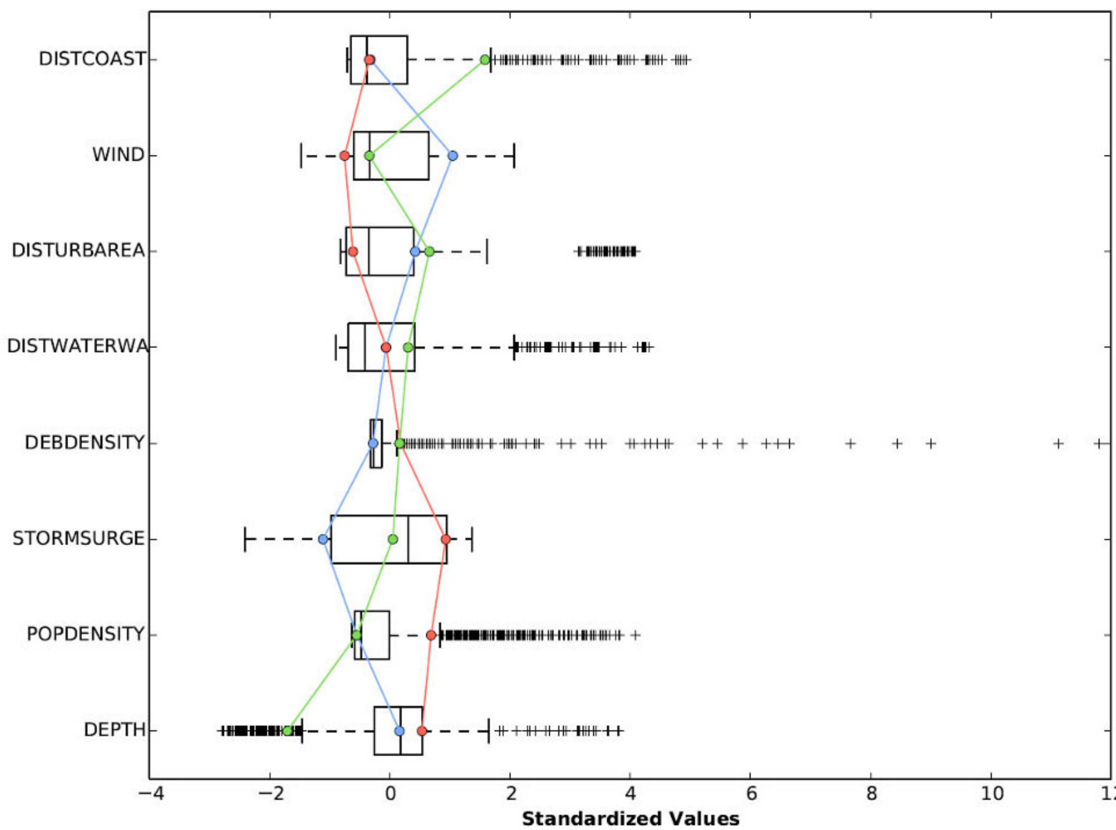

Figure 3.6: SSS-SD grouping analysis outcomes between debris density ("DEBDENSITY") and predictors: distance from the shoreline ("DISTCOAST"), maximum wind ("WIND"), distance from the urban area ("DISTURBAREA"), distance from waterway ("DISTWATERWAY"), maximum storm surge height ("STORMSURGE"), population density index ("POPDENSITY"), and average depth ("DEPTH").

The resulting Moran's I values show a similar trend for the GOMMDP and the SSS-SD data sets, with peaks at 3.5 km and 4.5 km respectively, but lower values in the SSS-ID data set (although with a consistent peak at 4.5 km). Such a difference could be explained by the fact that restoration efforts are more likely to have been applied in the intertidal zones due to their accessibility. The Getis-Ord Gi* test identified several clusters of points that have higher values than expected by chance. For the GOMMDP dataset, the analysis results suggest a relationship between the Hurricane Katrina track, urban areas and hot-spots of marine debris density (Figure 3.3). Several hot- and cold-spots are also present for the Sandy datasets (intertidal debris in Figure 3.4, and subtidal debris in Figure 3.5), although relationships with tracks and urban areas are less visually evident. The results from the hot-spot analysis are compatible with the LISA outcomes, and only a very limited number of possible outliers are present. An interesting result from the grouping analysis is the different number of groups (three rather than two) for the SSS-SD data set. As is clear in Pane C of Figure 3.5, the anomaly is spatially localized (the results of the grouping analysis are expanded in Figure 3.6 for reference) and almost exactly matches with an area assigned to a specific contractor. Thus, it is possible to speculate that this is most likely due to different (and likely stricter) criteria being followed in the target detection analysis by this contractor, or within this area. Consequently, the debris distribution in this area was removed from consideration within the remaining analysis (although the causes and procedures behind this difference are worthwhile of additional investigation).

3.3.4 Predicted Debris Distribution

After an exploratory regression based on the seven predictors listed in Table 3.1, both study areas exhibited similar results, indicating that storm surge, population density index, and distance from urban areas are generally good predictors of marine debris presence (R-squared higher that 0.5). The addition of other available predictors does not provide significant contributions to the R-squared values, adding decrements in terms of AIC and VIF values. Using the resulting model parameter coefficients, a prediction of debris distribution for the areas covering is presented in Figure 3.7 for the SSS-SD data set, and in Figure 3.8 for the GOMMDP data set.

The model outcomes highlighted higher likelihood of debris presence in areas that received both higher wind energy and storm surge water elevations during hurricanes, and which are proximal to more developed and populated urban areas. However, it is likely that not all of the drivers for marine debris generation have been captured.

Addition of similar rich databases would help in obtaining a clearer picture of how individual characteristics of hurricanes interact with human land use to generate various types and degrees of marine debris deposition. In fact, this deposition may or may not occur, or occur to varying degrees, depending upon individual hurricane characteristics (e.g., category, breakpoint, maximum wind speed, height of storm surge, and path after landfall). Landfall in a populous area, a post-landfall trajectory upriver toward a headwater region, or a relative slow speed of passage and others

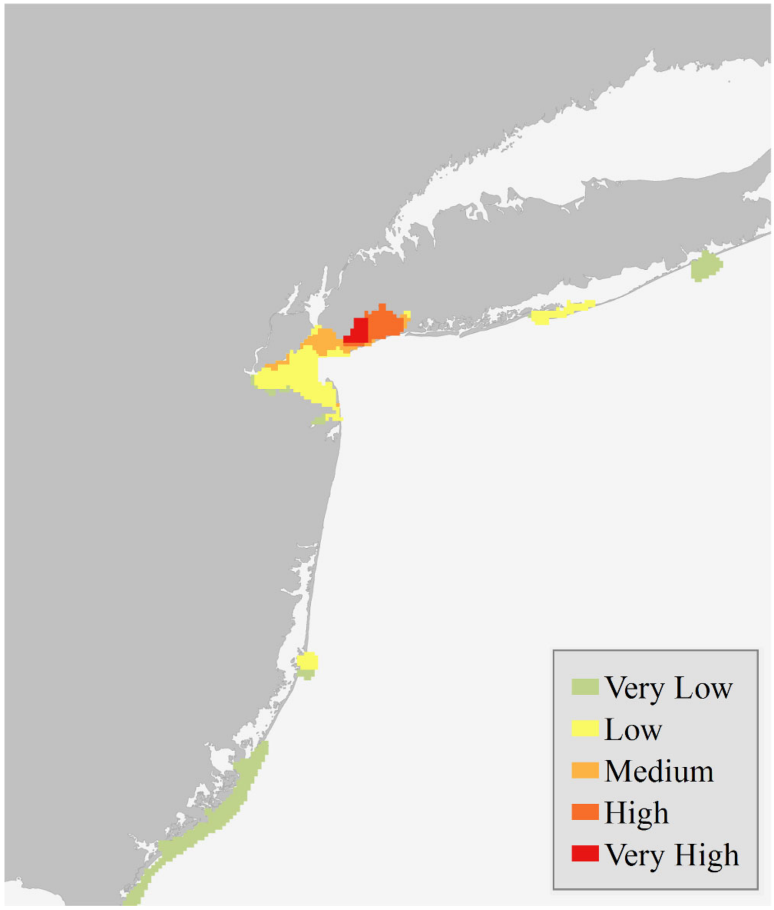

Figure 3.7: Predicted distribution density of marine debris in the SSS study area.

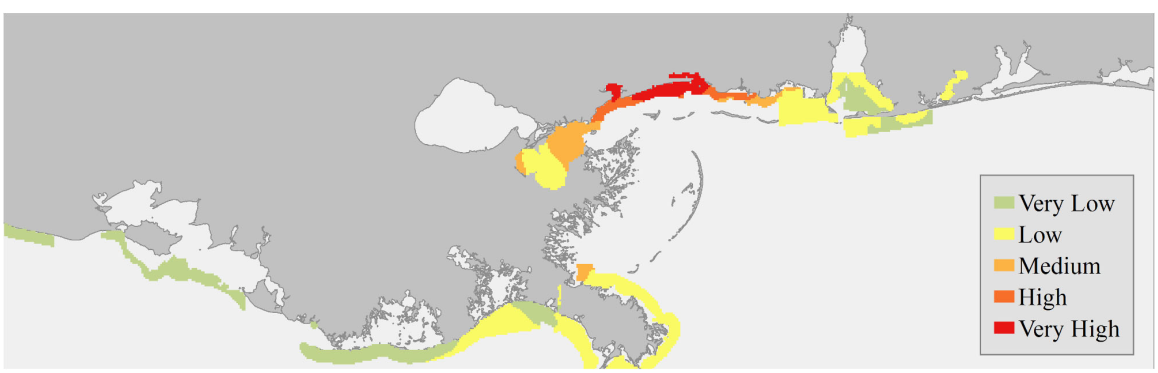

Figure 3.8: Predicted distribution density of marine debris in the GOMMDP study area.

can cause more damage and lead to increased marine debris. The different intensities and tracks for the hurricanes affecting the study areas are clear examples of how each storm-like event has its own peculiarities.

A practical difficulty common to these and similar data sets is the complexity involved in distinguishing between anthropogenic and natural, storm-generated and pre-existing targets. In order to make the analysis possible, it was assumed that each dataset provides a representative picture of the distribution of storm-related and anthropogenic marine debris. The model also relies on the assumption that the distribution of marine debris objects is essentially static, even months after the event occurred, so that it can use data sets collected variable amounts of time since the event. This is increasingly likely to be untenable as a function of the time passed since the event or if another storm-like event occurs after data set collection.

The seven predictors used do not completely capture all the possible causes of concentrations of marine debris. For instance, areas with particular activities (e.g., recreational marinas), specific land use in the neighborhood such as dumping areas, and strong energy impacts of wave run-up effects might behave differently. Additional predictors capturing such causes might be evaluated in future studies, but with the criterion of maintaining the model's spatial portability, this might be challenging.

3.4 Detection Model

Given that "marine debris" does not have a very good definition, a slightly more sophisticated approach than the ones usually applied in related fields of research was required (Figure 3.9). The overall idea here is that a selection of detection algorithms, each one not necessarily reliable when used on its own can together provide a more reliable output that can be used to provide a robust indication on where marine debris should be located.

The three primary considerations that were given weight in building a solution to this problem were:

- What products to use as data input (and their collection requirements);
- How to do the initial detection (i.e., selection of detection algorithms); and
- How to fuse together the outcomes of different algorithms.

3.4.1 Data Input and Related Collection Requirements

For inputs, only hydrographic standard products were considered. This means that the approach will not require the acquisition of particularly "exotic" data, which is mainly driven by the design goal of being able to work in a storm-like scenario, when a disaster response is in progress, and the users of such an approach will not have

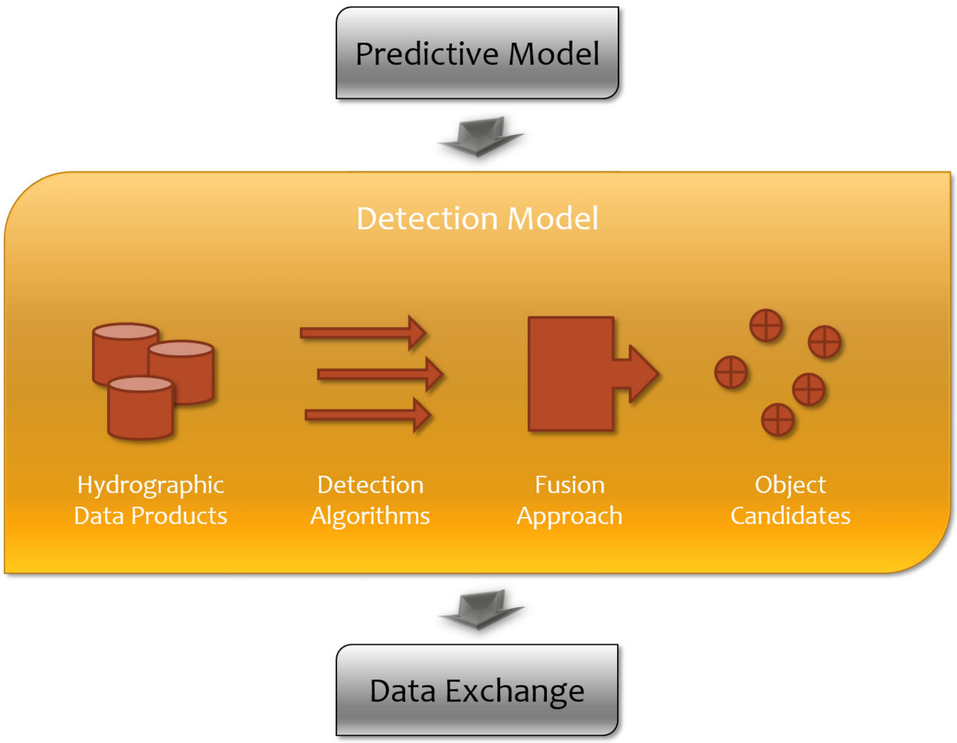

Figure 3.9: Diagram of the three sub-problems for the marine debris analysis theme. The core topic of the research is represented by the detection model (in orange). It takes hydrographic data products as input and provides a list of marine debris candidates based on the fusion of the outcomes of several detection algorithms.

time and resources to do anything beyond what is strictly necessary. Conventional bathymetry and backscatter are considered to be the most likely available datasets.

The data used must meet some requirements, however, for the process [45] to be successful. In particular, the acoustic system used should be fully understood, with particular attention to the internal backscatter processing, otherwise the appropriate corrections cannot readily be made. In addition, the system used to collect the data should be calibrated, and the resulting calibration parameters correctly applied (in real time or post processing), or the results may be misleading. Finally, the environment should be properly characterized (e.g., absence of issues with the sound speed profiles, correct absorption coefficients, etc.) for the corrections being done to be effective.

System calibration is mainly required by the fact that elements in the receive array do not usually have absolutely identical characteristics or mounting position [81], and such distortions could be significant for some algorithms. Similarly, any signal distortion of the backscatter time series collected around the seafloor detection point should be reduced or avoided.

Where available, pre- and post-disaster dataset comparison can be powerful. However, proof that the seabed changes observed (e.g., presence of marine debris) are not related to instrumental and integration artifacts requires confidence in the absolute accuracy of both the bathymetric and backscatter output of the integrated sonar system [82, 83]. Similarly, smaller objects require higher accuracy of calibration, and pre-existing datasets may not achieve this goal; care in comparison is therefore warranted.

Different systems have different achievable [83] (as well as theoretical) resolutions, and assessment of this is essential in data or system selection, and in evaluation of results. The system resolution is particularly important; for MBES systems, this is mainly a function of the beamwidth and pulse length [84], while for phase measurement systems, the resolution can be finer than the beam footprint [82]. Similarly, the type of beamforming and bottom detection can be important considerations, particularly the availability of high-density processing modes [85, 86] or multiping capabilities [82]. Uniformity of data density across all of the datasets is particularly important, since a spatially varying density can reduce the reliability of detection for small objects [87], as is motion compensation for the MBES, which can otherwise lead to variable density. This is particularly true of yaw stabilization, especially when surveying at low speed in order to maintain along-track data density [87]. Increasing along-track data density does not necessary imply better data quality, but it often provides a wider margin for data filtering and statistic tools application.

MBES along-track beamwidth is usually much wider than that used by conventional sidescan sonars, so that sidescan imagery tends to be better quality [88]. However, unless the sidescan is hull-mounted (which has its own difficulties) variable distortions are usually introduced due to the uncertainty in the towing fish position and inapplicability of the flat-seafloor assumption. A better solution, when feasible, is to integrate accurate MBES bathymetry and high resolution sidescan imagery. In such a case, the sidescan-based mosaic can also take advantage of being properly geometrically corrected by using the MBES-based DTM.

Many of the products used in the processing scheme developed are constructed from combinations of multiple survey lines; minimizing the total propagated uncertainty (TPU) is therefore important to ensure that the data are free of artifacts that could mask the presence of marine debris, or prompt false positive detections. Correct patch test procedures [89,90] and identification of any residual dynamics [91] are therefore essential. Combination of individual sources into the product can also limit the scale of change visible to the combined accuracy of the product, rather than the individual accuracies of the sources [82].

The characteristics of the water column change continuously both in time and in space [92]. As a consequence, there is not a simple direct relationship between the time since, and the distance from, the sound speed measurement in use and its applicability. The measurements of sound speed must be taken often enough to capture the actual spatial and temporal variability [93, 94].

Finally, there is no substitute for a survey team familiar with the sensor in use and its capabilities; some systems may have specialized operational modes [95] which might be useful for surveys targeted towards marine debris detection, for example. The workflow will naturally take advantage of well-collected and calibrated hydrographic data, but marine debris detection will still be possible, with expected increased false alarm rates, even if not all best practices are applied.

3.4.2 Detection Algorithms

Selection Criteria

A comparison of the SSS-SD data set and the original survey data was used to estimate the criteria used by the analyst for defining the presence of possible marine debris. From the analysis of the targets selected so far within the SSS-SD data set, several common selection patterns emerged [45]. For instance, a first group containing a rounded shape and/or a jump in seafloor reflectivity was common to many of the several hundred targets examined. A second group was based solely on bathymetry evaluation. A third group comes from an integrated analysis of the DTM and the acoustic backscatter. Finally, although such data can now be readily collected on many systems, there are no examples of debris selection based on water column data, although the extent of availability of this data (and appropriate tools) to the observers is unknown. It appears that operator debris detection was mainly based on the bathymetry and the reflectivity of the seafloor, assuming that any deviation from the "natural average background" was a hint of possible debris. From this observation, and given the intrinsic complexity of the targets, it is likely that a single algorithm will not be successful for robust marine debris detection. The proposed solution is therefore based on multiple algorithms to process different sources (mainly bathymetry and backscatter from acoustic systems, but easily extendable to water column data, as well as LIDAR data), fused together so as to be adaptive to the environment, the context, and *a priori* knowledge (if available) of the possible targets. The goal was to use a collection of algorithms working at different levels (e.g., using per beam, single swath, snippet and pixel level operators), which were then fused by the core engine. One of the primary advantages of this approach is that operating over different data with independent algorithms can reduce inter-algorithm cross-correlation and therefore the probability of false alarm [45].

Development was also driven by concern about false positive generation in the (large) areas where there are no real targets based on parameters extracted in areas with targets. In essence, applying a single algorithm globally can be problematic. Therefore, the algorithm is designed to break the overall area into local sub-areas, and then adapt to the conditions locally in the detection structure. This extra structure allows standard algorithms to be used without extra complications, and leads to more local feature extraction and adaptation.

Backscatter-based Algorithms

For the backscatter mosaic, as in many existing algorithms, target detection is based on the observation that denser material (often anthropogenic) makes debris returns much stronger than the surrounding background. However, the common approach to object detection of simple thresholding (e.g., based on the premise that in a mosaic the object return is brighter than the background) was modified since it tends to fail when the background is textured (i.e., simple detectors are not aware of image correlation). This algorithm is based on an acoustic backscatter mosaic, and takes advantages of previous NOAA-sponsored work at the Joint Hydrographic Center to properly geometrically and radiometrically correct the collected data [45, 96]. The resulting mosaic is segmented into areas with similar reflectivity values through a clustering analysis, and a histogram of backscatter values as a function of angle of incidence is then computed for each clustered area (effectively forming a bivariate histogram). A simple Bayesian classifier is subsequently used to identify areas in each segment where the statistics of a small window do not match that of the overall background distribution (as characterized by the appropriate marginalization of the histogram). Areas of low probability of background membership are identified as potential marine debris. Subsequent edge detection and hierarchical filtering are applied to remove misdetections along the mosaic boundaries (Figure 3.10) [45].

The backscatter information content, expressed as a variable angular response, is also used in a model-based detection algorithm (Figure 3.11). The angular response for each clustered area is formed, as is the angular response for each sequential series of pings, in both cases averaging to reduce levels of noise and improve the estimated statistics. These local angular responses capture angular variability that is lost in the process of generating a mosaic [45].

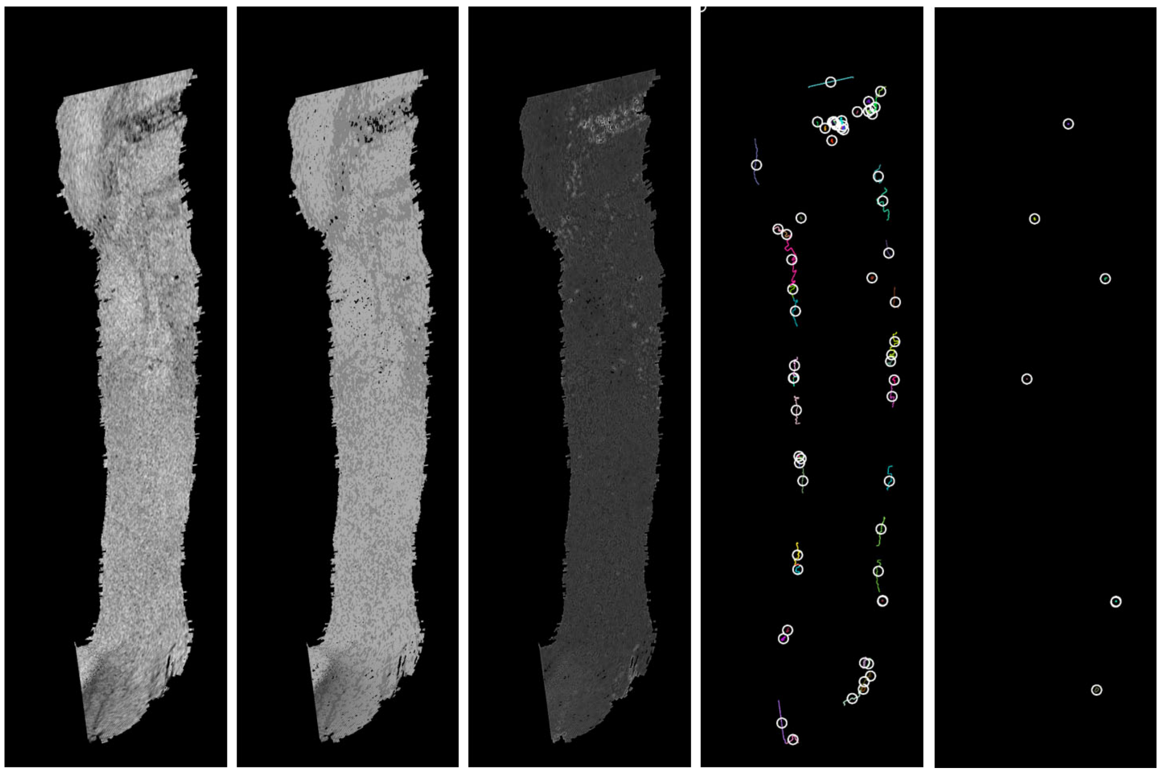

Figure 3.10: Stages in the Bayesian analysis of backscatter anomalies. The sub-images show, left to right: the geometrically and radiometrically corrected backscatter mosaic; the clustered mosaic (clustering is based on simple backscatter values in the mosaic); the probability map for membership of each analysis window in its surrounding background (high values indicate lack of membership); edge detected segments indicating potential objects; and hierarchically filtered objects showing those likely not associated with edge effects in the mosaic. The limited number of detections is promising (from the point of view of limiting false alarms), and corresponds well to operator inspection of the mosaic.

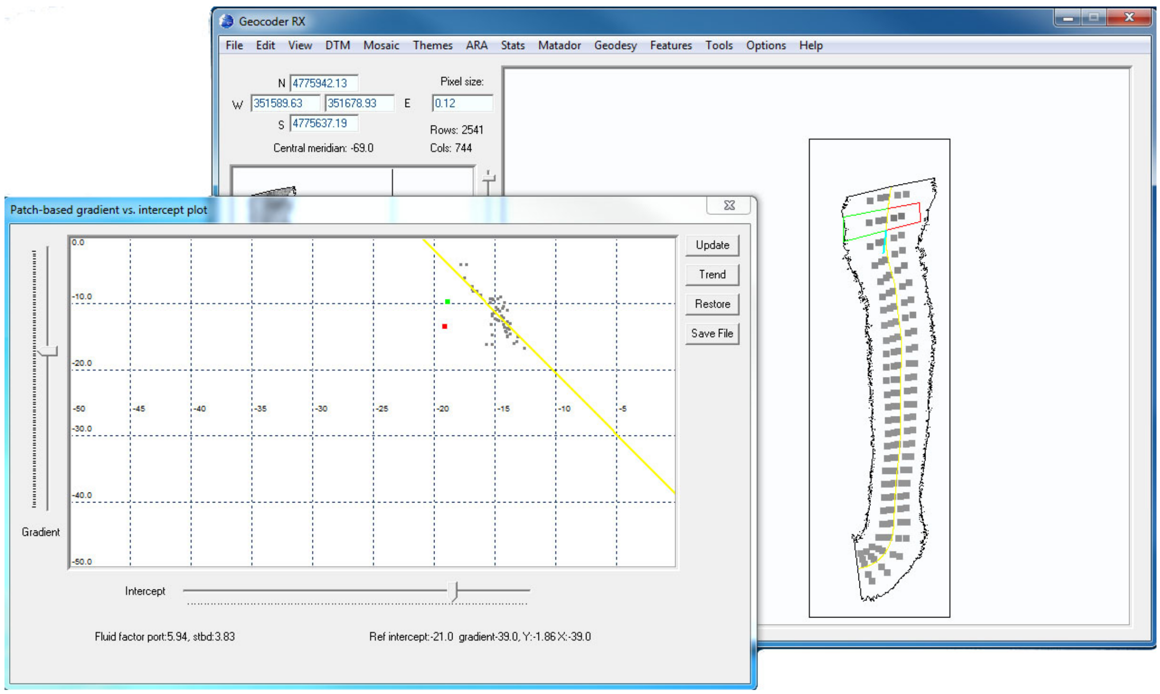

Figure 3.11: Bivariate plot of acoustic backscatter-derived features computed from a half-swath patch of MBES data. The red/green boxes indicate half-swaths having distinctly different behavior (as measured by the slope and intercept of a line fitted to the acoustic backscatter angular response in the patches) from the other patches, an indication of anomalous behavior. Use of multivariate combinations of features can help to clarify detections and reduce false alarm rates.

Finally, adaptations of well-known general-use image processing techniques to marine debris detection have been developed.

Bathymetry-based Algorithms

For the DTM, a few spatial indices were developed as proxies for discontinuities, which are interpreted as potential targets.

In particular, an algorithm was developed based on the Combined Uncertainty and Bathymetry Estimator (CUBE), a weighted depth estimation algorithm that processes large and dense bathymetric data sets, and which addresses issues such as efficiency, objectivity, robustness and accuracy [97]. The nodes independently assimilate propagated soundings to form depth hypotheses which are then tracked and updated as more data is gathered. CUBE manages groups of soundings that are mutually inconsistent, but internally consistent, by segregating them in alternate hypotheses, avoiding cross-contamination of estimates [97]. The state of knowledge about the data is summarized for each estimation node through a list of depth hypotheses.

The algorithm developed here uses CUBE's auxiliary products for marine debris detection (Figure 3.12). The map of hypothesis counts clearly shows areas of difficulty in the gridding process, and, together with CUBE's estimate of the correctness of the hypothesis selected by the disambiguation engine (known as hypothesis strength) [98], may be used as a proxy for debris presence. Low values of hypothesis strength are used to identify a node depth reconstruction that is sufficiently robust to be reliable [99].

Additional Remarks

For both backscatter and bathymetry, the adoption of classical estimation techniques usually generates point estimate or a confidence interval, which becomes important when fusion of target information coming from different products is attempted. In order to provide appropriate distributions for exploitation, Bayesian methods were adopted since they permit use of multiple-source asymmetric and discontinuous posterior distributions that may be transferred into further analysis. A hierarchical scheme is proposed where a series of modeling tasks are implemented through a probabilistic model, casting the debris detection problem as one of estimating properties of the posterior distribution, which represents the probability of objects occurring given the observed data products.

3.4.3 Fusion Approach

The predictive model developed indicates areas of higher likelihood of there being debris. The information obtained from the various detectors in use represents an estimation of how likely it is that there will be a detection given that there is an object present. Unfortunately, neither is the desired information, which is to know how likely it is that there is an object given the detections observed. A Bayesian analysis,

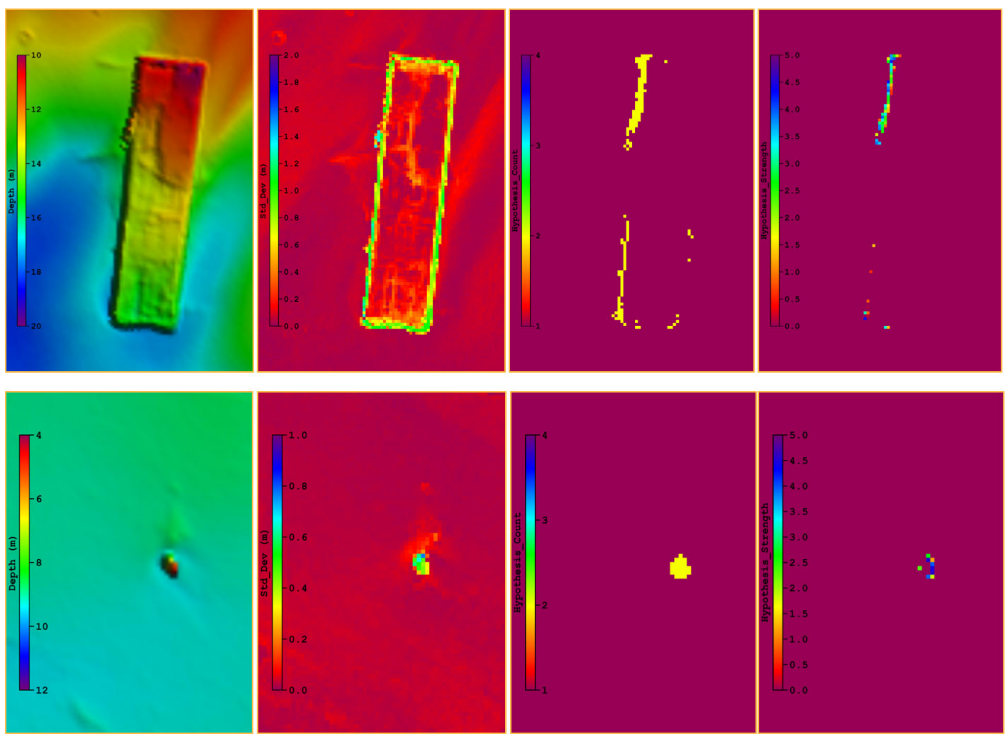

Figure 3.12: Examples of additional useful metrics related to the statistical bathymetric representation of two objects (from left to right, bathymetry, standard deviation, hypothesis count, and hypothesis strength).

however, does allow this inference. The Bayesian hierarchical model provides a probabilistic structure that can be used to combine together detector and predictive data, including any other available sources, such as the ENC. The outcome is an estimate of the probability of there being an object at any point, given the observations and the structuring information from the predictive model.

Bayesian methods have a very strong, and flexible, mathematical framework, and very well understood mathematical structure and supporting computational methods. This allows, in addition to specification of *a priori* information from the predictive model, direct specification of spatial auto-correlations. This can be used to model behaviors in detectors where true objects tend to generate multiple spatially coherent detections, while false detections do not, which can make the detection process more robust.

Hierarchical Spatial Modeling

In order to control the complexity of the detection problem, the algorithm developed uses a hierarchical spatial model, which allows complicated dependencies to be further broken down into problems that are simpler to evaluate. Although a hierarchical model can be flattened by marginalization/integration, there are multiple advantages that have driven the selection of a hierarchical form: ease of interpretation and specification of the various components, facilitation of the model fitting step, and proper propagation of the model uncertainty based on the reconnaissance of the uncertainty in each modeled unknown. In particular, a hierarchical model was adopted that treats the debris presence data as a realization of a spatial point process, whose intensity is driven by local features based on the outcomes of a set of target detection algorithms.

In this case, each detector operates on hydrographic data products, and generates a binary decision on whether debris is expected to exist at a point. The fusion problem is therefore defined over a set of binary indicators, and generates outputs from a binary class $C = \{t, n\}$ for presence or absence of a debris object. Similar to other classification models, the classifier produces an intermediate step that estimates membership probability to the "target" class for each cell. The application of a different threshold to such an estimate can be used to tune the classifier behavior, directly influencing its balance between hit rates and false alarm rates. For notational clarity, the label set $L = \{Y, N\}$ is specifically introduced for the detector output, to distinguish predictions from the actual class. The detector may reach four possible states, as summarized through the contingency table (Figure 3.13).

The classifier states can be combined in various classification metrics, such as:

- The true positive rate (ρ_{tp}), or sensitivity, evaluated as

$$\rho_{\mathrm{tp}} = N_{\mathrm{tp}}/N_{\mathrm{p}} \tag{3.1}$$

  where P represents the "real" total positives.

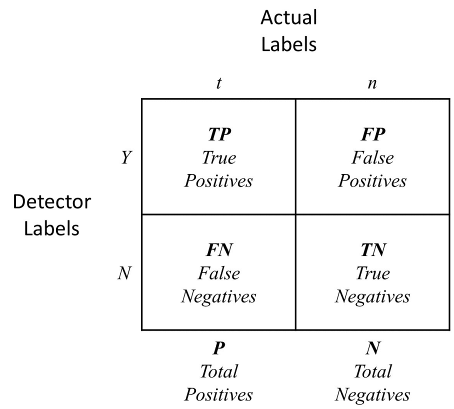

Figure 3.13: Contingency table and notations adopted for the marine debris detector.

- The specificity, S, directly related to the false positive (or false alarm) rate (ρ_{fp}),

$$S = \frac{N_{\text{tn}}}{N_{\text{fp}} + N_{\text{tn}}} = 1 - \rho_{\text{fp}} \tag{3.2}$$

The performance of the proposed detector can therefore be depicted using two-dimensional Receiver Operating Characteristics (ROC) graphs [100]. In these graphs, a diagonal line (i.e., $y = x$) is added to represent the strategy of randomly guessing a class. A single scalar representing the portion of the area of the unit square, called the Area Under the Curve (AUC), is commonly used to compare classifiers. Since random guessing produces an area of 0.5, no realistic classifier should provide a value less than 0.5.

The debris data are necessarily categorical: either binary (presence/absence) or abundance (number of objects at a given location). The developed workflow focuses on binary data, seen as the result of the fusion approach, that may be easily fitted using logistic regression, which is straightforward to implement using standard maximum likelihood [101]. However, like all linear models, logistic regression is incompatible with SAC observations since it assumes independence of errors. Thus, among several possible approaches for modeling SAC in binary data, the auto-logistic approach [55, 102], which extends the logistic model to allow dependence between nearby observations [55], was selected. Common past objections against the use of auto-models seem to be due to incorrect model implementations, providing a general conclusion of validity for auto-model analysis of SAC data [103].

Fitting the auto-logistic model can be difficult since the full likelihood is only known up to a (intractable) constant [104]. Although there are approximate methods to fit the auto-logistic model using maximum pseudo-likelihood estimation (MPLE), a simple Bayesian implementation of the auto-logistic model was adopted since it avoids many issues with MPLE including observed inaccuracies [105].

This solution can be used simultaneously for model fitting, based on covariates, and for making predictions about unsurveyed parts of the study area, and has been implemented previously in a Bayesian framework adopting the Markov Chain Monte Carlo (MCMC) methodology pioneered by Besag [55] and refined by Geman and Geman [106]. This methodology constructs a non-normalized posterior distribution for the unknown parameters and any missing observations (which are treated identically to parameters). The resulting distribution, conditional on the observations, is sampled according to one of the possible MCMC procedures (e.g., the Gibbs sampler) that guarantee that certain sequences of dependent samples (generated as successive states of a particular Markov chain) will converge to the target distribution. This Bayesian approach allows for a more flexible incorporation of possible complications (observer bias, missing data, and different error distributions) at the expense of higher computational requirements.

Case Study

Jamaica Bay, an area in the East Coast of U.S. affected by Super Storm Sandy, was selected as a test site. This area has optical imagery, bathymetry, and sidescan, as well as ground truth object detections done by hand (Figure 3.14). The area also has ENC coverage, and is covered by the predictive model.

Figure 3.15 focuses on a particular area, in the southwest region of Jamaica Bay, showing the marine debris prediction as a hot spot map. The map shows strong debris prediction in particular zones. Part of this prediction is related to there being anthropogenic structures in the area that can feed into the water there (or result in extra effects due to storm surge, for example).

Since the system is naturally scalable, it is possible to zoom in a particular subarea (Figure 3.16), so that is possible to increase the map resolution without being too computationally expensive. Figure 3.16 shows a good correlation between the high peaks in the hot spot probability map and where the human analyst selected objects.

In order to assess the benefit of adding spatial context, the detection outcomes from auto-logistic and logistic regressions were compared. The comparison was performed separately on two data sets: first, a data set was artificially created, injecting SAC as described in *Bardos et al.* [103], and second, the algorithm was applied to the Jamaica Bay data set. The resulting ROC graphs for both data sets are presented in Figure 3.17. The graphs for the artificial data set present AUC values of 0.923 (logistic regression) and 0.940 (auto-logistic regression); while, for the real survey data set, AUCs of 0.862 and 0.880 characterize the logistic and the auto-logistic regressions, respectively.

The auto-logistic implementation therefore outperformed the basic logistic model in removing residual auto-correlation. Thus, the auto-logistic model provides a better description of the observed clustering of objects, since the logistic model cannot represent clustering at all unless it is present in the covariates. Furthermore, the ROC

Figure 3.14: From top to bottom, bathymetry, backscatter mosaic, and analyst-based detection (with land/sea mask from the ENC) from Jamaica Bay, New York, NY.

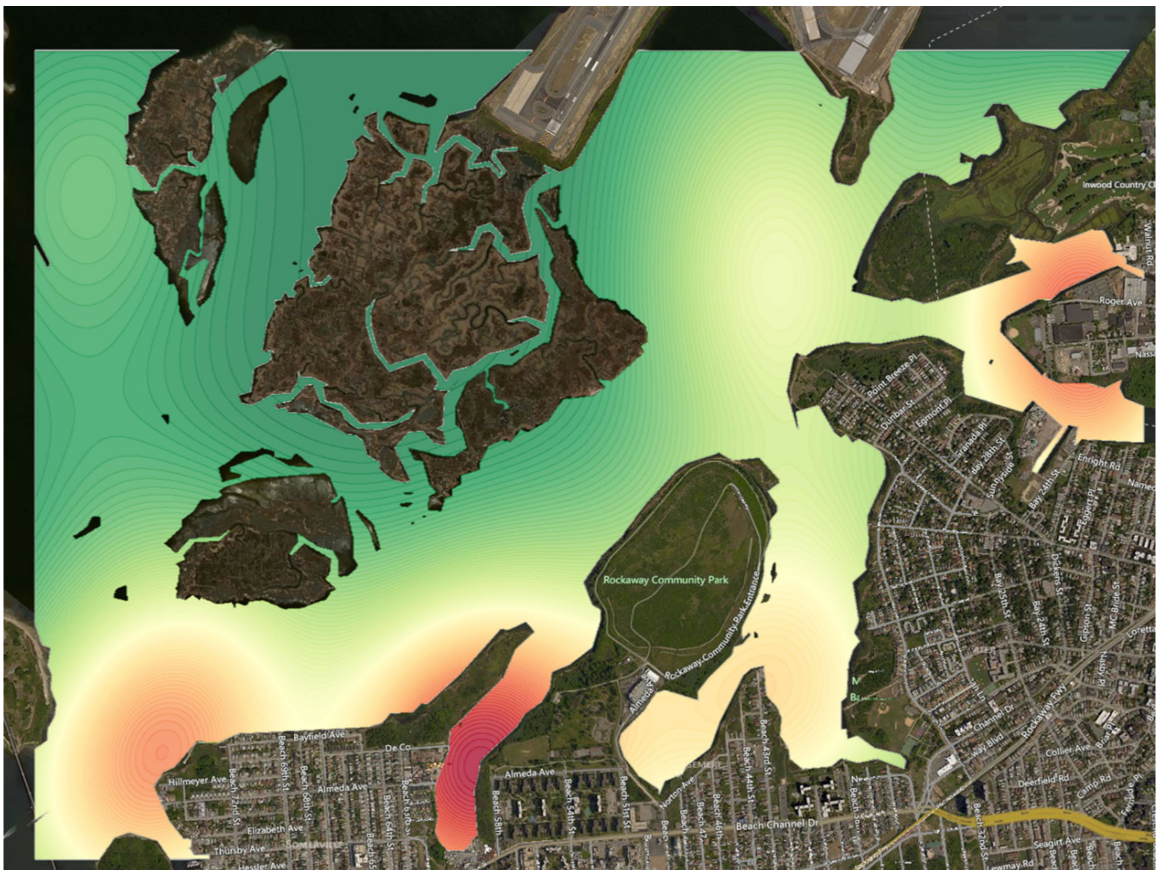

Figure 3.15: Hot spot map generated by the workflow for a particular area of Jamaca Bay, New York, NY.

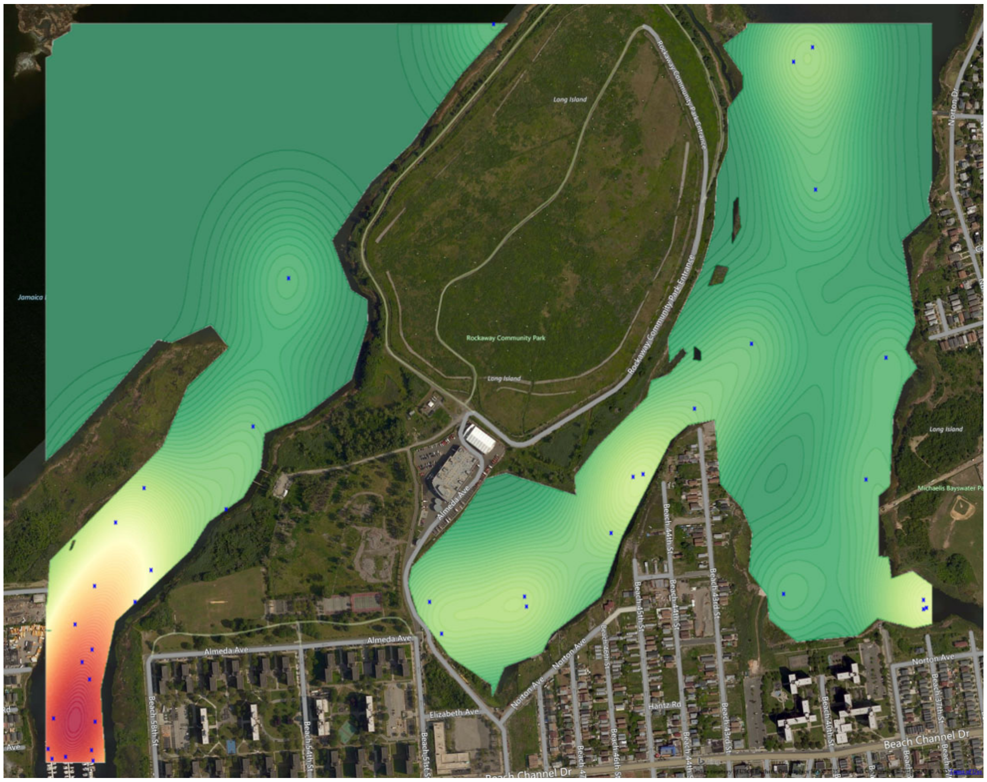

Figure 3.16: Results of the hot spot analysis in Jamaica Bay, New York, NY, with the ground-truth positions of the marine debris designed by human analysts showed as blue dots.

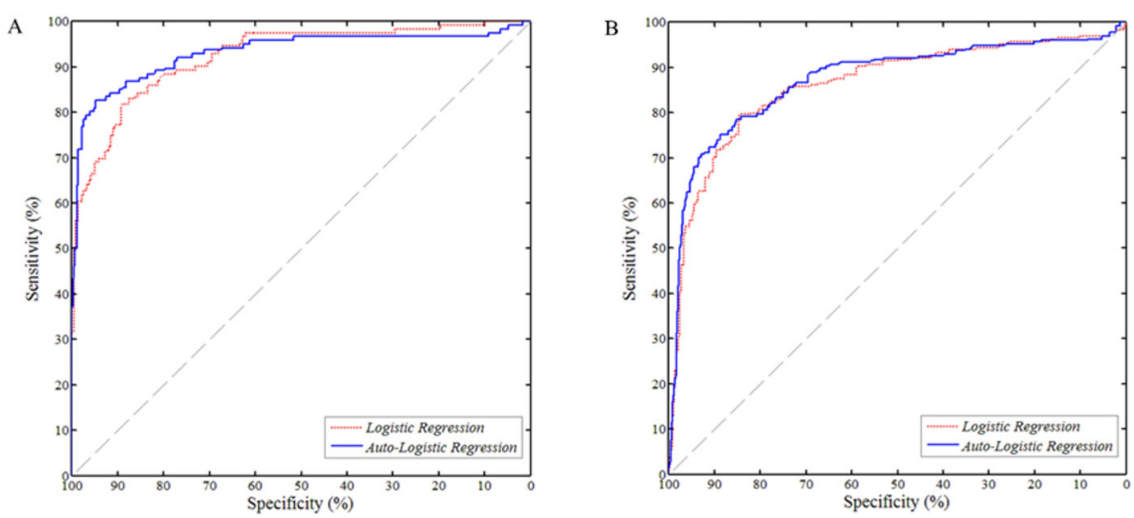

Figure 3.17: ROC curves for artificial data (pane A) and real survey data (pane B), for both logistic (no spatial context) and auto-logistic regression models.

plots indicate better overall predictive performance by the auto-logistic model due to much higher true positive rates at small false positive rates, although the logistic model slightly outperforms at low (artificial data set) and intermediate (real data set) specificity. Classifiers appearing on the left-hand side of a ROC graph (near the vertical axis), are usually evaluated as more "conservative", since they make positive classifications only with strong evidence (so they make few false positive errors) [100]. Since the marine debris detection domain is usually dominated by large numbers of negative instances, performance like the auto-logistic regression becomes more interesting.

3.5 Target Management and Data Exchange

3.5.1 Marine Object Manager

The combination of information present in bathymetric and imagery-based products is a key requirement for any modern feature-detection approach that aims to be adopted in coastal areas where the seafloor is deep enough that optic means are not reliable. If the data sources and the processing involved are correctly weighted in a fusion algorithm, the detection task can be extended beyond a simple binary (presence/absence) decision to provide a meaningful metric that evaluates confidence in the presence of new features. In combination with other existing information (such as that present in ENCs), this metric can become a proxy for areas with high probability of change (for features to be either added or removed) with respect to the baseline knowledge of the area. The dual, and partially contradictory, goals of such a system are to highlight areas with high probability of change, and to use the existing nautical documentation as a spatial filter to limit computational or operational resource consumption on known features. Determining an appropriate balance between these is an interesting challenge. However, it is recognized that the algorithms developed are never going to be perfect (very few algorithms actually are).

Based on such considerations, this work has developed an approach for how to effectively assist data analysts in combining the results of different target detection algorithms, as well as in comparing such results with existing features present on ENCs and in geographic databases (e.g., spatial database management systems). The main goal is to help the analyst in focusing on specific areas (with higher likelihood of new features), prioritizing them on safety-of-navigation criteria, and reducing the common pitfall of subjectivity in the processing workflow. Although mainly aimed at rapid response to the short-term increase in marine debris deposition related to major events like hurricanes and floods, the approach is also well suited for different scenarios such as reducing the "ping-to-chart" time.

Some prototype tools were therefore built in parallel with this workflow, with the expectation that there will always be a human operator in the loop. Objects can be detected very easily, but identifying whether they are natural or marine debris is not necessarily straightforward for an algorithm (Figure 3.18), without a level of

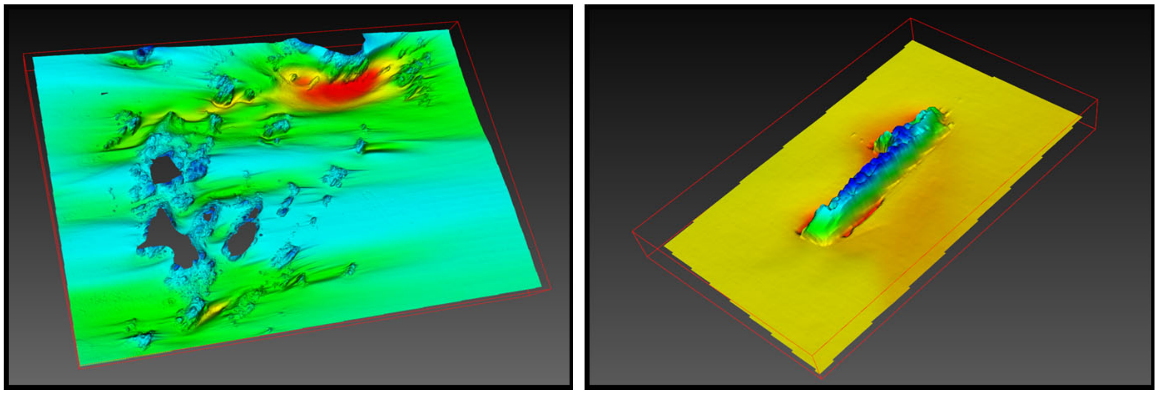

Figure 3.18: Examples of "natural" (left) and "marine debris" (right) candidates provided as output of the detection model.

sophistication in the algorithm that makes it very slow. Even the complexity of determining whether features are natural or artificial is variable, so the goal here is to provide tools to accelerate the process, supporting the human operator. Thus, for example, tools to provide useful visualization of the results of the analysis have been examined, as well as tools to assist in extraction of shape both automatically and by hand (Figure 3.19).

3.5.2 Marine Debris Markup Language

Algorithms that generate good results that go nowhere are not particularly useful. A specific consideration for this project was therefore to ensure that the results could be generated in a form that is exchangeable with other researchers and those responsible for responding to a storm event. After a marine disaster, many agencies conduct surveys collecting information that may be related in different ways to the presence of marine debris. The data acquired in these surveys can be used for planning purposes, operational support, and to manage risks associated with marine debris. Most surveys adhere to standards and best practices in creating outputs, but there is currently a lack of standardization for debris detections, which are typically delivered in unstructured CAD and GIS files. Although flexible, this lack of structure makes integration and interoperability with these files difficult. This make sharing marine debris data difficult.

A collaboration with NOAA's Marine Debris Program was therefore undertaken to jointly evaluate how this data can be better managed; the result is a Marine Debris Markup Language (MDML).

This model provides a common vocabulary to describe marine debris based on sound geo-information management principles and practice, which could be used to provide guidelines for the acquisition of marine debris data in future events. The

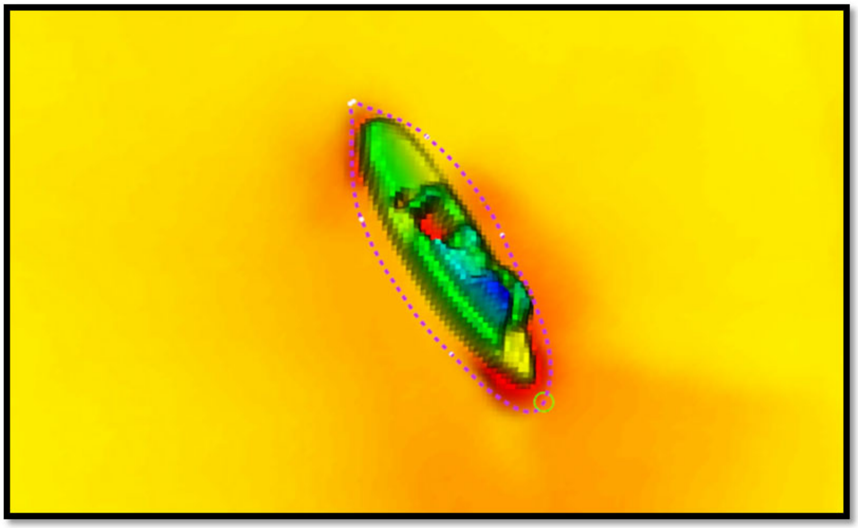

Figure 3.19: Example of an auxiliary tool provided to the analyst to define the shape of the target. Here, the analyst can define the shape of the object interactively; other techniques to assist in semi-automatic shape extract from objects have also been investigated.

MDML template is implemented using a GML[2]-aware XML[3] schema that is the *lingua franca* for geographic data exchange (Figure 3.20). However, in principle the data model can be implemented in any GIS and transferred via an open GIS data exchange format (Figure 3.21). Because the schema uses the Open Geospatial Consortium GML Encoding Standard and the GML Simple Feature Profile (Level Zero), many applications are already able to process MDML data files, thus supporting intra- and inter-community interoperability.

Building onto a standard feature profile provides the opportunity to build something that is easily reconstructed in standard OGC tools, such as GDAL, etc. The advantage is that output that uses the Marine Debris Markup Language can be readily imported in other tools, without any extra effort.

3.6 Summary

The problem of marine debris identification is complex, particularly because what is being sought is not particularly well defined (i.e., there is no real good definition of what marine debris really is). Thus the workflow developed assumes having to deal with this variable situation. The workflow defines a selection of algorithms that, although not entirely reliable individually, together permit fusion into a solution that

[2]Geographic Markup Language.
[3]Extensible Markup Language.

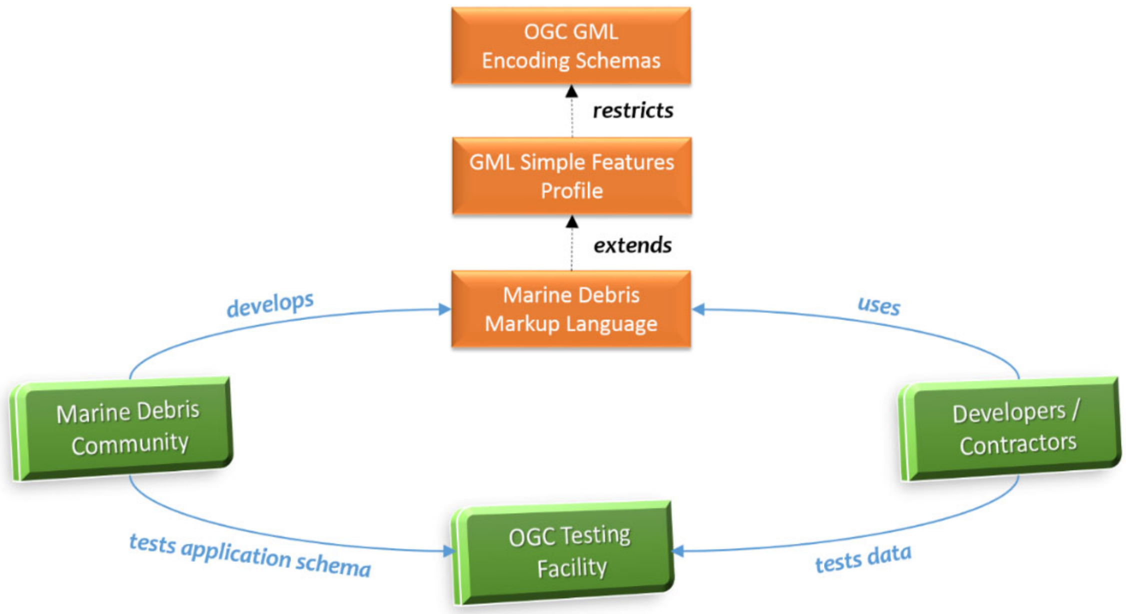

Figure 3.20: Interactions between the community interested to marine debris data and users of the Marine Debris Markup Language (MDML). MDML uses several of the primitives defined in GML Core Schemas as restricted by GML Simple Feature Profile (Level Zero).

is reliable and useful. Given this structure, extensions to the algorithm for better predictive models and detection algorithms are obvious.

As described in the previous sections, the current workflow provides a way to structure a complex problem by merging the output of different algorithms (including prior constraint information) into a probabilistic hot spot map that is easy to understand. A partially open question is whether including additional detection algorithms actually improves the performance. The current conjecture based on some testing is that is not always the case. These results can be explained by the fact that the more metrics that are generated from the algorithms and then used in the fusion, the more likely it is that they cause more confusion in the detection that is gained from having the extra algorithm included. What is desired is a limited number of independent algorithms that provide independent views to the data.

The Bayesian approach used here allows for a more flexible incorporation of possible complications (observer bias, missing data, and different error distributions) and prior beliefs at the expenses of higher computational requirements. Furthermore, a good understanding of the influence of prior distributions and convergence assessment of Markov chains is crucial to properly evaluate the method's results. The scalability of the fusion technique permits its straightforward extension to additional detection algorithms for *ad hoc* created data products, with expected improvements both in robustness against outliers and in detection performance. Given the flexibility of such

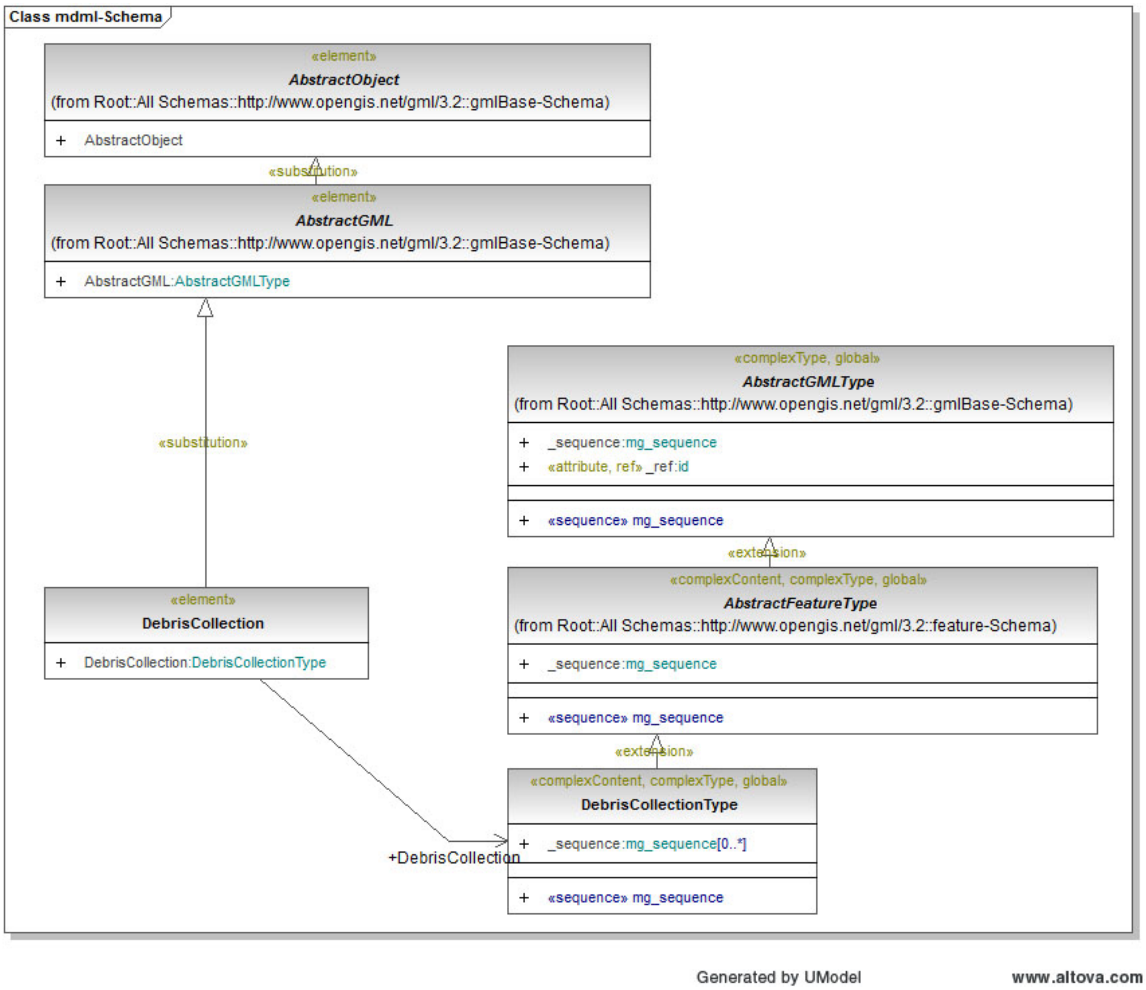

Figure 3.21: Details of the MDML implementation: each class, as the DebrisCollection class in the diagram, is derived from GML abstract elements that have proper counterparts within other spatial object models (e.g., ESRI Data Model).

a framework, it is possible to extend the detector with a set of *ad hoc* hydrographic products. Although the probability of false alarm based on a combined analysis of multiple data sources is expected to be generally lower than when a single source is used, there are particular cases where a particular object might only be observable within a single data source. For example, a semi-buried target, or one with a flattened shape, might only be visible through acoustic backscatter. A careful analysis of the benefits of different algorithms and different data sources is therefore indicated in case of future research along the direction shown by this approach.

From a more general point of view, it is believed that the outcomes of this project can be used to improve current hydrographic data processing for target detection. Since the current processing is usually subjective and time consuming, increasing the automation of the process would be beneficial in subjectivity reduction.

Chapter 4

Improving Storm-Response Surveying with PMBS Echosounders

4.1 Introduction

Hydrographic surveys are required after major storm events to ensure that navigationally significant waterways are sufficiently clear of debris to support delivery of recovery supplies and resume normal commercial activity. Under non-response conditions, hydrographic surveys in shallow ports and harbors typically employ multibeam echosounders (MBES) to acquire high-accuracy depth and uncertainty data with ample overlapping swath coverage on adjacent ship tracks. Survey operations in response scenarios are naturally limited in time available for planning and must necessarily focus on the rapid detection of new hazards and significant seafloor changes within channels and harbors. The efficiency of these operations depends to a large degree on the swath coverage achieved and swath overlap required to ensure detection of hazards. Thus, a major challenge for rapid response surveying in these shallow water environments has been the geometric swath width limitation of traditional single-head MBES systems, which yield typical across-track coverage of up to approximately five times the echosounder altitude above the seafloor.

In the last decade, a type of echosounder called a phase-measuring bathymetric sidescan (PMBS) has come into widespread use for shallow water applications. PMBS systems are also known colloquially as phase-differencing sonars, bathymetric sidescan, or interferometric sonar. These echosounders use multiple transducer arrays on the port and starboard sides to collect traditional sidescan backscatter amplitude data as well as to estimate the angles of arrival for acoustic returns at each sample range. Much like the range and angle data produced by MBES, the PMBS angle(s) of arrival calculated for sample ranges are used to estimate depths of bottom returns where the minimum amplitude (and other) criteria are satisfied. This "dual-head" PMBS configuration supports a broad swath width, up to and including angles above the depth of the echosounder (e.g., up to 220° total swath width for some models) to allow surveys of steep slopes and vertical features in shallow environments. Like MBES data, PMBS sounding accuracy decreases markedly at large ranges and shallow angles of incidence on the seafloor; however, the value of this outer swath region for object detection is augmented strongly by acoustic shadows in the co-located sidescan imagery.

PMBS systems can therefore have a number of advantages when applied to a storm response scenario. PMBS systems have had a limited application for hydrographic surveys due to the properties (and volume) of data that they produce. The work conducted during this project has attempted to assess the applicability of PMBS systems to storm response scenarios, developing techniques to mitigate the difficulties of using PMBS systems, and making recommendations on best practices for their use. Specifically, basic processing difficulties have been addressed through the use of semi-automated techniques, and questions of object detection and preservation, which are a significant concern for PMBS systems, have been examined as a function of processing parameters. The work also considers questions of how best to design surveys for storm response, how to integrate PMBS systems into standardized workflows in commodity software, and develops some ideas for how to better utilize all of the sources of information available from a PMBS. As part of the work reported here, a number of white papers and other reports have been generated, and are available on the project website, `http://sandy.ccom.unh.edu`. The reader is directed to these documents to provide greater detail on each topic[1].

4.2 Historical Challenges of PMBS

Challenges during adoption of PMBS systems into existing hydrographic workflows have historically been related to sparse sounding density near nadir, high sounding density away from nadir, lack of (or insufficient software support for) echosounder uncertainty information, and high standard deviations of soundings compared to bottom detections provided by beamforming echosounders (i.e., MBES). For example, Figure 4.1 demonstrates the density and "noisiness" of raw soundings over flat seafloor near Redbird Reef, Delaware, a site impacted by Super Storm Sandy.

A noteworthy problem with a number of PMBS systems has been low sounding density—or, in some cases, complete lack of data—in the nadir region. Figure 4.2 illustrates the issue, resulting primarily from the geometry of the intersection of the spherically spreading transmit pulse with a planar seafloor such that few measurements are possible. In addition, the effect of baseline de-correlation tends to increase the uncertainty in the receive angle measurement that is fundamental to PMBS bathymetry [107]. Because of these issues, the sounding density at nadir is often reduced when imaging a planar seafloor with most PMBS systems. Klein systems, for example, have, until recently, opted to omit data wholesale from this area, leaving a

[1]Footnotes are used to indicate specific locations within the website.

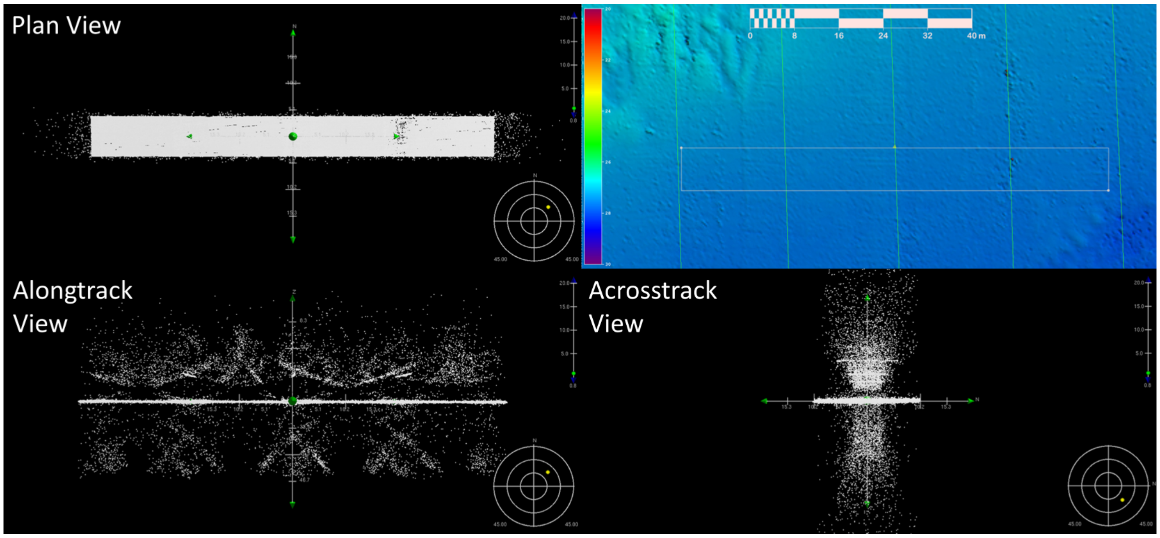

Figure 4.1: Example PMBS data collected at Redbird Reef, Delaware. All data from the middle three lines (top right) are shown, as well as depth estimates from approximately half the swath from the outer two lines. The along-track views highlight the elevated scatter in the raw soundings and the patterns in outliers along each line.

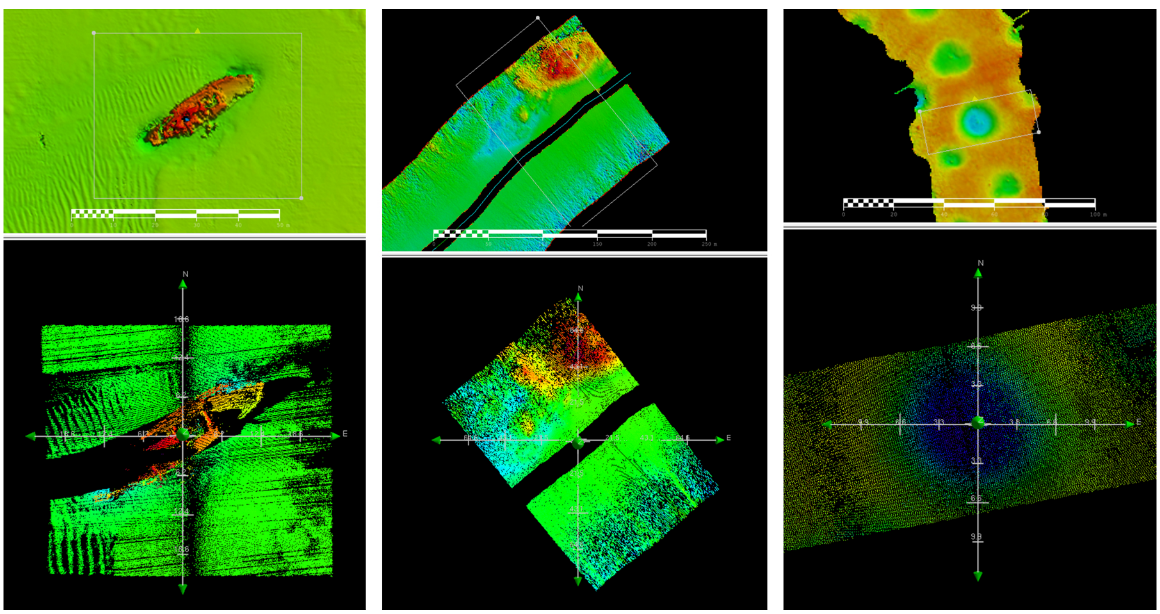

Figure 4.2: A subset of depth estimates collected in separate surveys with three different PMBS echosounders illustrating the nadir gap effect. Low data density is evident near nadir for the system on the left and no data is apparent in the middle example, though recent software supports reprocessing of raw data files to fill the nadir gap (2015). The effect of low sounding density near nadir is largely mitigated by wider bandwidth and different binning techniques for the system on the right.

large nadir gap below the sonar. However, in recent years, PMBS manufacturers have largely addressed this issue. For example, the EdgeTech 6205 PMBS[2] transmits wider bandwidth pulses ($\sim 65\,\text{kHz}$), decreasing the effective transmitted pulse length, and therefore increasing the number of soundings possible in the nadir region. Moreover, the decrease in raw data density in EdgeTech systems is frequently not apparent to the user, as raw measurements may be binned by angle or range within each ping to report only the average measurements within each bin. Any decrease in data density near nadir may not be apparent unless the gaps grow larger than the selected bin size. In addition, Klein systems now produce soundings through nadir[3], where no attempt to produce nadir data was made previously. Although uncertainty in the angle measurement increases at nadir, the geometry of the measurement is such that this translates to increased uncertainty primarily in horizontal positioning rather than vertical depth measurement. While this increase can make object recognition difficult it does not generally negatively affect object detection, especially when coupled with scrutiny of sidescan imagery.

As with any echosounder used for hydrographic purposes, a calibration must be performed to determine the angular offsets between the transducer arrays and active motion sensor. Conventional calibration procedures ("patch tests") use a series of survey lines over prominent features at various headings, across-track offsets, and speeds to determine the pitch, roll, and yaw of these systems as-installed. These tests are routinely applied for MBES systems but become complicated or impossible for PMBS systems that produce sparse or zero soundings near nadir. Working with Jonathan Beaudoin[4], a process has been developed (currently in preparation for publication) for calibrating PMBS systems by repeatedly surveying a distinct seabed feature in reciprocal directions at increasing across-track distances. Careful scrutiny of the calibration data allow the user to estimate the pitch bias (constant with across-track range) and yaw bias (proportional to across-track range) separately, while roll is determined using the conventional method of examining the outer swath on reciprocal headings over flat seafloor.

Therefore, while these issues are not wholly resolved, great strides have been made, largely by industry, in mitigating their negative effects. The decrease in nadir data density results from the physics and geometry of the measurement process and as such cannot be fully eliminated in all circumstances. However, in shallower waters ($< 15\,\text{m}$), with high-bandwidth systems and binning of data, the effect can be largely mitigated. In addition, the challenges to calibrating Klein systems that resulted from a complete omission of data at nadir are now eliminated with newer processing methods that produce a full swath of data. Echosounder uncertainty information is now provided by several manufacturers, allowing better use of statistical data cleaning and gridding methods such as CUBE to effectively address the data density and "noisiness" issues.

[2] Released in 2014

[3] As of SonarPro version 12.2, released in 2015

[4] Formerly of CCOM and now with QPS, b.v.

4.3 Considerations for Object Detection when using PMBS Echosounders

A primary task of response and routine surveying is to distinguish navigational hazards from measurement noise and outliers, and ultimately preserve the hazards throughout the processing chain. Though PMBS systems generate co-located sidescan imagery with the depth data, the investigation of hazards requires quantification of least depths through careful scrutiny of the available bathymetric data. Example datasets in Sandy-impacted regions were examined for object detection using depth data alone and in conjunction with sidescan imagery to improve hazard identification, especially in the outer swath region which is critical for increasing survey efficiency in response scenarios.

Figure 4.3 demonstrates an example of depth data collected with a PMBS system mounted on an autonomous underwater vehicle (AUV) while surveying over a sunken barge at Redbird Reef, DE. The raw soundings include widely scattered watercolumn targets and a transducer "ring-down" artifact following the path of the AUV. In this example, the primary challenge is to identify and preserve the barge and its railing in the processed data while rejecting less reliable, non-hazard soundings. The CUBE algorithm implementation in CARIS HIPS was applied to generate a "first-pass" surface which was then used as a reference surface for a subsequent round of data filtering to omit gross outliers and ensure the correct hypothesis is chosen. The result, shown in Figure 4.3, captures the barge and most of the top railing, highlighting the ability of statistical methods to extract the most likely targets in a noisy data set.

Registering the depth of an object, or a piece of marine debris, in the raw measurements from any sonar is not sufficient to ensure that the object is "detected." For that, the object has to be maintained throughout the processing chain until it is inspected by a human operator (or a suitable algorithm). The behavior of gridding algorithms, therefore, can be critical to the success of object detection. The Redbird Reef data set and another dataset collected at two sites near Long Island, NY, were used to examine the effects of gridding parameters on preservation of objects through data processing without manual editing, using commercially available software. Objects ranging from approximately 1–2 m in all dimensions (fish habitat structures) to at least 10 m horizontally and protruding more than 3 m from the seabed (shipwrecks) were present at both Sandy-impacted survey sites.

Trends in all datasets gridded at 10–100 cm suggested that broadening vertical distributions of soundings in the outer swath, as expected due to increasing angular uncertainties and refraction artifacts, presented the greatest challenges for object detection. The apparent data "noisiness" was effectively suppressed as grid size approached 100 cm but became a serious complication for object detection at grid sizes smaller than 30 cm (Figure 4.4). Depth anomalies present in regions covered by single survey passes could not be confirmed as objects or ruled out as purely acoustic artifacts. Such anomalies require additional data collection, highlighting the utility of a data acquisition method which examines bathymetry and sidescan imagery in real-

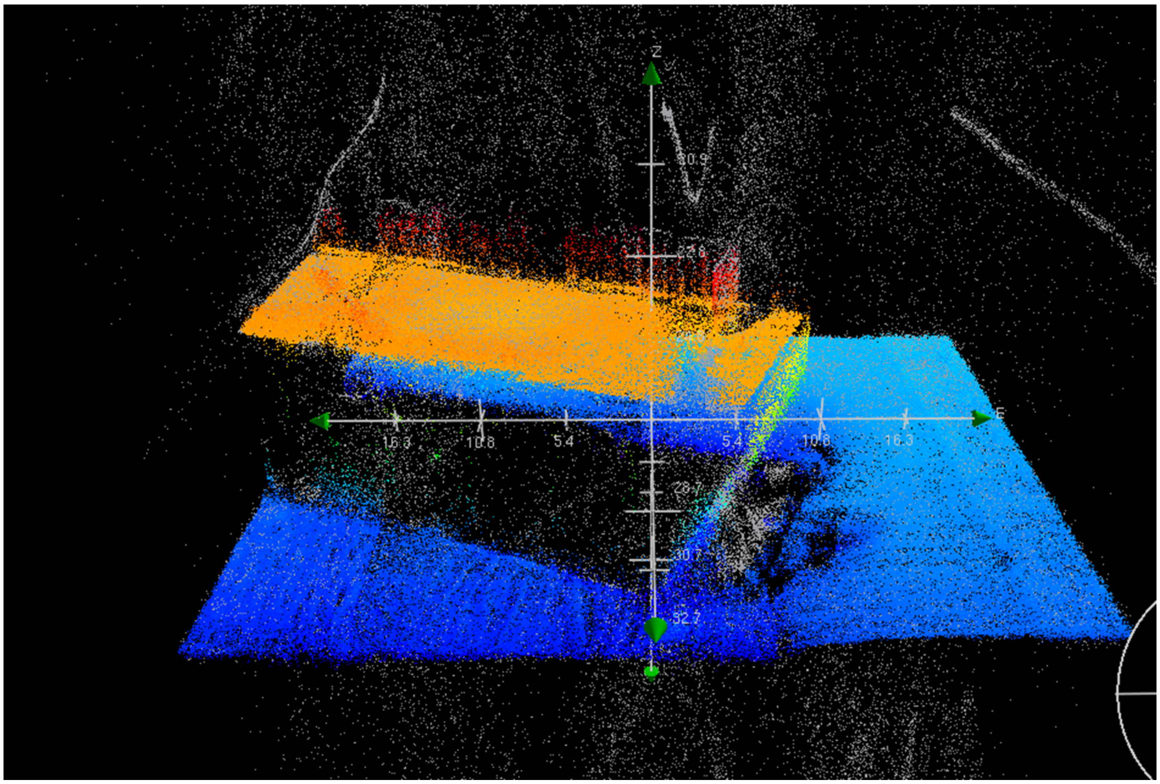

Figure 4.3: In this example of PMBS data collected at Redbird Reef off the Delaware coast, a combination of the CUBE algorithm and a subsequent surface filter for outlier rejection successfully omits a large portion of noise (gray soundings) while retaining a sunken barge and railing along its top edge (colored soundings). Coherent lines of noise in the top of this image result from the transmit pulse captured in the sonar data, depicting the approximate path of the autonomous underwater vehicle used for data collection; these points are correctly rejected in this example.

time, identifies targets requiring additional data, and resurveys these targets in swath regions where data quality may be higher. Toward this end, a conceptual interface for streamlined scrutiny of all PMBS data products was developed (Section 4.6).

In evaluating the ability to effectively locate objects of various sizes in PMBS bathymetric data, an important distinction was noted between detecting an object in the gridded surface (e.g., recognizing a region of elevated depth estimates) and identifying the object (e.g., recognizing the features of a sunken vessel). The gridded surfaces were found to preserve the general presence and shapes of objects of all sizes, but were insufficiently detailed for object recognition in most cases. Object identification was possible only after closer scrutiny of subsets of raw data from multiple viewing angles and benefitted greatly from the associated sidescan imagery. While this would also probably be the case for MBES data, the smallest objects of interest in these PMBS datasets (fish habitat structures 1–2 m in horizontal extent and 1 m in vertical relief) required additional scrutiny of the raw soundings to ensure that the objects were detected in multiple survey passes and were not simply acoustic artifacts (Figure 4.5).

The objects in the Redbird Reef and Long Island datasets were surveyed using different PMBS sonar systems and processed rapidly without manual editing. In both cases, the utility of a gridded bathymetric surface for object detection depended heavily on the grid size. Resolution of approximately 30 cm, which approximately matches the along-track sounding density, was found to provide a reasonable compromise between suppression of outliers and preservation of detail. In fact, comparison of gridded surfaces at multiple resolutions became a useful tool in evaluating changes in object appearance or contextual clues, such as scour and bedforms, to build confidence in detection of an object. All cases benefitted greatly from overlapping survey passes which were used to corroborate the presence of an object or support rejection of an artifact, highlighting the need for additional data when potential objects are identified. In this regard, the capability of the processing method for object detection and recognition depends heavily on the data acquisition method. Several recommendations for processing were provided in the document "Object Detection with Phase-Measuring Bathymetric Sidescan Sonar Depth Data."[5] These observations, in turn, correspond to additional recommendations for PMBS and MBES surveying outlined in the documents "Storm Response Surveying with Phase-Measuring Bathymetric Sidescan Sonar"[6] and "Object Detection and Storm Impact Evaluation with Bathymetric Sonar Systems."[7]

In summary, work with these data sets suggests that binning of data within a ping and reporting the average or median measurement within each bin is preferable, in general, to reporting raw soundings for object detection. Doing so reduces confusion in scrutinizing raw soundings to quantify hazards to navigation. When fixed bin sizes are used, they should be set commensurate with both the hydrographic requirements

[5] http://sandy.ccom.unh.edu/publications/library/Object_detection_with_PMBS.pdf

[6] http://sandy.ccom.unh.edu/publications/library/Response_surveying_with_PMBS.pdf

[7] http://sandy.ccom.unh.edu/publications/library/Object_detection_storm_impact_with_PMBS.pdf

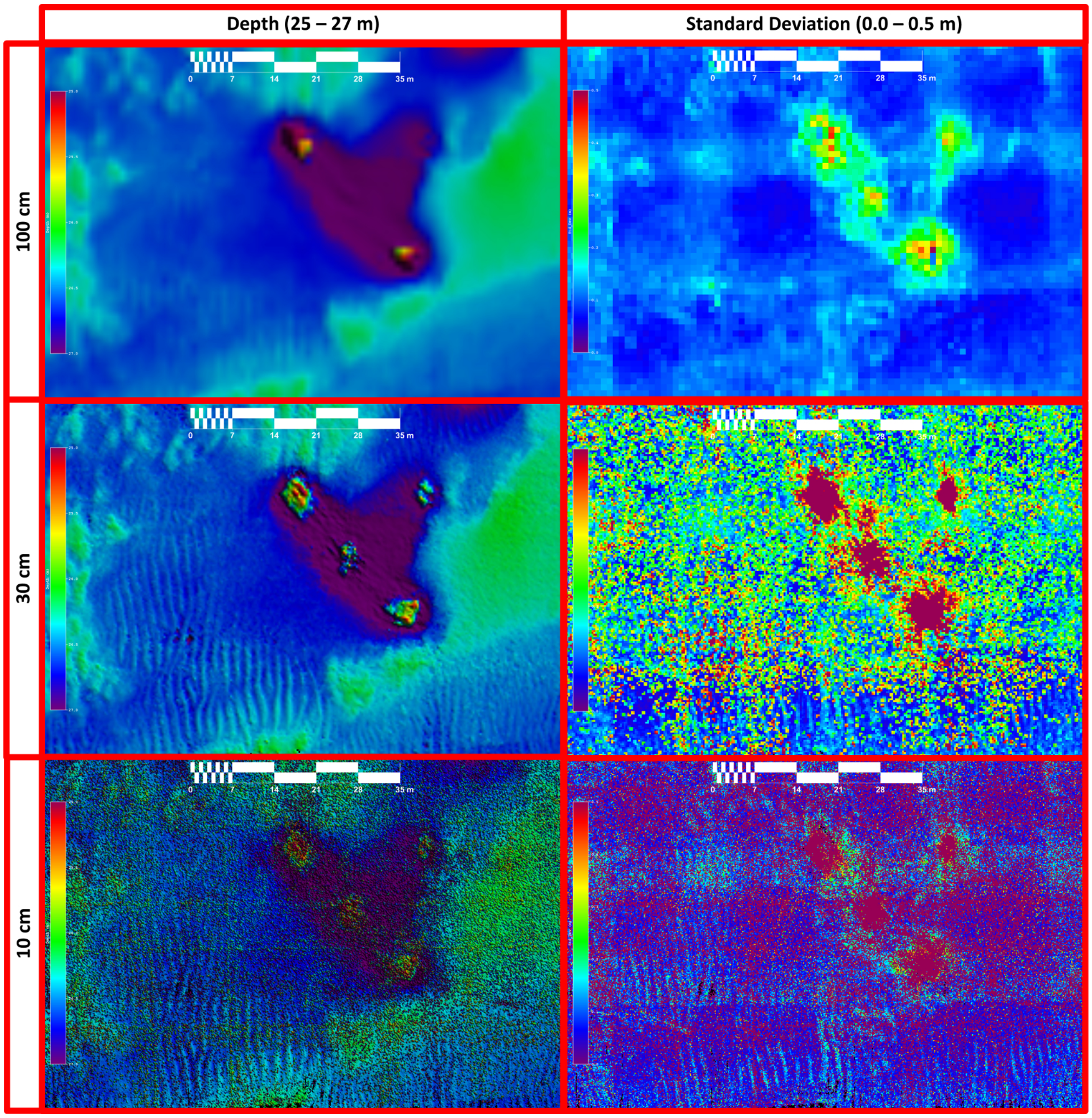

Figure 4.4: Depth and standard deviation of soundings in each grid cell may be used in conjunction to detect objects. The depth scale (left column) ranges from 25 m (red) to 27 m (purple) and the standard deviation scale (right column) ranges from 0 m (dark blue) to 0.5 m (purple); the scale bar is 35 m in total length in all images. The central portion of the overlapping subway cars is not visible in the depth surface gridded at 100 cm but stands out in the depth surfaces gridded at 10 cm and 30 cm; this region also stands out in all standard deviation grids. Sand waves on the order of 2–3 m in wavelength and 0.5 m in relief are clearly visible in the 30 cm grid, but appear overly smoothed in the 100 cm grid and partially obscured by surface artifacts in the 10 cm grid. These images demonstrate the utility of gridding at multiple resolutions to determine grid sizes appropriate for the dataset as well as highlight changes between grids which may indicate the presence of objects.

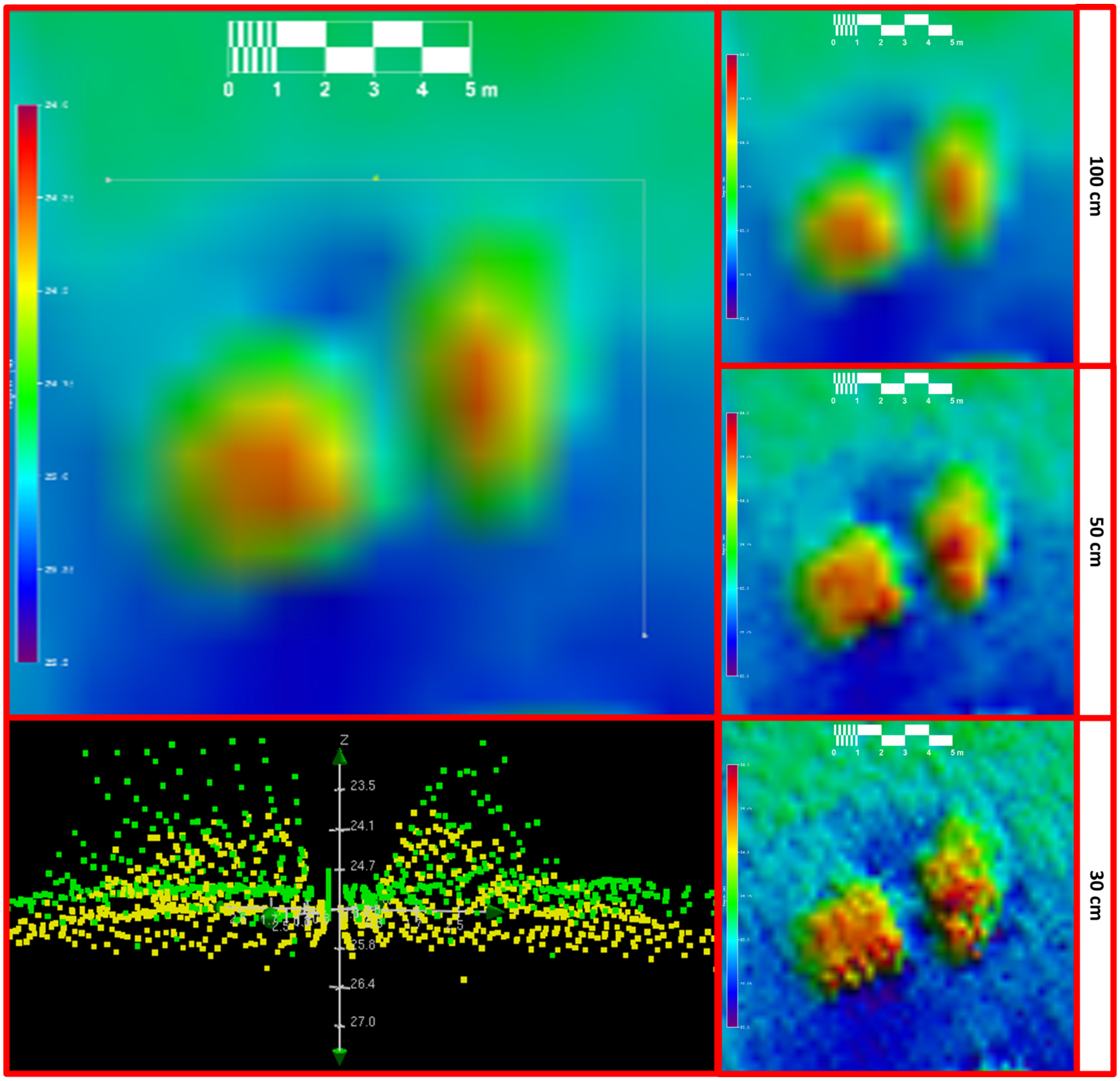

Figure 4.5: Two structures separated by approximately 5 m are clearly visible in bathymetric surfaces gridded at 100 cm (top two images), 50 cm (middle right), and 30 cm (lower right). The color depth scale ranges from 24 m (red) to 25.5 m (purple); the scale bar is 5 m total length in all images. A northwest-looking subset of the raw data colored by line (yellow and green soundings, lower left) indicates that these objects are evident in two independent survey passes, increasing confidence in their detection but not necessarily supporting their identification.

for object detection for the survey and not smaller than the along-track ping spacing to ensure sufficient data density for gridding. (Gridding itself is typically done at coarser resolution, however matching bin size with along-track ping spacing ensures a homogenous distribution of data to each grid node.) Furthermore, interpretation of bathymetric data is greatly enhanced by viewing it with the associated imagery simultaneously. These recommendations are elaborated upon in Section 4.5.

4.4 Storm Response Survey Protocols

The evaluation of typical PMBS sonar parameters and comparison of CUBE surfaces created with various line spacing strategies highlighted several factors to consider when planning storm response surveys intended to identify navigationally significant objects and seafloor features while maximizing efficiency of operations. In particular, low sounding density at nadir (typically between 0–30°) and elevated uncertainties of outer swath soundings collected with PMBS systems highlight the importance of the co-located sidescan imagery for effectively extending swath coverage (e.g., Figure 4.6). Recommendations for survey planning were developed to maximize the across-track distance over which hazards are likely to be detected, thereby increasing survey efficiency through wider line spacing and providing additional overlapping coverage only in areas identified as potential hazards. These recommendations include line spacing of 8× water depth with slightly larger sonar range settings to ensure overlap; evaluating sidescan imagery carefully in the outer swath where bathymetric measurements are more noisy; and resurveying hazards at favourable geometries of 1–3× water depth when quantifying their shoal-most extent. These suggestions are outlined in the document "Storm Response Surveying with Phase-Measuring Bathymetric Sidescan Sonar."[8] Six related "best practices" based on the examinations of PMBS and MBES data are detailed in the document "Object Detection and Storm Impact Evaluation with Bathymetric Sonar Systems"[9] and highlighted below for ready reference.

4.5 Best Practices for Post-Storm Operations

Here the "best practices" developed during this research are listed concisely for ready reference, with further discussion provided in the document "Object Detection and Storm Impact Evaluation with Bathymetric Sonar Systems."[10]

1. Collect acoustic water column or sidescan imagery. Interpretation of bathymetric data sets for object detection is significantly enhanced by the availability and use of full resolution acoustic imagery, such as sidescan backscatter amplitude

[8] `http://sandy.ccom.unh.edu/publications/library/Response_surveying_with_PMBS.pdf`

[9] `http://sandy.ccom.unh.edu/publications/library/Object_detection_storm_impact_with_PMBS.pdf`

[10] `http://sandy.ccom.unh.edu/publications/library/Object_detection_storm_detection_with_PMBS.pdf`

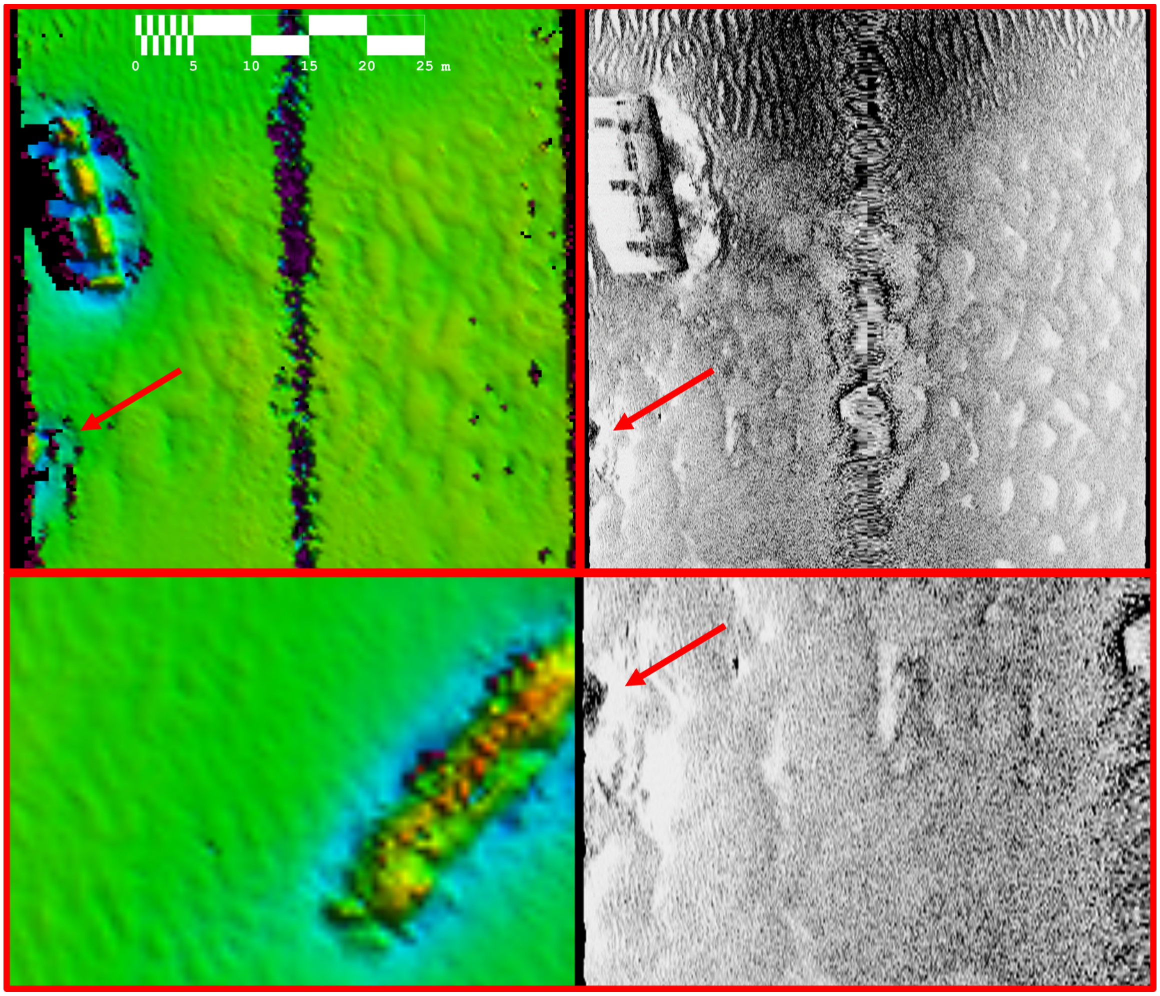

Figure 4.6: PMBS systems offer survey efficiency gains through increased angular swath width and real-time analysis of co-located bathymetry data and sidescan imagery. In the upper left image, one complete sunken subway car at Redbird Reef, DE, is detected in PMBS bathymetry data from a single survey line. The bathymetry includes a region of apparent scour (red arrow). PMBS sidescan imagery from the same line (upper right) assists in the identification of the complete subway car and also suggests the presence of scour and another object near the limit of the swath (red arrow). The lower composite image provides a closer view of the sidescan data showing the potential object in the outer swath (red arrow, lower right) with georeferenced bathymetry from additional survey lines (lower left) confirming the presence of a second subway car. This example demonstrates the potential for efficiency gains in response scenarios by increasing survey line spacing, evaluating sidescan imagery where bathymetric data may be inconclusive, and conducting more detailed surveys only when potential objects are detected.

for PMBS systems and water column backscatter data for MBES. Where the inspection of water column data is possible, it is preferable to seafloor backscatter or snippet data from MBES systems.

2. Examine data in real time. Small objects that are readily apparent in acoustic imagery frequently are not reliably captured in bathymetric measurements. For this reason, operators must scrutinize imagery in real-time or near-real-time, identifying potential hazards quickly enough to provide opportunities for additional data collection at a variety of headings and athwartship distances to better quantify their shapes and least depths.

3. Scrutinize the outer swath. Both dual-head MBES and standard PMBS systems provide the capability to generate swath widths beyond 65° ($\sim$ 4.25 times water depth, or WD) from nadir. When refraction conditions are favorable, swath widths meeting IHO Order 1 standards for bathymetry [108] are possible exceeding 75° ($\sim$ 7.5 WD), and object detection capabilities are enhanced by acoustic shadowing at these shallow angles. However, the object measurement capabilities of both systems typically suffer in the sounding data beyond 65°, such that these portions of the swath cannot be used reliably for object quantification. A strategy is required that carefully scrutinizes the outer swath for hazards to navigation and provides opportunity to revisit them in more favorable survey geometries for proper quantification of least depths.

4. Utilize systems with real-time uncertainty and in-ping averaging techniques. When using NOAA's standard metrics [109] for meeting IHO requirements for hydrographic surveys, PMBS systems that provide the capability to estimate real-time measurement uncertainty and to bin and average the raw bathymetric data across each ping have been shown to perform well and fit readily into the existing data processing pipeline. Bin averaging can be used to reduce uncertainty and density of the resulting soundings to acceptable levels while still maintaining significant features. In addition to examining the raw data, the ability to vary the bin size or method for processed soundings is also advantageous when investigating suspected targets. For example, binning by angle may achieve many of the density and uncertainty benefits while preserving separate targets observed at the same range. Acoustic imagery such as sidescan backscatter should always be retained at the full resolution for scrutiny of targets.

5. Use PMBS systems without real-time uncertainty and binning options only with great care. PMBS systems without real-time uncertainty of their bathymetric measurements and binning and averaging of data can still be used effectively for object detection and meeting of IHO standards for hydrographic survey. However, the methods used for processing these data sets and their quantification for IHO purposes are fundamentally different from other systems. Specifically,

because the data must be used to estimate the uncertainty empirically, care must be taken to filter data only for outliers and not the "tails" of the natural distributions of measurements, which may be wide or "noisy." It is important to consider the difficulty in establishing the quality of any individual raw sounding other than statistically when taken as part of a larger group of soundings. Given sufficient data quantity and quality (and while ensuring careful scrutiny of the raw soundings and sidescan imagery over hazards), it is appropriate to use gridded surface estimates in lieu of individual soundings to quantify potential hazards to navigation.

6. Generate CUBE surfaces using NOAA guidance for shallow water [110]. MBES and PMBS data should be gridded according to NOAA's current standard practices. Specifically, it is recommended that the CUBE algorithm be applied at a 0.5 m grid spacing for water depths less than 20 m. NOAA's standard CUBE processing parameters ensure that no single sounding contributes to more than one grid node, thereby avoiding any "smoothing" effects that could obscure detection of small objects.

   When these parameters are used, it is estimated that the lower limit of object size detectable by routine visual inspection of a bathymetric surface of this type is 1 m (the standard IHO requirement for object detection), only when the bathymetric uncertainty of the seafloor (taken as the standard deviation of the combined seafloor roughness and depth measurement) is less than 20 cm (1-sigma).

4.6 Improving Integrated Analysis of Bathymetry and Sidescan Imagery

The sidescan imagery provided by PMBS systems is critical for extending the swath width for which they are useful for detection of objects to longer ranges and lower angles of incidence on the seafloor, where depth data typically become least reliable for this purpose and may be filtered by gridding methods. For example, Figure 4.7 presents an example of a mooring chain that is detected in raw soundings and readily identified in the sidescan imagery but not represented in the gridded bathymetric surface. A noteworthy challenge of integrating PMBS systems for response surveying is to ensure rapid and complete review of all available data streams to ensure detection of all possible hazards.

However, the tools for examining sidescan imagery in traditional bathymetry processing software packages do not provide intuitive layouts for identifying correlated anomalies in depths and sidescan amplitudes which would be strong indicators for object presence. In an attempt to address this issue, NOAA's Hydrographic Surveys Division has created their own toolset called "Pydro" which, among many other things, allows 2D geographic plotting of targets previously identified in sidescan and

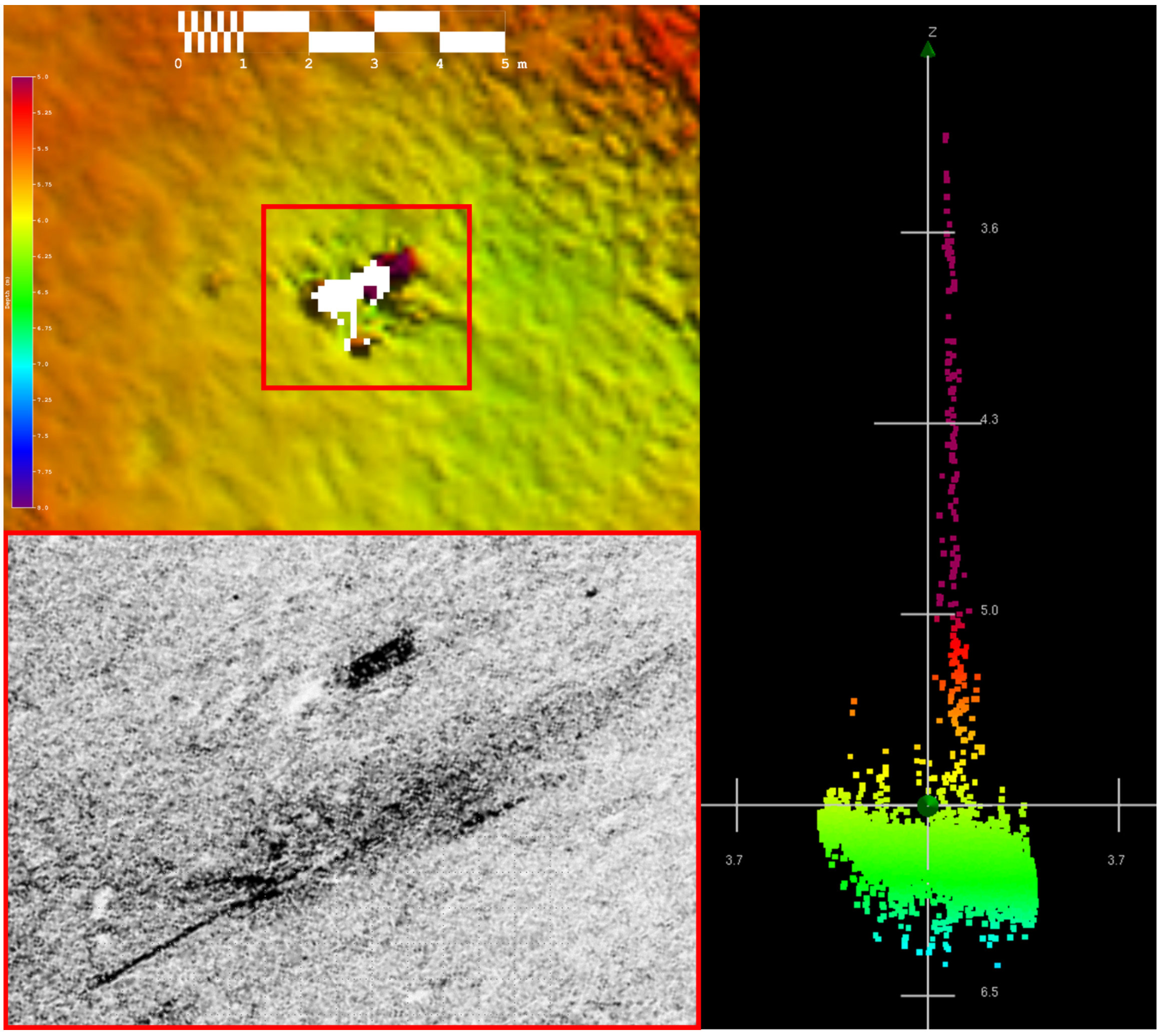

Figure 4.7: Example PMBS bathymetry (upper left) and sidescan imagery (lower left) over a mooring block and chain. The chain appears clearly in the sidescan imagery and is detected in a subset of raw soundings (right), but treated as an outlier in the gridding process.

bathymetry datasets, allowing users to correlate common hazards into a single target. This process could be improved by a new tool having a more ready and holistic view of the raw data when identifying the targets and correlating them between datasets. Towards this end, a conceptual data processing interface has been developed which enables the sonar operator to examine raw soundings, full-resolution sidescan imagery, and processed depths with on-the-fly adjustability for filtering and gridding parameters. Other tools available in the interface help the user to identify the same location in multiple displays (e.g., gridded bathymetry, sidescan, and sounding subset) and model the range from the vessel to a sidescan target within the sounding subset. This interface would ideally be used during the survey to quickly identify targets of interest and prioritize regions for more detailed data acquisition. Figures 4.8 and 4.9 present screenshots of the prototype interface, which is discussed alongside other acquisition and processing recommendations in the document "Object Detection and Storm Impact Evaluation with Bathymetric Sonar Systems"[11] available on the project website.

4.7 Integrating PMBS in the Traditional MBES Survey Framework

In order to more fully incorporate PMBS systems for routine and response surveying, it is important to demonstrate the performance of these systems in comparison to traditional "benchmark" survey platforms (e.g., MBES) and incorporate existing data processing paths. The Common Dataset collected for the Shallow Survey 2015 conference included overlapping PMBS (Figure 4.10) and MBES surveys in Plymouth Harbour, England, which provided timely examples for these considerations using commercially available current generation systems, as operated to (hopefully) the best of their capabilities by their manufacturers. Rapid processing of both datasets using the CUBE algorithm in CARIS HIPS (without manual editing) revealed a high degree of agreement over the vast majority of low-slope areas and indicated important differences in depths recorded over rugged terrain and edges of objects (Figure 4.11). The root causes of consistent differences in high-slope areas are not clear as of this report, although there is some evidence to suggest that positioning difficulties may be in part to blame.

Despite the differences between the "benchmark" MBES and PMBS survey results in high-slope areas, an important result is that the PMBS survey agrees to within a few centimeters over the vast majority of the survey area. A survey of similar seafloor in a shallow harbor environment under response conditions would likely require wider line spacing (for efficiency) and depend heavily on the sidescan imagery to increase the effective swath coverage for hazard detection in order to maximize survey coverage. The degree to which a traditional MBES survey plan can be modified for increased

[11] http://sandy.ccom.unh.edu/publications/library/Object_detection_storm_impact_with_PMBS.pdf

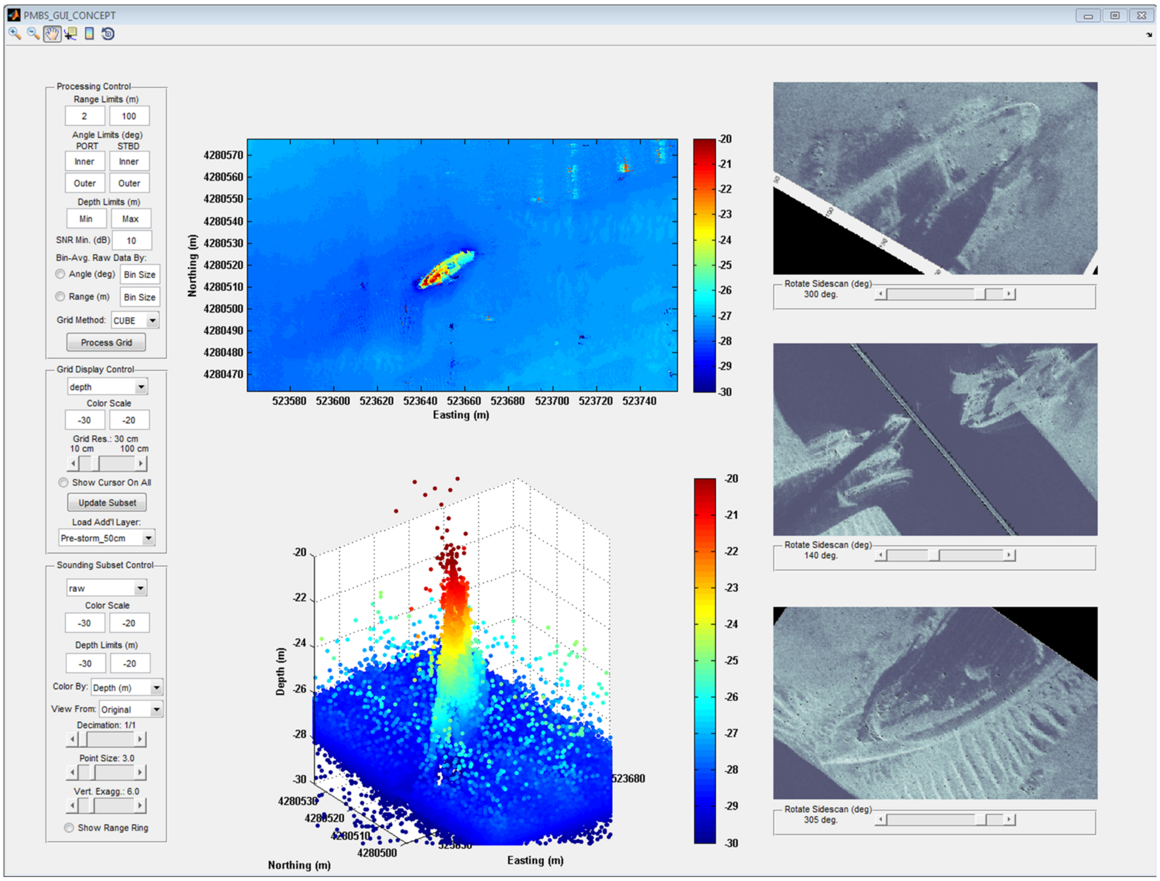

Figure 4.8: A conceptual PMBS graphical user interface (GUI) presenting raw soundings, gridded bathymetry layers, and sidescan imagery simultaneously for maximum data utility during review for object detection. Data shown here include a shipwreck and sand wave field at Redbird Reef, DE, surveyed with an AUV-mounted PMBS system shortly after Super Storm Sandy. This conceptual GUI combines visualization tools that are traditionally available only in separate software packages, potentially enhancing the object detection process by streamlining the visual correlation of targets in different data products.

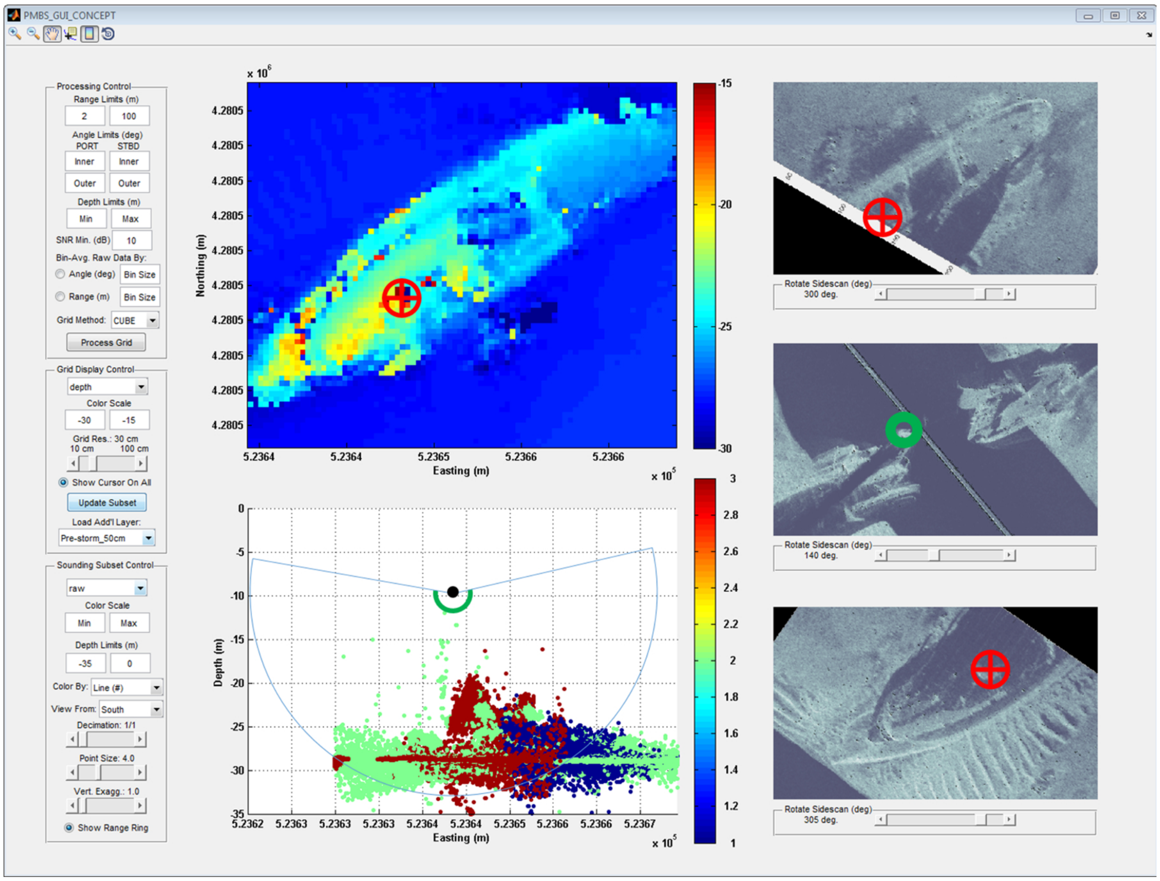

Figure 4.9: A closer view of the shipwreck with the “Show Cursor On All” option selected helps the user to identify the same location (red crosshairs) in the gridded bathymetry and the sidescan imagery from multiple passes for better context and correlation among targets. With the “Show Range Ring” option selected, the range to a high-amplitude target selected in one sidescan image (green cursor, middle right) is depicted in the 3D subset (green range ring, lower left); this option helps to confirm the relationship between shallow soundings in survey line 2 (light green soundings) and the corresponding shallow sidescan feature.

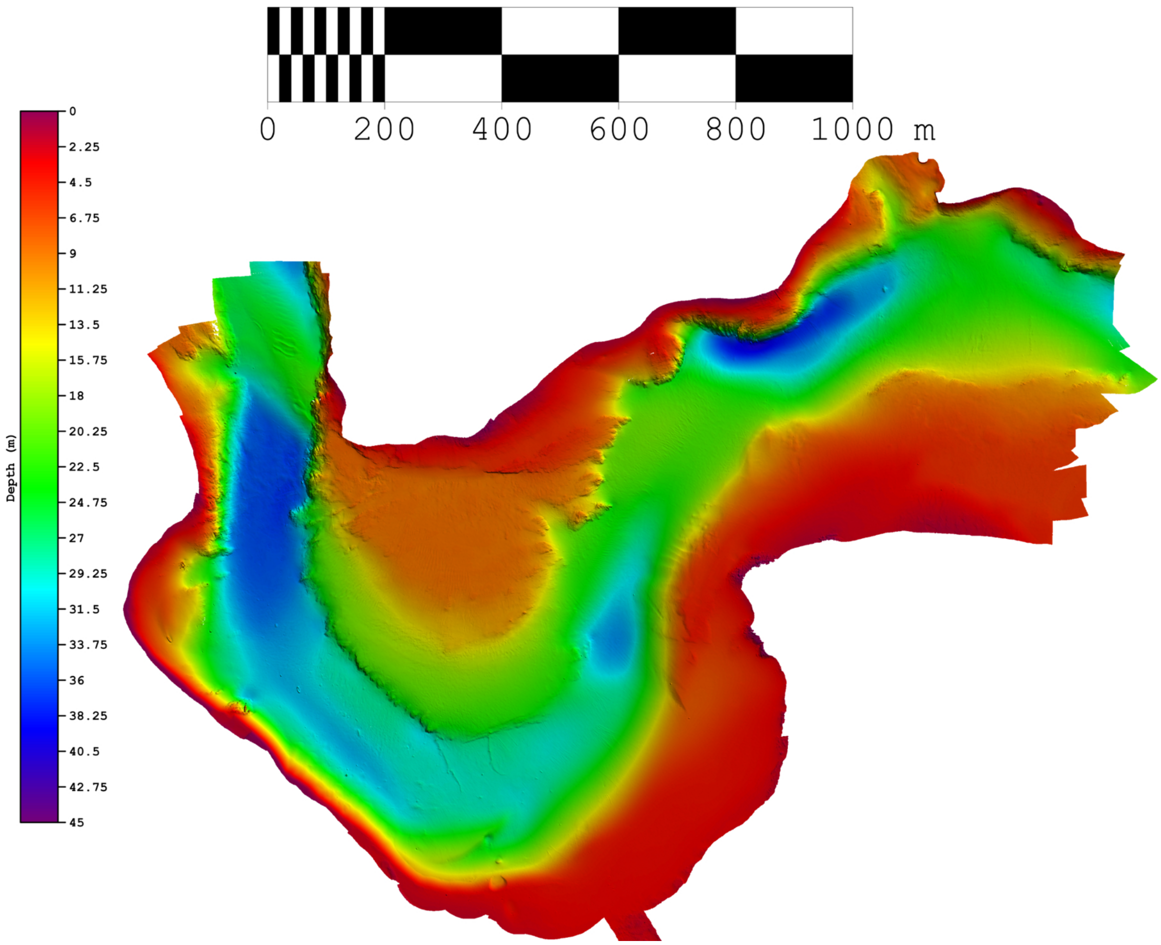

Figure 4.10: PMBS bathymetry in Plymouth Harbour, England, gridded at 50 cm using the CUBE algorithm in CARIS HIPS 9.0. The raw soundings were filtered and averaged using 25 cm range bins. The depth color scale ranges from 0–45 m. No manual editing has been performed.

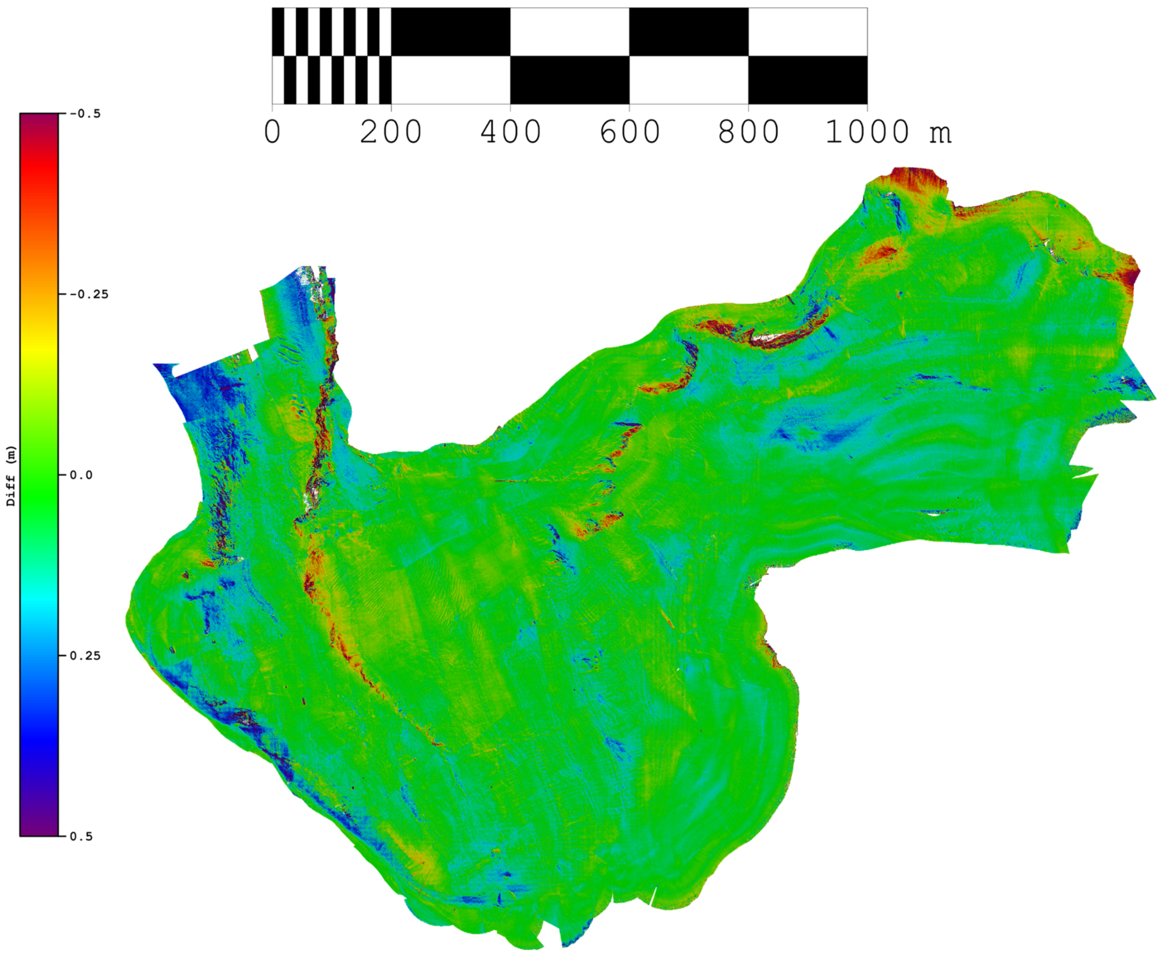

Figure 4.11: Difference between two example Shallow Survey 2015 PMBS and MBES bathymetric datasets gridded at 50 cm. The depth difference color scale ranges from -0.5 to +0.5 m, with positive values corresponding to shallower results in the PMBS bathymetric surface. Most of the low-relief areas show differences of ±0.10 m in depths up to 40 m, whereas larger differences appear highly correlated with slopes near rugged features.

PMBS swath coverage was investigated using the Redbird Reef PMBS dataset, creating combinations of survey lines to mimic line spacing strategies with different amounts of swath overlap (Figure 4.12) and evaluate the resulting CUBE bathymetric surfaces.

These trials showed that all major objects in the artificial reef, including scour around objects and bedforms in object-free areas, were readily apparent with line spacing of at least seven times the echosounder altitude. As with some other PMBS systems, a small data gap existed at nadir; this region would be subject to increased scrutiny in the sidescan imagery, along with the outer swath beyond the range of reliable depth soundings. Despite this data gap and increased vertical scatter in outer swath soundings, the CUBE surfaces created from PMBS data effectively represented all the reef objects apparent in traditional MBES data collected simultaneously from a surface vessel. Data quality in the outer swath suggest that the PMBS recording range could have been successfully extended during acquisition, though this was purposefully limited at the time to increase the ping rate and along-track sounding density under a more routine survey line plan. In a response scenario where the recording range would be extended considerably to ensure sidescan coverage in the outer swath, these simulated line plans suggest that a line spacing of up to ten times the echosounder altitude could be supported for object detection relying on sidescan imagery. It is not expected that bathymetric data quality will be sufficient to quantify hazards to navigation beyond 4–5 times echosounder altitude, however, requiring objects detected in sidescan to be resurveyed in a more favorable geometry.

4.8 Summary

Throughout the project, emphasis has been placed on understanding how data from PMBS systems can be incorporated into existing hydrographic workflows to improve efficiency in storm response situations. The inclusion of echosounder uncertainty data is critical for modern bathymetric processing algorithms used in commercial software, such as the CUBE algorithm. Several issues with current processing software were discovered and/or examined in more detail throughout the project and resolved in recent software releases. For instance, several CARIS processing functions have been updated: outlier rejection tools for GeoSwath and EdgeTech PMBS systems that were previously inoperable have been repaired; real-time uncertainty estimates for Klein systems are now interpreted properly; and a mistranslation of EdgeTech systems which previously caused across-track profile anomalies has been remedied. In short, the increased interest in using PMBS for routine and response hydrographic surveys has motivated echosounder and software vendors to improve acquisition and processing performance to better meet hydrographic survey standards.

A primary outcome of this project is the observation that many of the challenges faced during initial adoption of PMBS systems have been addressed in recent hardware and software updates. Current-generation data acquisition and pre-processing systems offer strategies for outlier rejection and data binning to achieve sounding den-

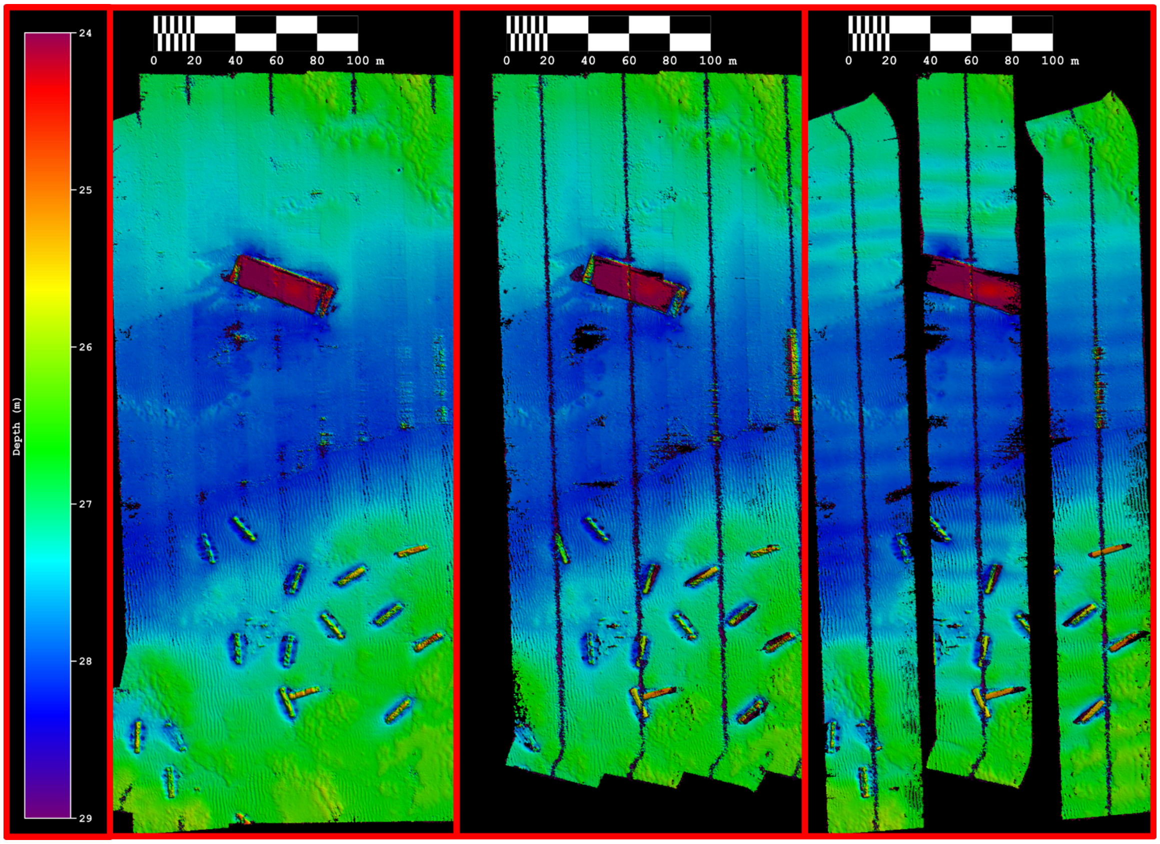

Figure 4.12: PMBS data collected at Redbird Reef, off the coast of Delaware, were rapidly processed without manual editing in a combination of line spacing strategies to evaluate bathymetric surfaces and the representation of objects with various levels of swath overlap. The survey was conducted using an autonomous underwater vehicle (AUV) at an altitude of 6 m above the seafloor with line spacing of approximately 20 m and a range limit of approximately 25 m, yielding half-swath overlap between adjacent lines. Under a response scenario with real-time analysis of sidescan imagery for detection of objects to be resurveyed at more favorable geometries, the acquisition range limit could likely be extended to 30–40 m and line spacing could be set to approximately 60 m or ten times the echosounder altitude.

sity and quality suitable for many purposes, from post-storm to routine surveys. The role of sidescan imagery in extending the useful swath coverage for hazard detection is a critical consideration for improved response survey efficiency with PMBS sonars. Furthermore, several systems now report echosounder uncertainty data that can be interpreted by commercial off-the-shelf software to better support CUBE processing and inform Total Propagated Uncertainty (TPU) estimates. In general, these advances represent a new generation of opportunities for PMBS data collection and processing which may offer efficiencies for response and routine survey operations, especially if they can be incorporated into the existing hydrographic processing pipeline.

Chapter 5

Visualization

5.1 Introduction

The visualization component of this project addressed the analytical process of determining whether potential marine debris targets are either natural features or actual debris that may need to be removed.

Finding and identifying marine debris is a tedious and time consuming task. Automatic target recognition algorithms can greatly speed up the task by searching vast survey datasets for anomalies that could be debris. However, they still leave analysts with thousands of potential marine debris targets that need to be individually examined.

A pair of tools that speed up and distribute this analytical process were developed: a rapid decision tool and a crowdsourcing website. Together, they can increase analysts' efficiency and decrease disaster response times.

The Marine Debris Rapid Decision Tool (MDRDT) increases analysts' efficiency by automating many of the common and repetitive steps in the marine debris target evaluation workflow. Using metrics based on the computer graphics concept of silhouette edges, the tool automatically calculates multiple optimal views for each debris target. These optimal views are likely to reveal enough shape information for analysts to make decisions without the need to manually reposition the (virtual) camera themselves.

These optimal views were also utilized within an experimental crowdsourcing website that allowed the public to participate in marine debris target evaluation. It was found that, even though participants were untrained and unexperienced in the task, most were able to understand and complete the task with reasonable accuracy (as high as 84% agreement with an expert). Their collective decisions can be used to greatly reduce the number of marine debris targets that must be evaluated by the limited pool of trained analysts. This can increase analytical capacity in time-critical disaster response situations when such analytical capacity can be in very short supply.

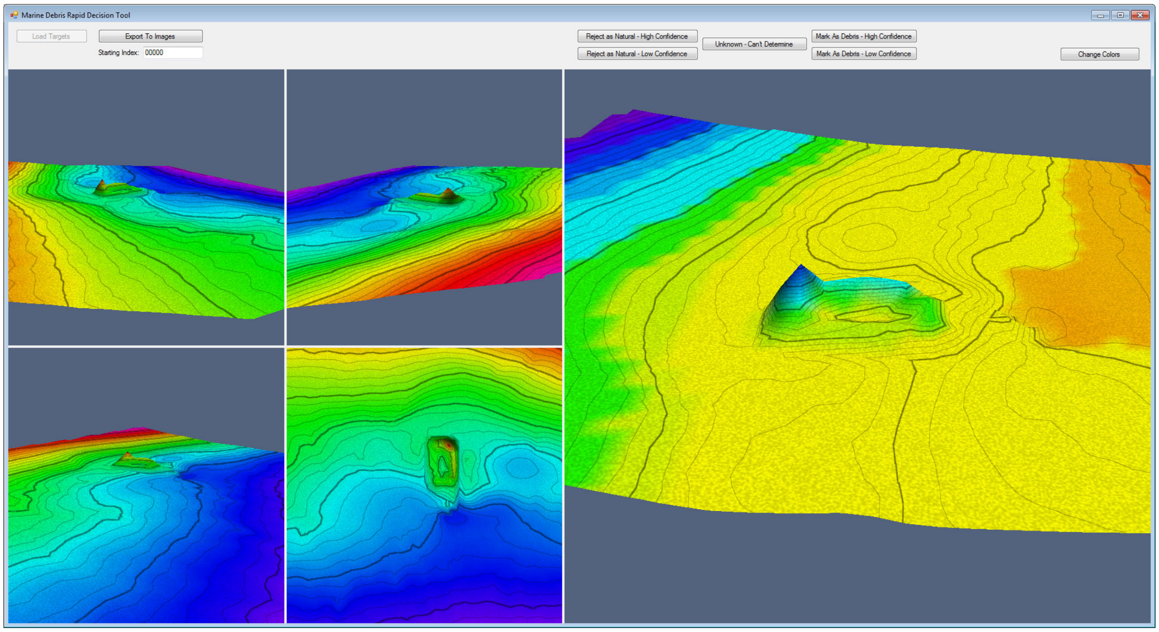

Figure 5.1: Screenshot of the Marine Debris Rapid Decision Tool.

5.2 Marine Debris Rapid Decision Tool

The Marine Debris Rapid Decision Tool (MDRDT), shown in Figure 5.1, streamlines the marine debris evaluation analytical workflow by eliminating or automating as many analyst interactions as possible.

Traditionally, marine debris target evaluation begins with an analyst loading a survey dataset, then iteratively navigating to and examining each target's location within the dataset. Instead of loading whole survey datasets, MDRDT loads individual targets. The tool automatically displays targets one after another, removing any need for navigation interactions between multiple targets in a dataset.

The targets themselves are generated external to the tool by whichever automatic target recognition algorithm is being used to process the survey data. Each time the algorithm detects a potential debris target, a file is created that contains a snippet of the survey data around that target. The most basic version of this is bathymetry data in the form of rasterized regular grids, stored in a BAG file. Exporting targets for the tool to ingest is simple, as the minimum data required is only raw bathymetry or a point cloud.

The use of multiple optimal views can save an enormous amount of analyst time. Traditional, single-perspective interfaces require users to repeatedly move and rotate the camera to view a target from multiple angles. MDRDT instead provides multiple viewing windows, each of which automatically show a different, optimized views of the debris object. Ideally, for the majority of cases, looking over the automatically chosen views will provide enough information to make a decision, and thus an analyst will not have to waste time repositioning the camera at all.

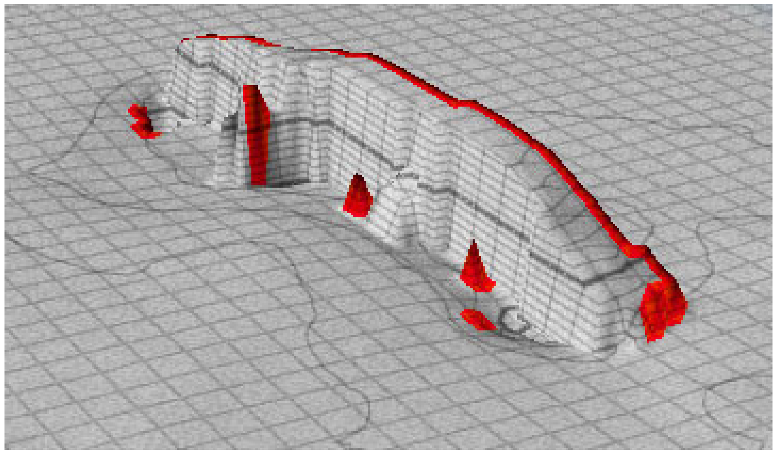

Figure 5.2: In this view of a debris target mesh, the faces highlighted in red have silhouette edges for the current camera viewpoint.

If the automatically chosen views are not sufficient, the analyst is able to manipulate each of them as necessary to get a better view. Each view is a fully-functional instances of CCOM's Virtual Test Tank 4D software, which is a 3D/4D interactive geospatial visualization and analysis package based on previous research projects regarding visual analysis of datasets such as dynamic ocean flow simulations and sediment transport models [111, 112].

The multiple optimal views are chosen based on a scoring system. The tool calculates how the target will appear as viewed from a wide range of possible camera locations and viewing angles. For each of these candidate views, a score is computed based on how many features it reveals. The candidate view with the highest score is selected, and its viewing angles are saved as the first optimal view. All of the remaining candidate views are then re-scored, removing any credit for features already revealed in the previously picked views. The highest scoring view is again saved, and this process continues until the desired number of optimal views is reached.

The primary metric used to score views is based on the concept of silhouette edges. In 3D computer graphics, a silhouette edge is an edge within a triangle mesh that, for a particular camera view-point, is shared between a front-facing (visible) triangle and a back-facing triangle. They are often used in non-photorealistic rendering to illustratively emphasize shape features. In geospatial and terrain models, these silhouette edge are most commonly encountered along the edges of prominent features or objects, where they generally form the boundary between the foreground and the background. This can be seen in in Figure 5.2, which shows faces with silhouette edges along a shipwreck from a single camera viewpoint.

Views that produce many prominent silhouette edges are likely to reveal the shape of target objects. Iteratively picking views that reveal different groups of silhouette edges helps to ensure all the shape information is being revealed across the multiple views. This effect can be seen in Figure 5.3, which shows the faces with silhouette

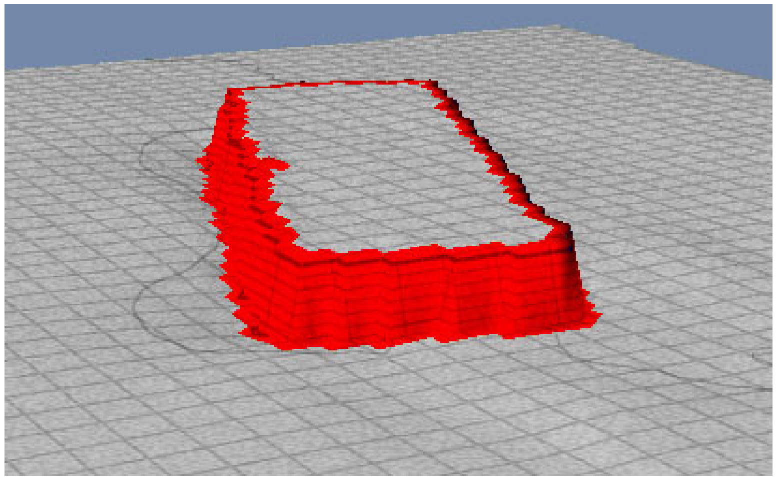

Figure 5.3: In this view of a debris target mesh, the faces highlighted in red have silhouette edges that have been cumulatively revealed by the top four viewpoints.

edges that have been revealed by picking the top four optimal views. Notice that the entire perimeter of the target object has been marked as revealed by the four views, indicating that the views provide a comprehensive depiction of the target's shape. An example set of these optimal views is shown in Figure 5.4.

Analysts can mark targets to indicate whether they are natural features or marine debris, as well as the confidence level of the decision, including a no-confidence "unknown" option. By having analysts include uncertainty measures in their decisions, it is possible to re-display the sub-set of ambiguous targets to other analysts for a second round of evaluations.

When a decision is entered, the tool records the decision, the user's estimated confidence level, and target information to a report file covering that analysis session. The tool then switches to the next target, and the process repeats until all targets have been evaluated.

The tool also provides a method for automatically rendering static images for each target, and then exporting all of the optimal views for each target to form datasets for use outside the tool. This is used to support a web-based analysis method intended to support the potential for crowdsourcing marine debris identification (as described in the following section).

5.3 Crowdsourcing Marine Debris Evaluation

After a disaster, minimizing response times is critical. While it is best to have trained analysts available to perform debris identification, the number available, and their time, is limited. A possible alternative to this is to consider the concept of using crowdsourcing to conduct marine debris identification, thereby increasing capacity during times of high demand.

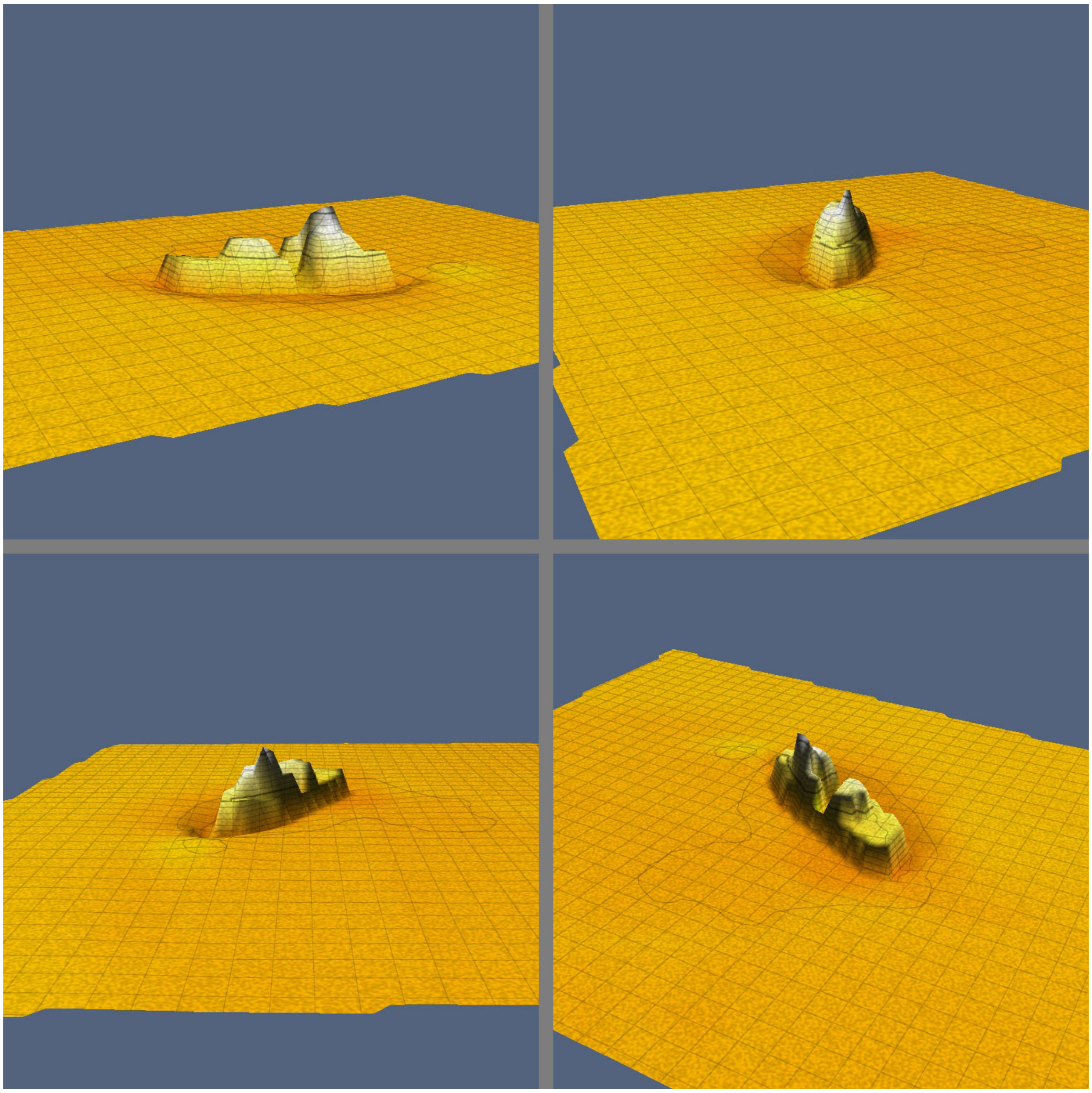

Figure 5.4: The top four views chosen for a debris object mesh of a shipwreck using the tool's optimal view algorithm.

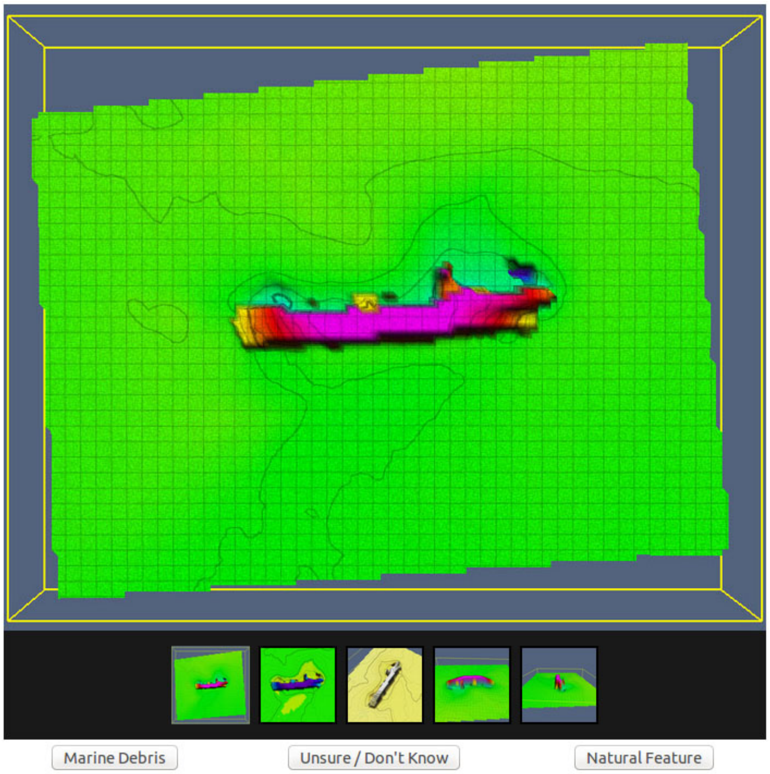

Figure 5.5: A screenshot of the web-based crowdsourcing interface. Users see a single zoomed-in image, and can scroll through or click on the thumbnail images at the bottom to view each of them as many times as needed.

Members of the general public were invited to conduct debris analyses via an interface on the project website[1], which displays the optimal views generated by the Marine Debris Rapid Decision Tool (Figure 5.5). While the users had no formal training, if large majorities make the same decision, the basic premise of crowdsourcing is that they are likely to be correct. (And it does not require a significant majority to be slightly better than average in order to achieve better than average results.) Even if their decisions are not 100% reliable, they can still be used to filter massive collections of targets into more manageable numbers for re-examination by trained analysts.

The project was advertised with links to the website through CCOM's social media accounts and the university's main webpage. Users were given a brief overview of the project's goals and motivations. They were provided with only the bare minimum of basic directions and examples, enough to ensure they understood the task, but not detailed or in-depth enough to be considered training.

A total of 82 targets were available for evaluation via the online interface. To assist in data quality assessment, image sets for 12 targets whose categorizations were

[1] http://sandy.ccom.unh.edu/participate.html

already known were included, which consisted of objects that were obviously debris or featureless seafloor. These quality assessment targets were distributed amongst the unknown targets, with the distribution skewed towards the beginning of the target set to ensure they were evaluated even by people who only assessed a few targets.

The quality assessment targets were of two types: four obvious debris targets of obvious shipwrecks, and eight snippets of barren seafloor devoid of any notable features. The design of the evaluation system is such that each participant evaluates the same targets as any other participant in the same fixed order.

Over the course of approximately one week, approximately 800 members of the public visited the crowdsourcing site, 34 of whom registered and participated in the project. Additionally, an expert familiar with interpreting hydrographic and bathymetric data was recruited to evaluate the targets using the interface in order to provide a baseline by which to compare the evaluations of the participants.

A total of 12 users (35%) evaluated all 82 targets, and 15 users (44%) evaluated at least half of the targets. An average of 45 evaluations were made per user.

The quality assessment targets were compared with user evaluations to identify any confused or possibly malicious participants, however all users appeared to be making evaluations in good faith.

To assess the quality of the data collected from participants, raw percentage agreements between users were computed as a rough metric of user quality. Of the 82 targets, 60 (73%) were agreed upon by a majority of the users who rated them. The inter-rater percentage agreements had a weighted average agreement of 77.4%. Comparing users to the expert's evaluations yielded a weighted average agreement of 78.9%.

Furthermore, when the quality assessment targets were used to filter out the lower-quality evaluators, there was a significant increase in agreement both between users (81%) and against the expert (84%).

This research indicates that crowdsourcing marine debris identification is a promising approach for increasing analytical capacity during time-critical disaster response, particularly for filtering and drastically reducing the number of targets that must be evaluated by trained analysts.

5.4 Summary

Finding and identifying marine debris is a tedious and time consuming task. Automatic target recognition algorithms can greatly speed up the task by searching vast survey datasets for anomalies that could be debris. However, they still leave analysts with thousands of potential marine debris targets that need to be individually examined.

A tool that automates many of the common and repetitive steps in the marine debris target evaluation workflow has been presented. Using metrics based on the computer graphics concept of silhouette edges, the Marine Debris Rapid Decision

Tool automatically calculates multiple optimal views for each debris target. These optimal views are likely to reveal enough shape information for analysts to make decisions without the need for manually repositioning the camera themselves, increasing analysts' efficiency.

These optimal views were also utilized within an experimental crowdsourcing website that allowed the public to participate in marine debris target evaluation. It was shown that, even though participants were untrained and unexperienced in the task, most were able to understand and complete the task with reasonable accuracy. Their collective decisions can be used to greatly reduce the number of marine debris targets that must be evaluated by the limited pool of trained analysts. This can increase analytical capacity in time-critical disaster response situations.

Complete details on the analysis tool, its optimal view algorithms, and the crowdsourcing website design and results can be found in the paper entitled "Streamlining the Evaluation of Potential Marine Debris Targets for Disaster Response", which was published in MTS/IEEE OCEANS 15, Oct., 2015 [113] and is available online[2].

[2] http://sandy.ccom.unh.edu/publications/library/OCEANS15-Butkiewicz-Nov15.pdf

Chapter 6

Outreach

6.1 Introduction

Outreach is now an essential part of any scientific program, and quite rightly so: the public, ultimately and for the most part, fund the science through their taxes, and so it seems only fair that scientists should invest some time and effort in explaining what it is that they do, what the implications are, and why the research is important enough to be funded.

This project is no different, and as part of the outreach component of this project, in addition to the project website (`http://sandy.ccom.unh.edu`), a number of static and interactive visualizations, infographics, and a museum exhibit were created. STEM[1] events were also conducted through interactions with the SeaPerch program, and the University's Ocean Discovery Day.

6.2 Interactive Mapping

To communicate to the public where and what is being cleaned up, an interactive online debris map was developed. The site (`http://sandy.ccom.unh.edu/visualizations/infographics.html`) features a fully interactive map (Figure 6.1) that merges a collection of Sandy-related debris records with public domain imagery and vector data. It allows the general public to quickly zoom into their particular region-of-interest and see not only where debris cleanup efforts are occurring, but explore and examine individual debris objects that have been cataloged and retrieved.

Comparison of datasets in an efficient manner is essential for many tasks, including marine debris identification, and object detection. Different methods of viewing multiple datatypes were therefore also considered, and demonstrated for the public through the project website. For example, WebLens, a web-based implementation of the "magic lens" visualization technique was developed (`http://sandy.ccom.unh.edu/visualizations/weblens.html`), which allows the user to examine a view a small portal

[1]Science, Technology, Engineering, and Math.

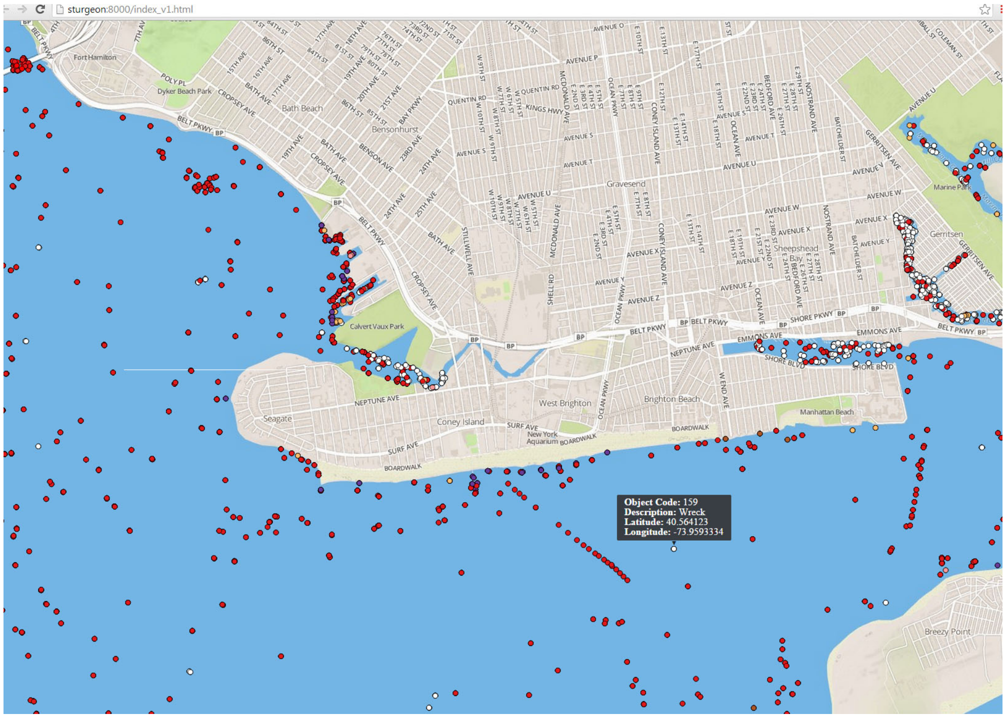

Figure 6.1: Zoomed-in view of individual marine debris records around Brighton Beach, Brooklyn, NY.

("lens") of one dataset overlaid on top of a background dataset (Figure 6.2); the base layer and lens can be readily moved, zoomed, and resized with a mouse, making it much more fluid as an interaction and correlation technique than other alternatives [114].

6.3 Infographics

Infographics are simplified, graphical descriptions of technical subjects, or representations of data, designed to convey the essence of the topic with clarity, but also with quantitative precision. Examples include simplified data visualizations that allow the general public to explore geo-spatial data without the complexity that this normally entails, or an abstracted representation of a topic that engages the public.

In an attempt to educate the public about both our related work at CCOM and the Sandy clean-up project as a whole, a series of visual infographics were developed. Visual infographics are stand-alone images that focus on single topics, explaining the issues and presenting supporting data and information with rich imagery and simple visualizations. Most importantly, they are easily shared and distributed by the general public over social media channels, which means that they reach more viewers than traditional web content or links to such content.

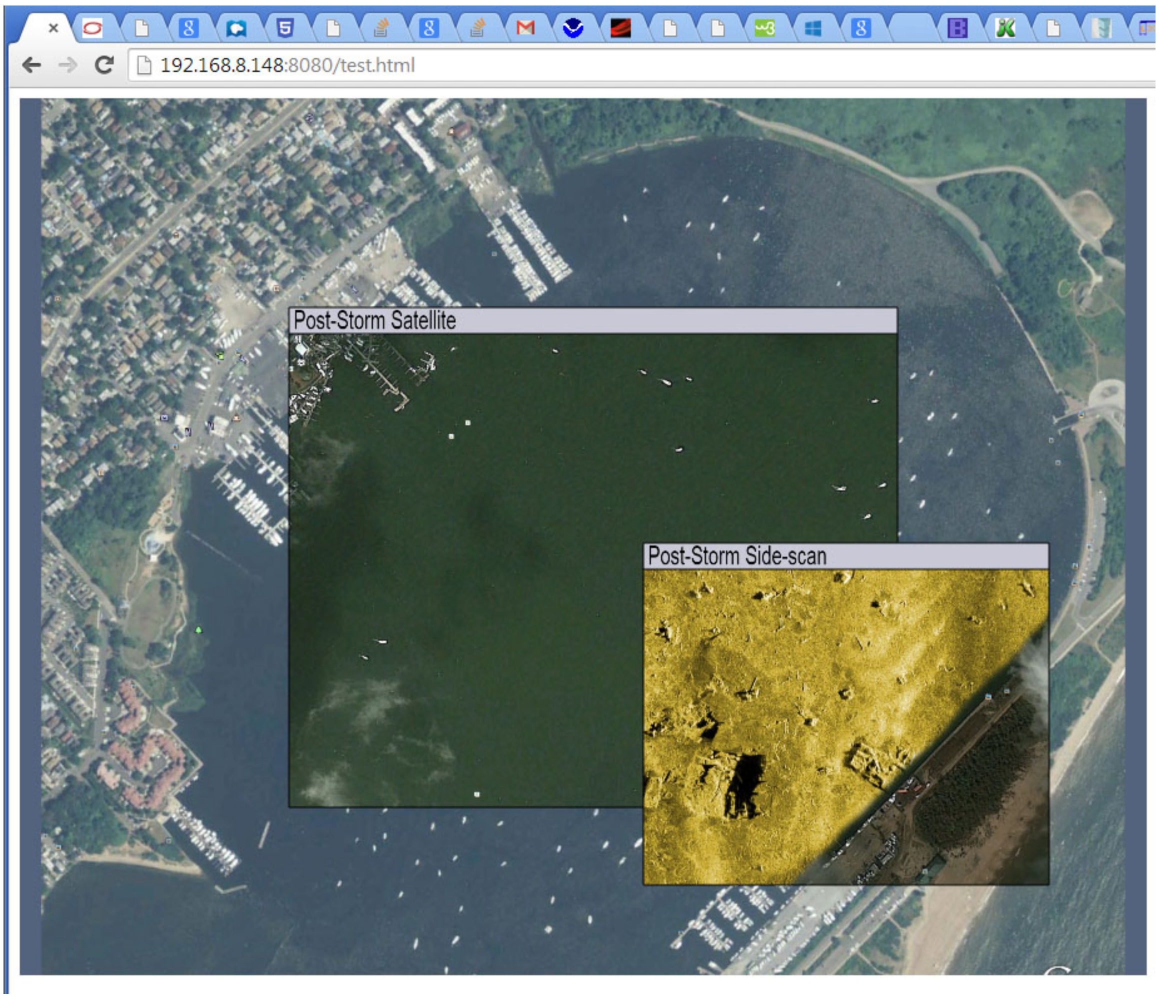

Figure 6.2: Example of the "weblens" paradigm for comparison of two datasets. Here, there are two movable "lenses" through which the user can see sidescan data, and post-storm aerial photography overlaid on the pre-storm imagery, so that comparisons can be readily made.

The visual infographics developed include "What do marine debris look like?—And how well can we see them?" (Figure 6.3) which demonstrates the capabilities of multi-beam sonar and LIDAR to reveal and resolve submerged objects (vehicles, shipwrecks, etc.), and "Marine Debris Identification and Processing" (Figure 6.4), which visually explains the process from deciding where to survey for debris to automatic target recognition, identifying debris, and finally salvage and cleanup. This includes explaining how the experimental techniques such as the rapid decision tool and the crowdsourcing website fit into and improve the overall process.

6.4 Permanent Museum Exhibit Development

A partnership between CCOM and The Seacoast Science Center (Rye, NH) has led to the development of an interactive museum exhibit that engages the public with a touchscreen based game revolving around the detection and identification of marine debris. "A Hurricane Hits Home" is a multi-station touchscreen exhibit (Figure 6.5) geared towards children, and integrates a large salvaged portion of a historical wooden shipwreck into its physical design.

The game invites people to examine a number of coastal regions and harbors in Sandy affected areas (Figure 6.6). It teaches them about modern mapping technology by letting them control boats with multibeam sonars and airplanes with LIDAR sensors. They drag these vehicles around maps to reveal the underlying bathymetry underneath the satellite photo backgrounds. They learn the applications and limitations of sonar and LIDAR through understanding where the vehicles can and cannot collect survey data (e.g. LIDAR does not work in deep water, and the boat cannot go in shallow areas).

As users collect bathymetry data, they occasionally reveal marine debris objects on the seafloor. Once all the debris objects in a level have been located, the game challenges them to identify them based on their appearance in the bathymetry data. They must compare the simulated bathymetry images of the debris targets to photos of possible objects, and choose the correct matches to achieve a high score.

This exhibit will have a permanent space at Seacoast Science Center, and should be installed and open to the public in late 2015 or early 2016.

6.5 STEM Events

For many educators, opportunities to expose students to science, technology, engineering, and maths (STEM) experiences are greatly prized. A particular example of this is the SeaPerch program (`http://www.seaperch.org`), developed by the MIT Sea-Grant program, and funded by the Office of Naval Research, where teams of three to four K-12 students (mostly from middle schools, although there are also home school groups, and 4-H groups represented) design and build a small remotely operated vehicle (ROV) using simple motors and plastic pipe (Figure 6.7). The students then

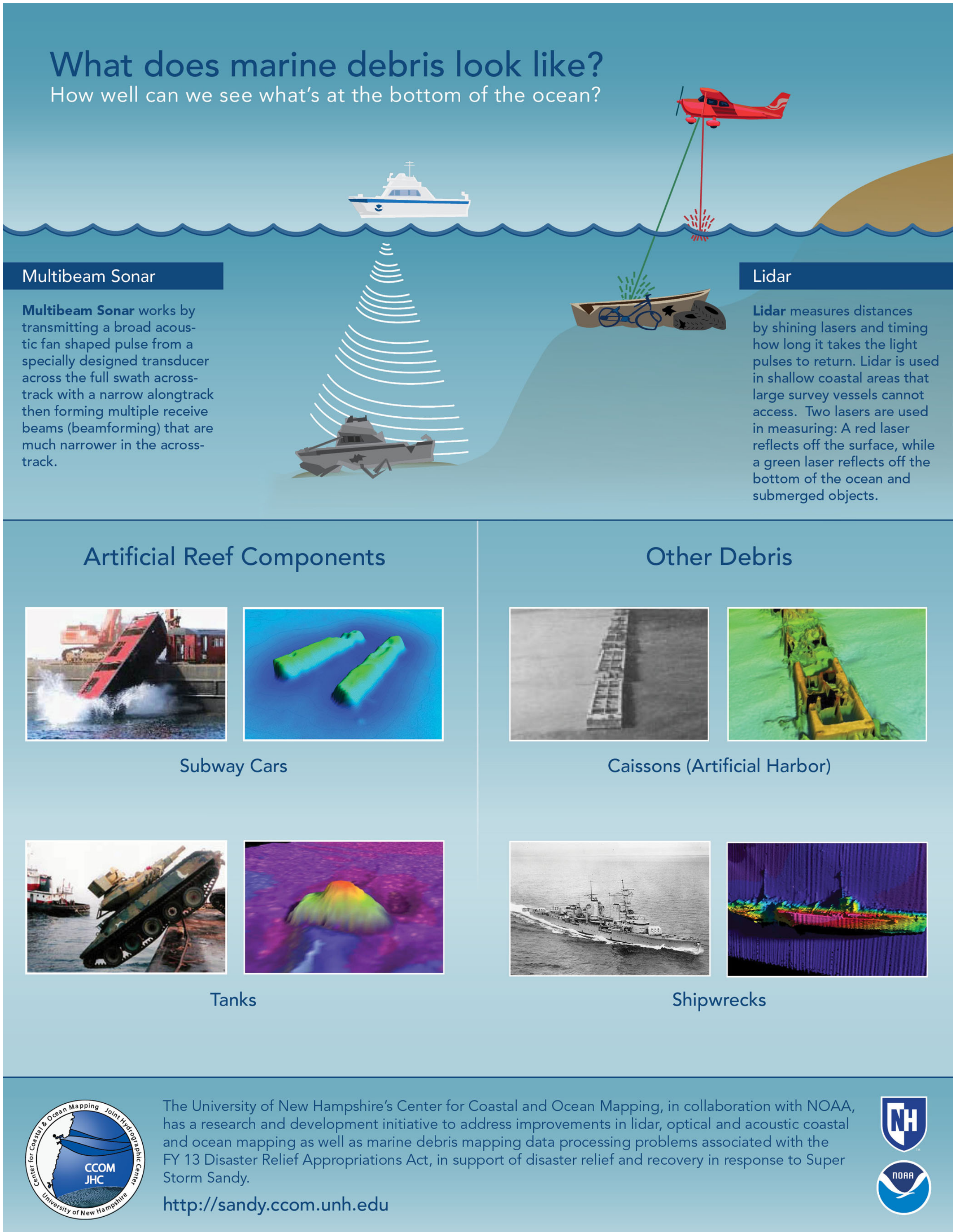

Figure 6.3: Example visual infographic showing detection capabilities of remote sensing systems.

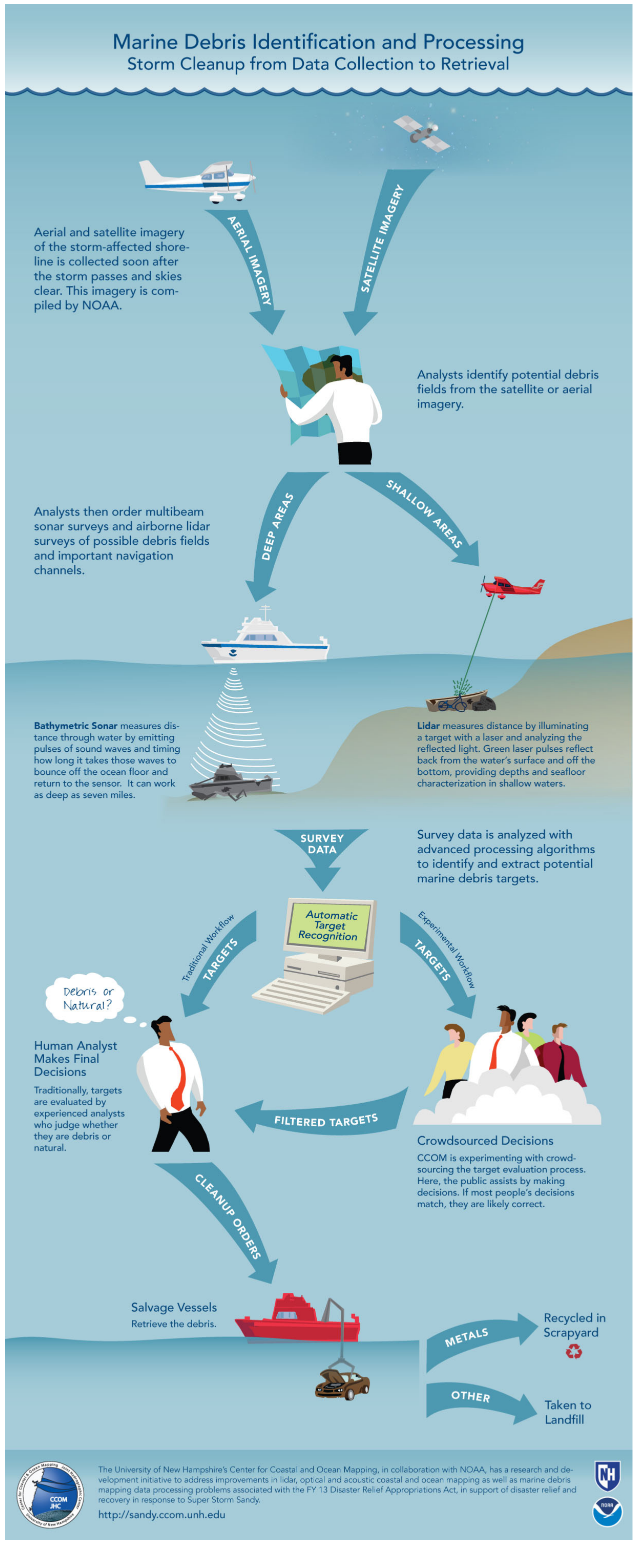

Figure 6.4: Example visual infographic explaining object identification processes.

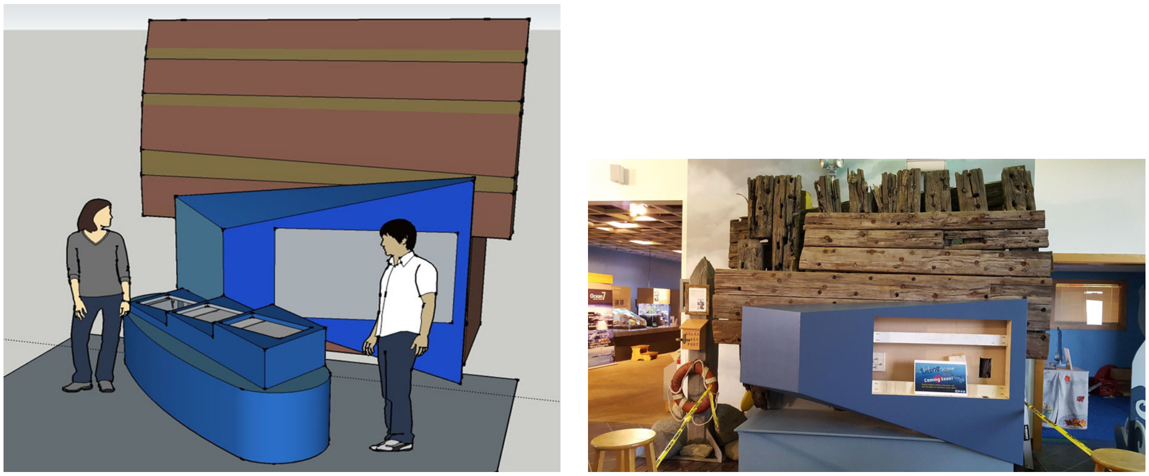

(a) Conceptual design. (b) Current implementation.

Figure 6.5: The “A Hurricane Hits Home” exhibit at the Seacoast Science Center, Rye, NH. The wooden structure behind the exhibit is part of the hull of a ship wrecked locally during a significant storm event.

Figure 6.6: Example screenshot from “A Hurricane Hits Home” during the opening stages of the game. The operator is guiding the multibeam across the survey area in order to gain insight into what might be on the seafloor, and understand the limits of this type of survey technology.

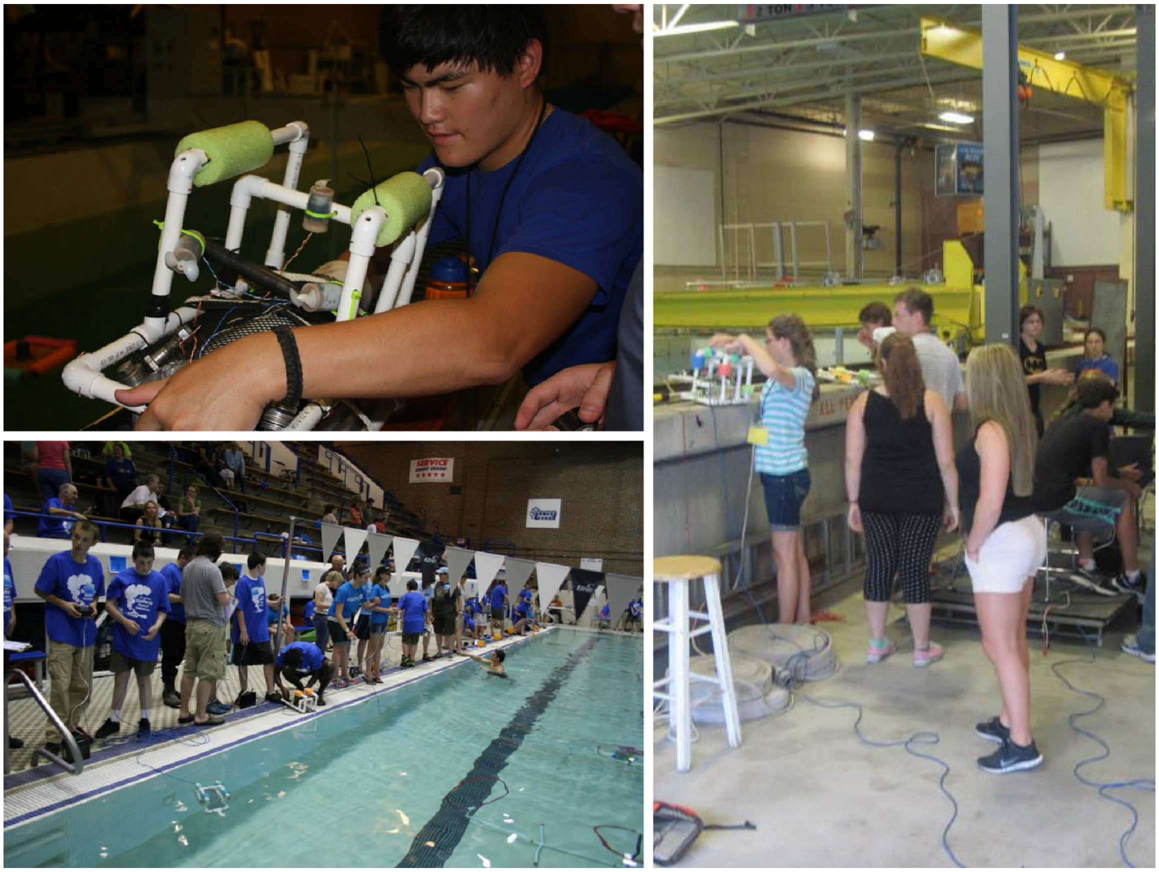

Figure 6.7: SeaPerch program events. Clockwise from top left: students building their SeaPerch ROVs; testing ROVs in the tank at UNH during Tech Camp 2014; morning events of the competition day in the UNH Fieldhouse pool, 7 June, 2014.

compete in a series of regional and national heats, carrying out obstacle course tests, and a dexterity challenge against the clock. During the regional SeaPerch competition at UNH in 2014, however, the project arranged for the afternoon event to be themed around marine debris. After a short briefing on the nature of marine debris, and its consequences, the students were challenged to modify their SeaPerch ROVs to make them capable of investigating and removing marine debris (Figure 6.8), which sparked a frantic wave of collaboration, re-design, and friendly rivalry between the dozen teams present, while at the same time communicating the ideas of discovery, identification, and restoration that are an essential concept in storm response scenarios.

A second opportunity for outreach took the form of the UNH Ocean Discovery Day event, which takes place annually around the beginning of October. Each year, a growing number of students take part in an "educators day" on a Friday, and then the University's Marine Program facilities are open to the public on the following Saturday; in 2015, approximately 1,600 K-12 students toured the Chase Ocean En-

Figure 6.8: SeaPerch afternoon "team challenge" event, 7 June 2014. Clockwise from top left: divers deploying simulated "marine debris" in the engineering test tank at the Chase Ocean Engineering Lab at UNH; a team collaborating on how to adapt their SeaPerch for the marine debris clean-up challenge; a collaborative "scoop" dual-Perch marine debris removal system; SeaPerch ROVs removing simulated debris from the tank.

Figure 6.9: Victoria Price explains LIDAR mapping technology and habitat mapping to a group of K-12 students during the educator's day of Ocean Discovery Day 2014.

gineering Lab and surrounding activities on educator's day, and approximately 600 members of the public visited on the following day.

In 2014 and 2015, the project provided communicators for Ocean Discovery Day (Figure 6.9) to explain the technology being used, and to explain the various aspects of habitat mapping, marine debris detection, and bathymetric mapping being used as part of the Super Storm Sandy project.

6.6 Summary

The outreach component of this project has attempted to provide a variety of different opportunities to communicate the goals, objectives, and research associated with the project to the public, and particularly to K-12 students, and their educators. This has taken the form of a public-facing website, some visual infographics, development of a museum exhibit, and some interactive STEM-oriented events. The website acts as both the archive for products generated by the project and an opportunity to communicate some of the objectives and results of the research to the general public; it has also been used as a means to test some of the ideas associated with visualization, including the ability to use crowdsourcing techniques to solve some of the semi-tractable problems associated with marine debris. Possibly the longest lasting results of the project, however, is the museum exhibit, which attempts to describe the nature of survey, the problems of identification of marine debris, and the trade-offs involved in storm response surveying to children.

Inevitably, it will likely be several years before any effect of the outreach efforts reported here bear fruit (e.g., with students becoming involved in the oceans, surveying, or marine debris due to their experiences). However, the project has at least demonstrated that it is possible to engage the public in the understanding of a complex research project, and thereby explain to them why they, ultimately, should provide funding for such projects in the future.

Chapter 7

Summary

7.1 Outcomes

7.1.1 LIDAR and Habitat

The essential objectives associated with the research in LIDAR and habitat mapping were to investigate the limits of existing techniques for the use of LIDAR and satellite imagery, and to develop new techniques for these data sources that could be used in a storm-response scenario.

The research demonstrated that there is significant potential for the development of LIDAR waveform features to assist with habitat mapping, in addition to conventional uses for nautical charting and shoreline assessment, particularly when coupled with appropriate normalization of the returned signals (such as reflectance maps from EAARL-B data) and classification techniques (such as the Object-based image analysis (OBIA) reported here). Although it was shown that the same features can be derived from different LIDAR systems and that the same OBIA analysis can be moved between datasets and locations, it is likely that the future direction of this work is going to be related to robustness and tuning of the algorithms, so that they become more automated.

In a storm-response scenario, one of the difficulties is gauging whether any changes observed in remotely sensed (or even physical observation) data is significant or not. That is, can the observed change be blamed on the storm, or is it natural variability of the area? To adequately answer this question requires a baseline estimate of change, which can be hard to achieve. (This might in itself argue for an active campaign to establish these baselines in preparation for future storm events, rather than hoping that such baselines can be derived *ad hoc* for each event.) The research reported here demonstrates that it is possible to establish such a time series from archives of satellite imagery, either for shoreline change, or for submersed aquatic vegetation, or from multiple LIDAR surveys, if available. This time series then allows for, e.g., seasonal variability to be established, and allows for an assessment of modeling and instrumentation variability, so that an estimate of "normal" variability can be established against which the change in the event of a storm can be assessed. The advantage of satellite imagery is simply that it is much more likely that the raw materials to establish a timeline will exist in extant archives than for LIDAR data.

Finally, the research demonstrated that although it might not be entirely possible to use satellite-derived bathymetry for direct update of charts, it is certainly possible to use this information to determine areas of significant change in the wake of a storm, and thereby use this to determine if further work is required on any particular chart (by some other means). As a means of prioritizing the distribution of survey resources in the wake of a storm such approximate indicators can be particularly effective.

7.1.2 Marine Debris

In the work on marine debris detection, characterization, and communication, the key objectives were to develop techniques for robustly identifying marine debris objects.

The research showed that the problem of marine debris detection was made significantly more difficult by the lack of uniformity in the definition of what constitutes "marine debris," leading to a much more complex problem than is typically found in object detection scenarios, e.g., in mine-like object detection, or pipeline inspection. The research did demonstrate, however, that by suitable choice of mathematical frameworks, it was possible to constrain the overall problem of marine detection through the use of an *a priori* model of marine debris production derived from observations in previous storm events, combined with a multiplicity of specific detection algorithms that are fused together to give a more robust solution than any detector on its own would achieve. This leads naturally to a map of the probability of debris presence that can be used for resource allocation as well as general detection. The method developed was shown to strongly match ground-truth estimates of debris location.

An observed difficulty with marine debris research was that there was no common vocabulary for the declaration of marine debris objects, and no mechanism by which the information could be readily transported between data collectors, analysts, and decision-makers. The research here demonstrated that it is possible to adapt a standard, well-implemented technology to this purpose, with a Marine Debris Markup Language that allows for well-controlled data transfer, and provides a standard vocabulary to discuss marine debris.

7.1.3 PMBS

Phase-measuring bathymetric sidescan (PMBS) systems have had a checkered history in the hydrographic world, mainly due to a number of difficulties in data generation, data formats, and processing options from the early manufacturers of such systems. The objectives for examining these systems were therefore to determine how they might be used for surveying, particularly when used in the response to a storm, where their characteristics lend them to the purpose, and the limits to which such systems might be subject.

The research demonstrated the PMBS systems have now resolved many of the issues that were previously problematic through a combination of improved hardware and processing techniques, including the development and wider adoption of uncertainty models. In particular, the research showed that with a non-conventional patch-test procedure and appropriate pre-processing it is now quite possible to process PMBS data with conventional hydrographic data processing tools.

A common, and much debated, question with PMBS systems is their ability to detect objects, and to preserve them through the processing chain until they can be "recognized" by the human operator at the end of the chain (or a suitable algorithm). The research here demonstrated the behavior of PMBS systems with respect to processing techniques, particularly grid resolution and object preservation, and developed a series of best practices to optimize the potential for object detection with this type of data.

PMBS systems generally have a significantly wider available swath than MBES systems. However, under conventional survey circumstances all of the data from this swath might not be entirely acceptable for charting purposes. In the case of a storm response, however, more lenient requirements might be operating, in which more of the swath could be considered usable, and thereby make for more efficient surveying. The work reported here considers this possibility, and developed protocols for survey line structure and survey best practices for PMBS systems.

Finally, it was argued that use of only bathymetry or backscatter information in the approach to object detection, and PMBS data processing in general, is suboptimal, particularly since these data are acquired simultaneously with a PMBS system in a sidescan-like geometry, and therefore are always available. A processing paradigm was proposed that would allow for simultaneous display of the bathymetry and backscatter within the same region, with suitable controls for processing of the various data types, and for their visualization and manipulation, along with tools for simultaneous localization of targets in all data. Although requiring further development, this proposed tool could significantly benefit the human operators tasked with examining such data in future storm responses.

7.1.4 Visualization

Visualization is a core component of much of the research reported here, but as a separate entity the specific objectives being addressed were to develop better methods of supporting marine debris identification, and leverage these methods to assist with the resource limitation problem that is common in storm response: there are only a finite number of trained analysts available to identify targets.

The research demonstrated a prototype of a new visualization tool for marine debris that attempts to improve on operator throughput by pre-selecting a series of views of the object being considered such that the chances of having to manipulate the viewpoint in order to positively identify the object as debris are minimized. Much of the time taken in identification (and hydrographic data processing in general) is in orienting the data such that the problem being remediated is correctly positioned to make the remediation simple. The more often this can be done automatically, the faster the operator can make each decision. Although this technique was developed specifically for marine debris recognition, the extension to, and benefit for, general hydrographic data processing is obvious.

Addressing the concern of operator availability, an extension to this viewpoint selection technique has been proposed, with the goal of making the problem of debris identification into something that can be successfully crowd-sourced. The concept of crowd-sourcing [115] is that a large group of untrained observers can be more successful at some tasks than a small group of highly trained specialists, primarily because it only requires a small majority of the untrained observers to be above average in order to sway the statistics of a decision towards the correct answer. In the context here, making the debris identification problem into something that can be passed to the general public unlocks the potential for a crowd of observers to deliver multiple votes on the same object, allowing for any misclassifications to be accommodated by the (possibly small) super-identifiers. The research conducted here shows that it is possible to attract a crowd to help with problems of this kind, and that the crowd can be almost as effective as a trained observer (except, of course, that there can be many more of them). This demonstration does not address, however, the difficulties of sustaining a crowd, or the number of observers per object required to guarantee a reliable classification of objects, which would be important in a full implementation. It does, however, indicate that such an implementation deserves further study.

7.1.5 Outreach

For outreach, the objectives are simple: communicate the goals and results of the research being conducted to the general public, engaging them in the science being conducted.

The research reported has attempted to build in this concept from the start within each effort, and express it within a number of different venues. Thus, for example, all of the research products that have been generated in the course of the project have been published on a specially-designed website, which has also included infographics in both electronic and printable form to attempt to explain the concepts behind the research to the (interested, but non-specialist) general public.

Similarly, there have been a number of opportunities to explain the principles, components, and outcomes of the research to the public. Specifically, the project has been represented within the UNH Marine School's Ocean Discovery Day for the duration of the project, allowing the researchers to talk directly with growing numbers of K-12 students and adults over the course of a two-day event each year. The project also assisted in a STEM-enrichment event for the region SeaPerch competition in 2014.

Finally, and probably most lastingly, the project has also collaborated with a local science museum to develop an exhibit that explains the effects of hurricanes on the coast, and the limitations, difficulties, and techniques used to respond to such events. The exhibition will be permanently on display at the museum, but could be readily reproduced for either a touring display, or reimplementation at other museums.

In addition to the public outreach, the results of the research have also been communicated with the scientific community through a number of conference and journal papers (see p. 133).

7.2 Broader Impacts

The research described here has covered a wide variety of topics across a broad range of technologies and fields, and has made positive contributions to each. Some of the contributions, however, have the potential to have broader impact beyond the scope of the project.

The first topic with potentially broader impact is the use of LIDAR waveform features for habitat classification and monitoring. While techniques for habitat mapping with acoustic remote sensing techniques are now common, they are always limited to the requirement that there is an instrument in the water, so that the rate of advance is necessarily slow—and more so in shallow water where there is risk of damage to the sensor. In the same way that hydrographic LIDAR surveys can potentially cover ground much more quickly than MBES surveys, use of LIDAR waveform features for habitat could open up the potential for much wider habitat studies, which are more frequently repeated. Of course, as with hydrographic surveys, there is also the issue that the spot-spacing for LIDAR surveys can be limited, which has implications for the smallest resolvable habitat area. Given that habitat tends to be an areal estimate, however, this is unlikely to be as much of a difficulty as it is in hydrographic surveys. In addition, the new generation of topo-bathymetric LIDAR systems promise significantly smaller spot-spacing than purely bathymetric LIDAR systems, mitigating this difficulty. The impact of this idea is therefore more likely to be limited by the robustness with which the techniques can be applied to different areas and LIDAR sensors, which, notwithstanding the results reported here, is still a partially-open question.

Generation of calibration baselines from LIDAR, but particularly from satellite imagery databases is also potentially impactful. In many fields, there is a significant lack of a formal uncertainty model for the instruments in use, and very few repeated observations of the same area over a long time period. Consequently, it is often difficult to determine whether a change observed is the result of instrument error, or of natural variability of the field being observed (e.g., seasonal or decadal variability of SAV). The development of an analysis technique that can be applied relatively readily to a data source that has a significant time series opens up the possibility of generating a usefully-scaled time history of variability for "normal" behavior of the system under study, and thereby provides an estimate of what "significant" change needs to look like in order to warrant the name. The techniques reported here allow for the use of satellite imagery to address questions of SAV variability, and therefore to provide an estimate of change rates, even if they are approximate, that can potentially be transferred to other remote-sensing modalities.

The marine debris detection problem is difficult, and is likely to remain so for at least the near future. Part of this difficulty is in the variety of different things that can be considered marine debris, and therefore the irreducible difficulty of specifying what it is that various detection schemes need to look for in order to identify it. Consequently, the concept, developed here, of a multi-component hierarchical model with semi-empirical prior and a pool of partially-skillful detectors could potentially have impact significantly beyond the immediate application. Adding prior structure to the problem results in an emphasis on the solutions that are considered more likely, and allowing for a group of detectors, each of which is allowed to be fallible (so long as they are not fallible simultaneously), makes for a much more robust solution than would otherwise be the case. The advantage of the solution developed is in its flexibility, so that it is readily possible for other prior structuring information to be substituted, and for other detectors to be added to augment, or replace, those currently in use (e.g., for different datasets). Thus, the method proposed can act itself as a structuring framework on which other analyses can be built.

PMBS systems have been the subject of intermittent attention within the hydrographic community for at least the last fifteen years. With the research reported here demonstrating that many of the fundamental problems that have limited their more widespread adoption have been resolved with advancing hardware and software capabilities, the observations described here and in the white paper reports developed during this project point to a future where PMBS systems could be more commonly used for wide scale hydrographic mapping, which could be very impactful from the point of view of efficiency of survey. Although it is not yet entirely clear that there is particular benefit in the increased potential swath of PMBS systems with respect to bathymetric data, the results reported here do indicate that the potential of the backscatter from these devices is not being exploited to the extent that it could be, and that a suitable processing system that optimally combined the use of both sources of information might make a significant difference on the potential for object discovery and anomaly detection in a hydrographic context, which leads to some interesting potential applications.

The use of automatic tools for computer-assisted hydrographic processing of data has been a major change in the field over the last fifteen years, and adoption of new technologies appears to be keeping this trend moving into the foreseeable future. However, the methods by which operators interact with data have not changed nearly as significantly, and the ultimate remediation tool for hydrographic data (editing individual soundings by hand) is essentially the same now as it was in the last century, and remains a significant bottleneck to processing speeds. Any tool that would accelerate that process could have very significant impact on data processing throughput, and in particular the hydrographic ping-to-chart time. The techniques developed here to automatically select viewpoints for analysis of marine debris could therefore be a very interesting addition to the field when applied more generally. For example, consider the potential for this technique applied to general data, where the operator, when faced with an anomalous depth surface reconstruction, has the viewpoint automatically aligned to highlight the difficulty (with auxiliary views to assist), and therefore finds that making the choice of what to do is significantly easier. Or, consider the case where the operator, faced with a sounding remediation, automatically has the viewpoint computed so that the soundings likely to be removed are highlighted against a blank background so that removing them can be accomplished without demanding the time required to reposition the viewpoint. Such extensions of the technique developed here are not necessarily axiomatic, but could be extremely fruitful if pursued, particularly if pursued in conjunction with the combined backscatter and bathymetry decision-making tool outlined with respect to PMBS systems.

Finally, the last topic of research developed here that could have potential impact beyond the immediate use in this project is the concept of making debris identification into a crowd-sourced problem. Crowd-sourcing has been used previously in the context of debris through efforts to document material that is directly observed (e.g., during beach cleanups), but applying it to the problem of marine debris could solve one of the problems for which the FFO was initially developed: how to deal with the volume of data that is collected in response to a storm event. The research here demonstrates the potential for a crowd to make appropriate decisions about marine debris, and in the wake of a storm the potential for recruiting a crowd from the many people that would like to assist, but lack the resources to do so directly, is high. Properly applied, this idea has the potential to significantly alter the mechanisms by which trained operators are expected to deal with data identification, moving from rote mechanical review of data to skilled assessment of the success of the crowd, and targeted review of the more obstinate cases for which the crowd's assessed skill is poor. This potentially impacts not only the volume of data that the operators would be required to assess, but also the types of operator skill sets and training expected.

Of course, the individual research results, taken individually, are not the only potential for broader impacts: combinations of the techniques developed could also be profitably pursued. For example, there is obvious complementarity between the work done on marine object detection, combined analysis of backscatter and bathymetry from PMBS systems, and multi-view data visualization that could result in significantly more powerful tools for marine debris detection, but also for object detection in general hydrographic contexts. Similarly, combinations of satellite imagery and its derived products with the LIDAR waveform analysis techniques could provide auxiliary products for IOCM purposes. The results reported here should, therefore, correctly be viewed as a basis for further research in addition to their immediate benefits, rather than an end in themselves.

7.3 Conclusion

Support of IOCM operations in the wake of a storm is challenging. However, the research developed as part of this project demonstrates that there are improvements to be had, and better methodologies to be used, to develop new IOCM multi-use products and accelerate the collection, processing, and dissemination of data and products.

The trick, however, might very well be ensuring that these facilities, once developed, remain current and available until the next storm arrives.

Products from this Project

Journal Papers

C. Parrish, J. A. Dijkstra, J. P. M. O'Neil-Dunne, L. McKenna, and S. Pe'eri, "Post-Sandy Benthic Habitat Mapping using new Topobathymetric LIDAR Technology and Object-based Image Classification," *J. Coastal Res.*, In Press, 2015.

Conference Papers and Presentations

T. Butkiewicz and A. H. Stevens, "Streamlining the Evaluation of Potential Marine Debris Targets for Disaster Response," In *Proc.* MTS/IEEE *Oceans*, Washington, D.C., 2015.

R. Freire, S. Pe'eri, B. Madore, Y. Rzhanov, L. Alexander, C. Parrish, and T. Lippmann, "Monitoring Near-Shore Bathymetry using a Multi-Image Satellite-derived Bathymetry Approach," In *Proc.* U.S. *Hydrographic Conf.*, National Harbor, MD, 2015.

G. Masetti and B. R. Calder, "A Bayesian marine debris detector using existing hydrographic data products," In *Proc.* MTS/IEEE *Oceans*, Genoa, Italy, 2015.

G. Masetti and B. R. Calder, "Marine Object Manager as Information Fusion Tool for Detected and Database-Stored Shipwrecks," In *Proc. Wrecks of the World III: Shipwreck Risk Assessment*, Gothenburg, Sweden, 2015.

G. Masetti, B. R. Calder, and M. Wilson, "A Marine Object Manager for Detected and Database-stored Features," In *Proc. 6th Int. Conf. on High-Resolution Surveys in Shallow Water*, Plymouth, UK, 2015.

G. Masetti and B. R. Calder, "Development of an adaptive fusion algorithm for marine debris recognition within the post-Sandy restoration framework," In *Proc. Canadian Hydrographic Conf.*, St. John's, NL, Canada, 2014.

L. McKenna, J. A. Dijkstra, and C. Parrish, "Assessing Hurricane Sandy Impacts on Benthic Habitats in Barnegat Bay with new Topographic-Bathymeric LIDAR Technology," In *Proc.* AGU *Ocean Sciences Meeting*, 2013.

C. Parrish, J. Rogers, L. Ward, and J. A. Dijkstra, "Enhanced Coastal Mapping using LIDAR Waveform Features," In *Proc. 15th Annual* JALBTCX *Airborne Coastal Mapping and Charting Workshop*, Mobile, AL, 2014.

C. Parrish and N. Wilson, "Topobathymetric LIDAR Waveform Features for Habitat Mapping and Hurricane Sandy Response," In *Proc. 16th Annual* JALBTCX *Airborne Coastal Mapping and Charting Workshop*, Corvalis, OR, 2015.

V. Price, J. A. Dijkstra, and E. Nagel, "Mapping eelgrass beds after Hurricane Sandy in Banegat Bay, New Jersey using LIDAR and RGB imagery," In *Proc. 24th Annual Zoosterpalooza*, Boston, MA, March, 2015.

V. Price, J. A. Dijkstra, E. Nagel, J. P. M. O'Neil-Dunne, C. Parrish, and S. Pe'eri, "Developing Methodology for Efficient Eelgrass Mapping across LIDAR Systems," In *Proc.* GEOHAB *8*, Salvador, Brasil, 2015.

White Papers

Note: all white papers are available through the library section of the project website, `http://sandy.ccom.unh.edu/publications/library.html`.

P. Johnson, "Imagery Distribution using ArcGIS Mapping Services."

B. Madore, "Morphological Change Procedure using Satellite-derived Bathymetry."

B. Madore, "Obtaining Submerged Aquatic Vegetation Coverage from Satellite Imagery and Confusion Matrix Analysis."

B. Madore, "Shoreline Change from a Storm Event: Procedure using the Digital Shoreline Analysis System."

G. Masetti, "Marine Debris Analysis: A Workflow for Identification of Submerged Debris Objects."

E. Nagel, "Procedures for Processing LIDAR Point Cloud Files to Create Digital Elevation Models, Contours, and Elevation Changes."

E. Nagel, "Procedures for Processing LIDAR Point Cloud Files to Create Digital Elevation Models, Contours, and Elevation Changes in ArcGIS 10.2.2."

V. Price, "Submerged Aquatic Vegetation Mapping using Object-Based Image Analysis with LIDAR and RGB Imagery."

V. Schmidt and K. Jerram, "EdgeTech 4600 and 6205 Data Processing with CARIS HIPS 8.1 and 9.0 in Support of Sandy Supplemental Research."

V. Schmidt and K. Jerram, "Effective Object Detection with Bathymetric Sonar Systems for Post Storm Response."

V. Schmidt and K. Jerram, "GeoAcoustics GeoSwath Plus Data Processing with CARIS HIPS 8.1 in Support of Sandy Supplemental Research."

V. Schmidt and K. Jerram, “Object Detection with Phase-Measuring Bathymetric Sidescan Sonar Depth Data.”

V. Schmidt and K. Jerram, “Storm Response Surveying with Phase-Measuring Bathymetric Sidescan Sonars.”

Project Participants

Name	Role
Dr. Brian R. Calder	Principal Investigator
Dr. Larry A. Mayer	Co-Principal Investigator
Dr. Thomas Butkiewicz	Visualization and Crowd-sourcing
Dr. Jennifer A. Dijkstra	Habitat
Dr. Giuseppe Masetti	Marine debris
Dr. Christopher Parrish	LIDAR
Dr. Shachak Pe'eri	LIDAR and satellite remote sensing
Christina Fandel	PMBS
Kevin Jerram	PMBS
Paul Johnson	Data management
Brian Madore	Satellite remote sensing
Lindsay McKenna	LIDAR and habitat
Erin Nagel	LIDAR, habitat, and data management
Victoria Price	LIDAR and habitat
Val Schmidt	PMBS
Andrew Stevens	Visualization and Crowd-sourcing

Glossary

ABBREVIATION	DEFINITION
ADCIRC	Advanced Circulation, a hydrographic model.
AIC	Akaike Information Criterion, a measure of the information value of a classification problem.
ALB	Airborne Lidar Bathymetry.
ALPS	Airborne Lidar Processing System, a software package used to process EAARL-B data.
AUC	Area Under the Curve, a metric used to assess the overall behavior of a classifier using the area under the receiver operating characteristic curve.
AUV	Autonomous Underwater Vehicle.
CCOM	Center for Coastal and Ocean Mapping, a research center at the University of New Hampshire.
CEI	Coastal Engineering Index.
CMECS	Coastal and Marine Ecological Classification Standard.
CO-OPS	Center for Operational Oceanographic Products and Services, a part of NOAA's National Ocean Service.
CRSSA	Center for Remote Sensing and Spatial Analysis, a research group at Rutgers University.
CSR	Complete spatial randomness, a reference model for spatial statistical analysis.
CUBE	Combined Uncertainty and Bathymetry Estimator, an algorithm for processing raw high-density hydrographic data.
CZMIL	Coastal Zone Mapping and Imaging Lidar.
DEM	Digital Elevation Model.
DSAS	U.S. Geological Survey Digital Shoreline Assessment System, a software package for ESRI ArcMap to assist in shoreline change analysis.
DTM	Digital Terrain Model.
EAARL-B	Experimental Airborne Research Lidar, model B.
ERMA	Environmental Response Management Application.

Abbreviation	Definition
ENC	Electronic Navigational Chart.
FFO	Federal Funding Opportunity.
FGDC	Federal Geographic Data Committee.
GIS	Geographic Information System.
GML	Geographic Markup Language, an xml-derived language for describing geospatial data.
GPS	Global Positioning System, usually a synonym for any Global Satellite Navigation System, but also specifically the U.S.-based NavStar system.
GUI	Graphical User Interface.
IHO	International Hydrographic Organization.
IOCM	Integrated Ocean and Coastal Mapping, a NOAA program to encourage multi-role mapping missions, and the reuse of mapping data. Also a NOAA research center located at the Joint Hydrographic Center, University of New Hampshire.
LIDAR	Light Detection and Ranging, a remote sensing methodology where rapid pulses of light are reflected off the land or seabed, and ranges are computed based on time of flight. Modern instruments also record the intensity of light returned for further analysis.
LISA	Local Indicator of Spatial Association, a method for assessing the spatial correlations in a dataset.
JHC	Joint Hydrographic Center, a NOAA-UNH research center at the University of New Hampshire.
MBES	Multibeam echosounder, a remote sensing methodology where acoustic means are used to determine the depth of water, and the magnitude of acoustic return from reflectors (usually the seafloor) below the survey platform.
MCD	Marine Chart Division, part of NOAA's Office of Coast Survey.
MCMC	Markov Chain Monte Carlo, a technique for evaluating the posterior distribution in a Bayesian analysis problem.
MDML	Marine Debris Markup Language, an XML-derived specification language for marine debris.
MDP	Marine Debris Program, part of NOAA's National Ocean Service.
MDRDT	Marine Debris Rapid Decision Tool, a software application developed during the project to assist in marine debris identification through use of automatically generated 3D views and a simplified feedback interface.

ABBREVIATION	DEFINITION
MHW	Mean High Water, a tidal datum.
MLLW	Mean Lower Low Water, a tidal datum.
MPLE	Maximum pseudo-likelihood estimation, a technique used to approximately fit auto-logistic spatial models to observed binary detection data.
MSI	Multi-spectral Imagery, a type of optical remote sensing data where the visible (and possible other) light bands are split into numerous sub-bands so that spectral characteristics can be estimated.
NAIP	National Agriculture Imagery Program.
NGS	NOAA's National Geodetic Survey.
NJDOT	New Jersey Department of Transportation.
NOAA	The U.S. National Oceanic and Atmospheric Agency.
NSDE	NOAA Shoreline Data Explorer, an on-line service providing information on the national shoreline.
OBIA	Object-based Image Analysis, an analysis technique used for classification of imagery and other multi-dimensional spatial datasets.
OCS	NOAA's Office of Coast Survey.
PMBS	Phase Measuring Bathymetric Sidescan, a remote sensing methodology that uses comparison of received signal phase on two or more sonar receivers to distinguish angle of arrival for reflected acoustic energy, and thereby compute sounding positions.
ROC	Receiver Operating Characteristic, a measure of the performance of a classifier.
ROV	Remotely Operated Vehicle.
RSD	Remote Survey Division, part of NOAA's National Geodetic Survey.
SAC	Spatial Auto-Correlation, a measure of the strength of the statistical relationship between spatially separated elements of one or more fields.
SAV	Submersed Aquatic Vegetation.
SDB	Satellite-Derived Bathymetry, a remote sensing methodology where optical imagery from satellites is used, along with some physical measurements of depth, to develop an estimate of bathymetric depths.

Abbreviation	**Definition**
SSS	Super Storm Sandy.
STEM	Science, Technology, Engineering, and Mathematics.
TPU	Total propagated uncertainty, a measure of the overall uncertainty of measurements.
UNH	University of New Hampshire.
USACE	U.S. Army Corps of Engineers.
USGS	U.S. Geological Survey.
UVM	University of Vermont.
VIF	Variance Inflation Factor, a measure of the significance of multi-colinearity in an ordinary least squares problem.
VNIR	Visible-Near Infrared, a specification for satellite imaging products.
WV-2	World View II, an imaging satellite.
XML	eXtensible Markup Language, a commonly-used text-based language for description of data.

Bibliography

[1] K. D. Sullivan and L. W. Uccellini. Service assessment: Hurricane/post-tropical cyclone Sandy, October 22–29, 2012. NOAA/NWS, 2012.

[2] Q. Guo, N. P. Psuty, G. P. Lordi, S. Glenn, M. R. Mind, and M. D. Gastrich. Hydrographic study of Barnegat Bay, New Jersey. Technical report, New Jersey Department of Environmental Protection, Trenton, NJ, 2004.

[3] M. J. Kennish, B. M. Fertig, and G. P. Sakowicz. In situ surveys of seagrass habitat in the northern segment of the Barnegat Bay–Little Egg Harbor Estuary: eutrophication assessment. Technical report, Rutgers University, New Brunswick, NJ, 2013.

[4] F. C. Moser. Sources and sinks of nitrogen and trace metals, and benthic macrofauna assemblages in Barnegat Bay, New Jersey. In *Dissertation Abstracts International Part B: Science and Engineering*, volume 58(11), page 5849. University Microfilms International, May 1998.

[5] R. G. J. Lathrop and S. M. Haag. Assessment of seagrass status in the Barnegat Bay-Little Egg Harbor Estuary System: 2003–2009. Technical report, Rutgers University, New Brunswick, NJ 2011.

[6] New Jersey Department of Transportation. Double Creek Inlet Channel closed because of navigation hazards in Barnegat Bay, Ocean County: News release. URL: `http://www.state.nj.us/transportation/about/press/2014/041714a.shtm`, 2014.

[7] S. Pe'eri, B. Madore, L. Alexander, C. Parrish, A. Armstrong, C. Azuike, and E. Tetteh. LANDSAT 8 satellite-derived bathymetry. In K. Marks, editor, IHO-IOC GEBCO *Cook Book*, number B-11 in IHO Publication, pages 243–304. International Hydrographic Office/International Ocean Commission, Monaco Cedex, Monaco, 11.1.13 edition, 2013.

[8] S. Pe'eri, C. Parrish, C. Azuike, L. Alexander, and A. Armstrong. Satellite remote sensing as a reconnaissance tool for assessing nautical chart adequacy and completeness. *Marine Geodesy*, 73(3):293–314, 2014.

[9] B. Madore. Morphology change procedure using satellite-derived bathymetry. Technical report, CCOM, University of New Hampshire, 2014.

[10] R. Freire, S. Pe'eri, B. Madore, Y. Rzhanov, L. Alexander, C. Parrish, and T. Lippmann. Monitoring near-shore bathymetry using a multi-image satellite-derived bathymetry approach. In *Proc. U.S. Hydrographic Conference*, National Harbor, MD, 2015. The Hydrographic Society of America.

[11] E. A. Himmelstoss. DSAS 4.0 installation instructions and user guide. In E. R. Thieler, E. A. Himmelstoss, J. L. Zichichi, and A. Ergul, editors, *Digital Shoreline Assessment System (*DSAS*) version 4.0 - An Arc*GIS *extension for calculating shoreline change*, number 2008-1278 in Open File Report. U.S. Geological Survey, 2009.

[12] C. J. Hapke, E. A. Himmelstoss, M. Kratzmann, J. H. List, and E. R. Thieler. National assessment of shoreline change: Historical shoreline change long the New England and Mid-Atlantic coasts. Technical Report 2010-1118, U.S. Geological Survey Open File Report, 2010.

[13] B. Madore. Shoreline change from a storm event: procedure using the Digital Shoreline Analysis System. Technical report, CCOM, University of New Hampshire, 2014.

[14] S. White, C. Parrish, B. R. Calder, S. Pe'eri, and Y. Rzhanov. Lidar-derived national shoreline: empirical and stochastic uncertainty analyses. *J. Coastal Res.*, S62:62–74, 2011.

[15] C. Parrish, J. A. Dijkstra, J. P. M. O'Neil-Dunne, L. McKenna, and S. Pe'eri. Post-sandy benthic habitat mapping using new topobathymetric LIDAR technology and object-based image classification. *J. Coastal Res.*, in press, 2015.

[16] V. Price, J. A. Dijkstra, E. Nagel, J. P. M. O'Neil-Dunne, C. Parrish, and S. Pe'eri. Developing methodology for efficient eelgrass mapping across LIDAR systems. In *Proc.* GEOHAB *8*, Salvador, Brasil, 8–12 May 2015.

[17] C. Parrish, J. N. Rogers, and B. R. Calder. Assessment of waveform shape features for LIDAR uncertainty modeling in a coastal salt marsh environment. *Geosci. and Remote Sens. Letters*, 11(2):569–573, 2014.

[18] M. Pfennigbauer and A. Ullrich. Improving quality of laser scanning data acquisition through calibrated amplitude and pulse deviation measurement. In *Proc. Laser Radar Technology and Applications* XV, volume 7684, page 76841F. SPIE, 2010.

[19] M. J. Kennish, S. M. Haag, and G. P. Sakowicz. Seagrass demographics and spatial habitat characterization in Little Egg Harbor, New Jersey, using fixed transects. *J. Coastal Res.*, S55:148–170, 2008.

[20] M. J. Kennish, S. M. Haag, and G. P. Sakowicz. Seagrass decline in New Jersey coastal lagoons: A response to increasing eutrophication. In M. J. Kennish and H. W. Paerl, editors, *Coastal Lagoons: Critical habitats of environmental Change*, pages 167–202. Taylor and Francis, Boca Raton, FL, 2010.

[21] M. J. Kennish, B. M. Fertig, and R. G. J. Lathrop. Assessment of nutrient loading and eutrophication in Barnegat Bay-Little Egg Harbor, New Jersey in suport of nutrient management planning. Technical report, Rutgers University, New Brunswick, NJ, 2012.

[22] R. G. J. Lathrop, S. M. Haag, D. Merchant, M. J. Kennish, and B. M. Fertig. Comparison of remotely-sensed surveys vs. in situ plot-based assessments of seagrass condition in Barnegat Bay-Little Egg Harbor, New Jersey, USA. *J. Coastal Conservation*, 18:299–308, 2014.

[23] C. W. Wright. USGS EAARL-B: Missions, calibration, and validation. In *Proc. 15th Annual* JALBTCX *Airborne Coastal Mapping and Charting Workshop*, Mobile, AL, 2014.

[24] D. Nagle and C. W. Wright. Algorithms used in the Airborne Lidar Processing System (ALPS). Technical report, U.S. Geological Survey Open File Report, in revision.

[25] C. W. Wright, R. J. Troche, C. J. Kranenburg, E. S. Klipp, X. Fredericks, and D. B. Nagle. EAARL-B submerged topography–Barnegat Bay, New Jersey, post-hurricane sandy, 2012-2013. Technical Report 887, U.S. Geological Survey Data Series, `http://dx.doi.org/10.3133/ds887`, 2014.

[26] C. Parrish and N. Wilson. Topobathymetric LIDAR waveform features for habitat mapping and Hurricane Sandy response. In *Proc. 16th Annual* JALBTCX *Airborne Coastal Mapping and Charting Workshop*, Corvallis, OR, 2015.

[27] S. Pe'eri, J. R. Morrison, F. Short, A. Mathieson, and T. Lippmann. Eelgrass and maroalgal mapping to develop nutrient criteria in New Hampshire's estuaries using hyperspectral imagery. *J. Coastal Res.*, S76(in press), 2015.

[28] J. T. Tou and R. C. Gonzalez. *Pattern Recognition Principles.* Addison-Wesley, London, 1974.

[29] P. Mather and M. Koch. *Computer Processing of Remotely-Sensed Images: An Introduction.* Wiley-Blackwell, 2011.

[30] L. Dunkin. Coastal Engineering Indices to inform regional management. In *Proc. 14th Annual* JALBTCX *Airborne Coastal Mapping and Charting Workshop*, Mobile, AL, 2013.

[31] V. Price. Submerged aquatic vegetation mapping using object-based image analysis and LIDAR and RGB imagery. `http://sandy.ccom.unh.edu/publications/library/Procedures_SAV_Mapping.pdf`, 2015.

[32] B. R. Calder and L. A. Mayer. IOCM research in support of Super Storm Sandy disaster relief. `http://sandy.ccom.unh.edu/publications/library/2015-04-30_Q2FY15_ProgressReport.pdf`, April 2015.

[33] J. Kinney, S. Wolfskehl, S. Bruce, M. Bogonko, C. Bongiovanni, A. Armstrong, E. Nagel, S. Pe'eri, and C. Parrish. Update on NOAA's IOCM Sandy project for charting and habitat mapping using topobathymetric LIDAR surveys. In *Proc. 16th Annual* JALBTCX *Airborne Coastal Mapping and Charting Workshop*, Corvallis, OR, 2015.

[34] D. Li, M. R. Azimi-Sadjadi, and G. J. Dobeck. Comparison of different neural network classification paradigms for underwater target discrimination. In *Proc. SPIE*, volume 4038, pages 334–345, 2000.

[35] J. Stack. Automation for underwater mine recognition: current trends and future strategy. In *SPIE Defense, Security, and Sensing*, pages 80170K–80170K–21. International Society for Optics and Photonics, 2011.

[36] B. A. Telfer, H. H. Szu, G. J. Dobeck, J. P. Garcia, H. Ko, A. C. Dubey, and N. H. Witherspoon. Adaptive wavelet classification of acoustic backscatter and imagery. *Optical Engineering*, 33(7):2192–2203, 1994.

[37] G. Masetti and B. R. Calder. A marine object manager as an information fusion tool for detected and database-stored shipwrecks. In *Wrecks of the World III: Shipwreck Risk Assessment*, Gothenburg, Sweden, 2015.

[38] G. Masetti, B.R. Calder, and M. Wilson. A marine object manager for detected and database-stored features. In *Proc. 6th International Conference on High-Resolution Surveys in Shallow Water*, Plymouth, UK, 2015.

[39] C. A. Ribic, T. R. Dixon, and I. Vining. Marine debris survey manual. *NOAA/NMFS Technical Report 108*, 1992.

[40] S. Katsanevakis. Marine debris, a growing problem: Sources, distribution, composition, and impacts. *Marine Pollution: New Research. Nova Science Publishers, New York*, pages 53–100, 2008.

[41] G. Masetti and B. R. Calder. A risk index methodology for potentially polluting marine sites. *Environment Systems and Decisions*, 34(3):391–405, 2014.

[42] G. Masetti and B. R. Calder. Design of a standardized geo-database for risk monitoring of potentially polluting marine sites. *Environment Systems and Decisions*, 34(1):138–149, 2014.

[43] N. Barnea, J. Michel, B. Bray, Z. Nixon, G. Imahori, and C. Moegling. Marine debris response planning in the north-central gulf of mexico. NOAA *Technical Memorandum* NOS-OR&R-*31*, 2009.

[44] Z. Nixon and N. Barnea. Development of the Gulf of Mexico marine debris model. NOAA *Technical Memorandum* NOS-OR&R-*35*, 2010.

[45] G. Masetti and B. R. Calder. Development of an adaptive fusion algorithm for marine debris recognition within the post-sandy restoration framework. In *Proc. Canadian Hydrographic Conference*, page 14, St. John's, NL, Canada, 2014.

[46] N. A. C. Cressie and C. K. Wikle. *Statistics for spatio-temporal data.* Wiley series in probability and statistics. Wiley, Hoboken, NJ, 2011.

[47] S. Banerjee, B. P. Carlin, and A. E. Gelfand. *Hierarchical modeling and analysis for spatial data.* CRC Press, 2015.

[48] J. Lubchenco and L. Furgione. Service assessment: Hurricane Irene, August 21–30, 2011. NOAA/NWS, 2012.

[49] NOAA. ERMA Atlantic. `https://erma.noaa.gov/atlantic/erma.html`, (2015-02-21) 2015.

[50] S. Lang. Object-based image analysis for remote sensing applications: modeling reality. In T. Blaschke, S. Lang, and G. J. Hay, editors, *Object-Based Image Analysis*, Lecture Notes in Geoinformation and Cartography, book section 1, pages 3–27. Springer Berlin Heidelberg, 2008.

[51] NOAA. Gulf of Mexico marine debris project. `http://www.ncddc.noaa.gov/website/GOM_MarineDebris/viewer.htm`, (2015-02-21) 2015.

[52] D. L. Johnson. Service assessment: Hurricane Katrina, August 23–31, 2005. NOAA/NWS, 2006.

[53] G. Masetti and B. R. Calder. A Bayesian marine debris detector using existing hydrographic data products. In *IEEE Oceans Conference*, Genoa, Italy, 2015.

[54] W. R. Tobler. A computer movie simulating urban growth in the detroit region. *Economic Geography*, 46:234–240, 1970.

[55] J. Besag. Spatial interaction and the statistical analysis of lattice systems. *Journal of the Royal Statistical Society. Series B (Methodological)*, pages 192–236, 1974.

[56] L. Anselin. Under the hood issues in the specification and interpretation of spatial regression models. *Agricultural Economics*, 27(3):247–267, 2002.

[57] J. Besag, J. York, and A. Mollié. Bayesian image restoration, with two applications in spatial statistics. *Annals of the Institute of Statistical Mathematics*, 43(1):1–20, 1991.

[58] T. H. Keitt, O. N. Bjørnstad, P. M. Dixon, and S. Citron-Pousty. Accounting for spatial pattern when modeling organism-environment interactions. *Ecography*, 25(5):616–625, 2002.

[59] L. Palma, P. Beja, and M. Rodrigues. The use of sighting data to analyse Iberian lynx habitat and distribution. *Journal of Applied Ecology*, 36(5):812–824, 1999.

[60] P. Grabarnik and S. N. Chiu. Goodness-of-fit test for complete spatial randomness against mixtures of regular and clustered spatial point processes. *Biometrika*, 89(2):411–421, 2002.

[61] J. N. Perry, A. M. Liebhold, M. S. Rosenberg, J. Dungan, M. Miriti, A. Jakomulska, and S. Citron-Pousty. Illustrations and guidelines for selecting statistical methods for quantifying spatial pattern in ecological data. *Ecography*, 25(5):578–600, 2002.

[62] F. Wang. *Quantitative methods and applications in* GIS. CRC Press, 2006.

[63] A. Getis and J. K. Ord. The analysis of spatial association by use of distance statistics. *Geographical Analysis*, 24(3):189–206, 1992.

[64] L. Anselin. Local indicators of spatial association—LISA. *Geographical Analysis*, 27(2):93–115, 1995.

[65] J. K. Ord and A. Getis. Local spatial autocorrelation statistics: distributional issues and an application. *Geographical Analysis*, 27(4):286–306, 1995.

[66] A. K. Jain. Data clustering: 50 years beyond k-means. *Pattern Recognition Letters*, 31(8):651–666, 2010.

[67] T. Caliński and J. Harabasz. A dendrite method for cluster analysis. *Communications in Statistics*, 3(1):1–27, 1974.

[68] C. F. Dormann, J. M. McPherson, M. B. Araújo, R. Bivand, J. Bolliger, G. Carl, R. G. Davies, A. Hirzel, W. Jetz, W. D. Kissling, I. Kühn, R. Ohlemüller, P. R. Peres-Neto, B. Reineking, B. Schröder, F. M. Schurr, and R. Wilson. Methods to account for spatial autocorrelation in the analysis of species distributional data: a review. *Ecography*, 30(5):609–628, 2007.

[69] N. H. Augustin, M. A. Mugglestone, and S. T. Buckland. An autologistic model for the spatial distribution of wildlife. *Journal of Applied Ecology*, pages 339–347, 1996.

[70] D. Umpierre and G. Margoles. Broward county's web-based hurricane debris estimation tool (HurDET). In *Proc.* ESRI *International User Conference*, 2005.

[71] FEMA. *Appendix B -* USACE *Hurricane Debris Estimating Model*, page 260. Federal Emergency Management Agency, FEMA-325 / July 2007 edition, 2007.

[72] FEMA. HAZUS-MH *2.1 - Hurricane Model - User Manual*. Multi-hazard Loss Estimation Methodology. Department of Homeland Security, Washington, D.C., 2013.

[73] M. D. Powell, S. Murillo, P. Dodge, E. Uhlhorn, J. Gamache, V. Cardone, A. Cox, S. Otero, N. Carrasco, and B. Annane. Reconstruction of Hurricane Katrina's wind fields for storm surge and wave hindcasting. *Ocean Engineering*, 37(1):26–36, 2010.

[74] NOAA. The Extratropical Surge and Tide Operational Forecast System. URL: `http://www.stormsurge.noaa.gov/models_obs_modeling.html`, (2015-03-20) 2015.

[75] B. W. Eakins and P. R. Grothe. Challenges in building coastal digital elevation models. *Journal of Coastal Research*, pages 942–953, 2014.

[76] NOAA. International best track archive for climate stewardship (IBTRACS). `http://www.ncdc.noaa.gov/ibtracs/index.php?name=ibtracs-data`, (2015-02-22) 2015.

[77] K. R. Knapp, M. C. Kruk, D. H. Levinson, H. J. Diamond, and C. J. Neumann. The international best track archive for climate stewardship (IBTRACS). *Bulletin of the American Meteorological Society*, 91(3):363–376, 2010.

[78] P. Wessel and W. H. F. Smith. A global, selfconsistent, hierarchical, high-resolution shoreline database. *Journal of Geophysical Research: Solid Earth (1978–2012)*, 101(B4):8741–8743, 1996.

[79] USACE. U.S. Waterway Data - National Waterway Network. `http://www.navigationdatacenter.us/data/datanwn.htm`, (2015-03-25) 2015.

[80] F. R. Broome and D. B. Meixler. The TIGER data base structure. *Cartography and Geographic Information Systems*, 17(1):39–47, 1990.

[81] T. Meurling and B. Volberg. The evolution and future of multibeam echo sounder technology. In *Underwater Technology and Workshop on Scientific Use of Submarine Cables and Related Technologies*, Tokyo, Japan, 2007.

[82] J. E. Hughes Clarke. Optimal use of multibeam technology in the study of shelf morphodynamics. *Sediments, Morphology and Sedimentary Processes on Continental Shelves: Advances in technologies, research and applications (Special Publication 44 of the* IAS*)*, 108:3, 2012.

[83] L. A. Mayer, R. Raymond, G. Glang, M. D. Richardson, P. Traykovski, and A. C. Trembanis. High-resolution mapping of mines and ripples at the martha's vineyard coastal observatory. *Oceanic Engineering, IEEE Journal of*, 32(1):133–149, 2007.

[84] X. Lurton. *An introduction to underwater acoustics : principles and applications*. Springer, published in association with Praxis Publishing, Chichester, UK;, Heidelberg; New York, 2nd edition, 2010.

[85] G. Masetti and B. R. Calder. Remote identification of a shipwreck site from mbes backscatter. *Journal of Environmental Management*, 111(0):44–52, 2012.

[86] Kongsberg Maritime. Sector coverage and beam spacing modes for multibeam echosounders. Report, Kongsberg Maritime, December 2013.

[87] Kongsberg Maritime. The advantages of yaw stabilization in multibeam surveying. Report, Kongsberg Maritime, September 2013.

[88] F. Pohner, J. Bakke, O. Nilsen, T. Kjaer, and L. Fonseca. Integrating imagery from hull mounted sidescan sonars with multibeam bathymetry. In *Proc. U.S. Hydrographic Conference*, page 16, Norfolk, VA, 2007.

[89] G. E. Wheaton. Patch test, a system check for multibeam survey systems. In *Proc. Hydrographic Conf*, pages 12–15, 1988.

[90] J. Eisenberg, M. Davidson, J. Beaudoin, and S. Brodet. Rethinking the patch test for phase measuring bathymetric sonars. In *Proc. U.S. Hydrographic Conference*, Tampa, FL, 2011.

[91] J. E. Hughes Clarke. Dynamic motion residuals in swath sonar data: Ironing out the creases. *International Hydrographic Review*, 4(1):6–23, 2003.

[92] W. S. Burdic. *Underwater acoustic system analysis*. Prentice Hall New Jersey, 1991.

[93] J. Beaudoin, B. R. Calder, J. Hiebert, and G. Imahori. Estimation of sounding uncertainty from measurements of water mass variability. *International Hydrographic Review*, pages 20–38, 2009.

[94] M. J. Wilson, J. Beaudoin, and S. Smyth. Water-column variability assessment for underway profilers to improve efficiency and accuracy of multibeam surveys. In *U.S. Hydrographic Conference*, page 24, 2013.

[95] Kongsberg Maritime. Detector modes in SIS for EM 2040, EM 2040C and EM 3002. Report, Kongsberg Maritime, September 2013.

[96] L. Fonseca and B. R. Calder. Geocoder: An efficient backscatter map constructor. In *Proc. U.S. Hydrographic Conference*, 2005.

[97] B. R. Calder and L. A. Mayer. Automatic processing of high-rate, high-density multibeam echosounder data. *Geochemistry, Geophysics, Geosystems*, 4(6):1048, 2003.

[98] B. R. Calder and D. E. Wells. CUBE user's manual. CCOM/JHC, UNH, *Durham,* NH, USA, 2007.

[99] B. R. Calder. Automatic statistical processing of multibeam echosounder data. *International Hydrographic Review*, 4(1):53–68, 2003.

[100] T. Fawcett. An introduction to ROC analysis. *Pattern Recognition Letters*, 27(8):861–874, 2006.

[101] D. Collett. *Modelling binary data*. CRC Press, 2002.

[102] B. A. Wintle and D. C. Bardos. Modeling species-habitat relationships with spatially autocorrelated observation data. *Ecological Applications*, 16(5):1945–1958, 2006.

[103] D. C. Bardos, G. Guillera-Arroita, and B. A. Wintle. Valid auto-models for spatially autocorrelated occupancy and abundance data. *arXiv preprint arXiv:1501.06529*, 2015.

[104] F. W. Huffer and H. Wu. Markov chain monte carlo for autologistic regression models with application to the distribution of plant species. *Biometrics*, 54(2):509–524, 1998.

[105] C. J. Geyer and E. A. Thompson. Constrained monte carlo maximum likelihood for dependent data. *Journal of the Royal Statistical Society. Series B (Methodological)*, 54(3):657–699, 1992.

[106] S. Geman and D. Geman. Stochastic relaxation, gibbs distributions, and the bayesian restoration of images. IEEE *Trans.* PAMI, 6(6):721–741, 1984.

[107] X. Lurton. Precision analysis of bathymetru measurements using phase difference. In *Proc.* IEEE OCEANS *'98*, volume 2, pages 1131–1134, Oct. 1998.

[108] IHO. IHO S-44*—Standards for Hydrographic Surveys*. IHB, Monaco, 5th edition, 2008.

[109] Office of Coast Survey. *NOS Hydrogaphic Surveys Specifications and Deliverables*. National Oceanic and Atmospheric Administration, May 2015.

[110] Office of Coast Survey. *Field Procedures Manual*. National Oceanic and Atmospheric Administration, 2014.

[111] T. Butkiewicz and C. Ware. Multi-touch 3D exploratory analysis of ocean flow models. In *Proc.* MTS/IEEE OCEANS, Kona, Hawai‘i, 2011.

[112] C. Englert, T. Butkiewicz, L. A. Mayer, A. Trembanis, J. Beaudoin, V. Schmidt, and C. Duval. Designing improved sediment transport visualizations. In *Proc.* MTS/IEEE OCEANS, San Diego, CA 2013.

[113] T. Butkiewicz and A. H. Stevens. Streamlining the evaluaton of potential marine debris targets for disaster response. In *Proc.* MTS/IEEE OCEANS, Washington, D.C. 2015.

[114] E A. Bier, M. C. Stone, K. Pier, W. Buxton, and T. D. DeRose. Toolglass and magic lenses: The see-through interface. In *Proc.* SIGGRAPH, 1993.

[115] J. Howe. *Crowdsourcing: Why the power of the crowd is driving the future of business*. Crown Business (Random House), New York, 2008.